Investigating neurocognition in design creativity under loosely controlled experiments supported by EEG microstate analysis

Wenjun Jia

A Thesis
in
The Concordia Institute
for
Information Systems Engineering

Presented in Partial Fulfillment of the Requirements
For the Degree of
Doctor of Philosophy (Information and Systems Engineering) at
Concordia University
Montréal, Québec, Canada

July 2021

CONCORDIA UNIVERSITY
School of Graduate Studies

This is to certify that the thesis prepared

By: **Wenjun Jia**

Entitled: **Investigating neurocognition in design creativity under loosely controlled experiments supported by EEG microstate analysis**

and submitted in partial fulfillment of the requirements for the degree of

Doctor of Philosophy (Information and Systems Engineering)

complies with the regulations of this University and meets the accepted standards with respect to originality and quality.

Signed by the final examining committee:

_____ Chair
Dr. Pouya Valizadeh

_____ External Examiner
Dr. Weiping Zhu

_____ External to Program
Dr. Jonathan Cagan

_____ Examiner
Dr. Nizar Bouguila

_____ Examiner
Dr. Arash Mohammadi

_____ Thesis Supervisor
Dr. Yong Zeng

Approved by _____
Dr. GPD, Graduate Program Director

August 20, 2021 _____
Dr. Mourad Debbabi, Dean
Gina Cody School of Engineering and Computer Science

Abstract

Investigating neurocognition in design creativity under loosely controlled experiments supported by EEG microstate analysis

Wenjun Jia, Ph.D.

Concordia University, 2021

Design is a recursive process to create original and useful artifacts to meet human needs. Creativity is a critical ability for designers to create original and useful artifacts. Design creativity focuses on creativity mechanisms during the design process. Even though many studies endeavor to understand cognition in design creativity by protocol analysis, neurocognition underlying design creativity remains unknown. Such scarcity can be explained by the intrinsic characteristics of the design process and the data analysis approaches. Loosely controlled experiments are capable of simulating the intrinsic characteristics of the design process, whereas they would increase difficulties of data analysis due to unstructured data and hidden causal relationships between a stimulus and its response. Therefore, this research aims to: (i) test the effectiveness of loosely controlled experiments through comparing its findings on phenomena that have been effectively studied by validated experimental research; (ii) structure and segment unstructured electroencephalography (EEG) signals through EEG microstate analysis; (iii) identify EEG-defined large-scale brain networks and uncover their temporal dynamics in design creativity; (iv) capture the temporal dynamics of EEG-defined large-scale brain networks to classify different cognitive activities in design creativity through RNN techniques under the autoencoder framework. The loosely controlled experiments supported by EEG microstate analysis appear to offer an effective approach to facilitating an ecologically valid neurocognitive study.

Acknowledgments

Changing is the most appropriate word to summarize my Ph.D. journey. I used to afraid of uncertainty, but now I begin to accept certain degrees of uncertainty with peaceful and open minds. I was a solution-driven engineer, but now I am a problem-driven engineer. I used to prefer pursuing knowledge aimlessly, but now I prefer pursuing knowledge along with many right questions.

I would like to express my sincerest gratitude and appreciation to my supervisor, Prof. Yong Zeng, for changing my emotion, skills, and knowledge to do creative research, supporting and encouraging me when I encountered difficulties.

I would like to thank Concordia University for providing me the opportunity to do research, NSERC CRD project, and NSERC Discovery Grant for supporting me financially, as well as NRC, CAE, and Marinvent for offering me the chance to collaborate with and learn from domain experts.

I would like to thank all members of the Design Lab for their help in my research and life during the past five years.

I would like to express my deepest love to my family. My parents always support me to explore the world without any preconditions and encourage me when I meet obstacles. Dr. Hui Yang often huohuo me to make real research contributions to human beings.

Contents

List of Figures

List of Tables

Chapter 1

Introduction

Design is a ubiquitous phenomenon in our daily life [1]. We have designed the room for living; we have designed the phone for communication; we have designed the car for driving. Except for physical products, we have designed the course materials for learning; we have designed the organization's rules for operation; even more, we have designed our thinking for everything.

Formally, design is a recursive process to create original and useful products that are able to serve its environment without breaking natural laws and social and technical regulations in the environment [2]. The environment of products is everything other than products; alternatively, the environment of products is anything existing and known [3]. Products, which are anything non-existing and unknown, come from the environment, serve the environment, and change the environment [4].

Design involves complex cognitive activities that may trigger the creative process and the creative product that is original and useful. The creative product can be considered as the result of the creative process. Design creativity focuses on creativity mechanisms while involving in design activities. Understanding the creativity mechanisms during the design process is particularly important in that it can improve products' quality and cost and designers' capability and performance.

Modeling the design process is the first step to understand the creativity mechanisms involved in design activities. Simon [5] viewed design from the perspective of a rational problem-solving process, which would search well-defined problem and solution spaces. The search spaces are supposed to be stable, while the designers' information processing capacity limits iteration steps toward the solution. Alternatively, Schön [6] provided a constructionist perspective for scholars to model the design process as a 'reflective conversation with the situation', in which problems are actively framed by designers who take action improving the current situation, approaching to solutions (see Dorst and Dijkhuis, 1995 for a comprehensive comparison [7]). This interaction between problem framing and solution generation is formulated into the recursive logic [2], representing the nature of design, which is seen in general human cognition and reasoning [8–10]. The recursivity of design implies a co-evolutionary construction of problem and solution spaces [11, 12], and calls for environment-oriented design methodology.

With the help of modeling the design process, design cognition further investigates designers' mental processes and representations while involving in design activities [13]. Such design cognition is worth studying as they not only support designers' mental activities throughout the design process but also serve as fundamental parts of the evolving environment [14, 15]. Design cognitive may involve a few mixed cognitive activities: remembering, understanding, applying, analyzing, evaluating, and creating based on Bloom's taxonomy [16]. For instance, recalling, which belongs to remembering, refers to retrieve relevant knowledge from long-term memory. Designers would recall past design experiences to accomplish a routine design task.

Protocol analysis is a widely used method to investigate designers' mental processes and representations during the design process [17–21]. Protocol analysis applied in design research can be defined as a series of means to extract 'reliable information about what

people are thinking while they work on a task' [22], the form of which can be verbalization, video, audio, sketches, and eye-tracking. Verbal protocol analysis is valuable in that designers can interpret a design problem, elaborate on a design solution, and explain their decision-making process verbally. Verbal protocols are typically collected during and after the design process, corresponding to concurrent and retrospective verbal protocols. For example, the concurrent verbal protocols are collected when designers to report all their thoughts verbally while involving in design activities [18]. These collected verbal protocols are then split into sequences of semantic segments and analyzed by a coding scheme.

Sketch protocol analysis is also usable when inferring designers' mental processes and representations. Schon and Wiggins indicated that sketch makes unintended discoveries by allowing designers' to inspect their own sketches [23]. When designers sketch ideas on paper and inspect sketches, this inspection allows designers to see new relations and features that would help designers refine and revise their ideas [24]. Indeed, Athavankar suggested that sketch can be considered as an external memory [25]. Along with similar thoughts, Zeng and colleagues suggested that sketch provides mental relaxation and helps in generating new ideas through reducing cognitive workload and encouraging the free flow of creativity [26]. Bilda and colleagues found no significant differences in design outcome scores, the total number of cognitive actions, and overall density of idea production between conditions of blindfold and full-version [27]. Bilda and Gero concluded that expert designers are capable of using knowledge and spatial information stored in long-term memory to facilitate the design process without the use of sketches [28].

Protocol analysis revealed that design is either a searching process or an exploration process [13]. An optimal design solution can be determined by searching well-defined problem and solution spaces under certain degrees of constraints. The searching target and spaces will not be changed significantly over time. Goel proposed that there are two searching strategies: lateral- and vertical-first [29]. The lateral-first strategy refers to 'movement

from one idea to a slightly different idea', while the vertical-first strategy refers to 'movement from one idea to a more detailed version of the same idea' [29]. Chan proposed that designers need to retrieve declarative and procedural knowledge from long-term memory given a design problem and activate this knowledge in working memory [30]. This knowledge is manipulated and updated through operations of synthesis and evaluation until an optimal design solution is determined [25, 30, 31].

Alternatively, a satisfactory design solution can be determined through a co-evolutionary process between ill-defined problem and solution spaces [11, 12]. The search target and spaces will be changed significantly over time. This co-evolutionary process between problem and solution spaces does not result in a predefined and optimal solution. Indeed, this co-evolutionary process follows the recursive logic that the design problem, design solution, and design knowledge would evolve simultaneously and interdependently throughout the design process [2, 32, 33]. As a result, a perceived design problem can determine a design solution, which in turn will change the perception of design problem.

1.1 Motivations

These models about the design process have established solid foundations to understand the creativity mechanism involved in design activities. The important involvement and impact of designers' brain activities during the design process have been realized by more and more researchers, whereas related research is still at an early stage. Brain activities are worth studying as they not only support designers' mental processes and representations throughout the design process but also as fundamental parts of the evolving environment [14, 15].

However, little is known about how brain activities support and influence designers' mental processes and representations during the design process. This insufficient investigation may result from the intrinsic characteristics of the design process and data analysis

approaches. In neurocognitive science, a strictly controlled experiment involves observing the effects of a design activity on brain responses with control of all extraneous variables [34]. Such a strictly controlled experiment provides a reliable approach to identifying repeatable/reproducible causal relations between a stimulus and a response [34]. The strictly controlled experiment is not the most appropriate to simulate creativity underlying the design process in that one cannot control whether, when, or how a designer generates a creative solution. Moreover, the strictly controlled experiment ignores the positive effects of incubation and mind wandering on creativity underlying the design process [35–38].

A loosely controlled experiment may be a proper way to simulate the creative process while involving design activities [15, 39]. The loosely controlled experiments will be conducted without control of all extraneous variables, such as task response time. Under this loosely controlled setting, designers have sufficient time to explore potential solutions freely; some of the solutions may be creative. In addition, this loosely controlled experiment is able to simulate some critical characteristics of design, such as recursivity. A design problem will identify relevant knowledge to generate a tentative solution, which will, in turn, further re-identify relevant knowledge to reformulate the design problem.

Although the loosely controlled experiment is capable of stimulating the creative process while involving design activities, its effectiveness remains unknown. Also, this loosely controlled experiment will increase the difficulties of electroencephalography (EEG) signals analysis. First of all, the EEG signals collected from the loosely controlled experiment are unstructured, which results in hidden causal relationships between a stimulus and its response. Secondly, the hidden causal relationships are very complex since one stimulus may trigger many brain responses while many stimuli may trigger one brain response. The brain responses may involve complex activities that are associated with large-scale brain networks. Thirdly, a stimulus for design activities may always keep changing in that the design problem, design solution, and design knowledge keep evolving simultaneously and

interdependently throughout the design process.

1.2 Objectives

This research aims to address the difficulties in EEG signals analysis when a loosely controlled experiment simulates the creative process while involving design activities. The main objectives are summarized as follows:

- test the effectiveness of loosely controlled experiments through comparing its findings on phenomena that have been effectively studied by validated experimental research;
- structure and segment the unstructured EEG signals collected from the loosely controlled experiments in design creativity;
- associate the segmentations of structured EEG signals with EEG-defined large-scale brain networks and their functions in design creativity;
- investigate neural oscillations and temporal dynamics of network oscillations in design creativity through measuring temporal properties of EEG-defined large-scale brain networks;
- capture the temporal dynamics of network oscillations in design creativity and use this characteristic to classify cognitive activities in design creativity.

1.3 Organization

Chapter 2 presents a review on design methodologies, design creativity, cognition in design creativity, neurocognition in design creativity, and challenges in design creativity studies. Chapter 3 presents a framework of loosely controlled experiments supported by

EEG microstate analysis to address these challenges, as mentioned in Chapter 2. Chapter 4 reports findings of network oscillations in design creativity when applying the framework as mentioned in Chapter 3. Chapter 5 reports findings of temporal dynamics of network oscillations in design creativity through investigating the temporal dynamics of EEG-defined large-scale brain networks. Chapter 6 reports findings of capturing temporal dynamics of EEG-defined large-scale brain networks and classifying cognitive activities in design creativity. Chapter 7 concludes the thesis.

Chapter 2

Background

2.1 Design methodologies

Intuitively, 'design is an activity that aims to change an existing environment to a desired one by creating a new artefact into the existing environment' [4]. An original and useful product must be able to satisfy design requirements constituted by a set of human needs. A product can be considered as a solution to a design problem, while the environment of a product can be viewed as all objects other than the product itself [3]. A design problem is a set of statements about the product-environment system, which includes a product and its environment [3]. According to focused respective parts of the product-environment system, design methodologies can be classified into three categories: product-based design methodologies, function-based design methodologies, and environment-oriented design methodologies [40].

Product-based design methodologies consider a product as their focus in that one must have a product at the beginning of design. Theory of Inventive Problem Solving (TRIZ) is a product-based design methodology for developing a new product in a structured and systematic manner [41]. TRIZ pays more attention to how to generate innovative solutions rather than understanding and analyzing the design problem. TRIZ analyzed contradictions

of desired features of a product and uses 40 inventive principles, separation principles, or substance field analysis to design a new product through solving contradictions [42]. There are two major types of contradictions, which are technical and physical. The technical contradictions illustrate that an attempt to improve one aspect of desired features of a product results in deteriorations of other aspects of desired features of a product. The physical contradictions illustrate that desired features of a product cannot be satisfied at the same time in physical conditions. Later, the 40 inventive principles can be used to deal with technical and physical contradictions conceptually. The separation principles can be applied to understand and solve complex physical contradictions with what appeared to be unresolvable contradictions. This too rigid and definite direction to the thinking process has been challenged because of inflexibility in a variety of situations and difficulty in learning this thinking process [43].

Function-based design methodologies consider functional structures of a product as their focus in that functional structures implied in the design problem embody the expectations of a product. Function-Behaviour-Structure (FBS) is a widely used methodology to design a new product through transforming a set of functions into design descriptions [44]. A design description represents the components of a product and their relations, which is labeled as structure. Behaviour represents the attributes that can be derived from structure. Transformation among function, structure, and behaviour constitutes basic design activities, which are formulation, synthesis, analysis, evaluation, reformulation, and production of design description. A Design prototype is a conceptual schema for representing a set of generalized concepts from similar design cases. The design prototype consists of function, behaviour, and knowledge, which provides the basis for the start of a design. Initial design prototype may consist of more function and behaviour while subsequent design prototype may have more details on structure. The design process can be considered as retrieval and transformation of the design prototype.

Environment-oriented design methodologies consider the environment of a product as their focus. Environment-based Design (EBD) [3], User-Centred Design (UCD) [1], and Situated Function-Behaviour-State (S-FBS) [45] are widely used approaches to design a product in a creative manner, which start a design process from the environment of a product. In the cases of EBD, the environment of a product represents everything except the product itself. It is easier and more intuitive for designers to start an activity from the environment of a product, which is already existing and known for designers. Next, a transformation between environment and product constitutes basic design activities, such as formulation, evaluation, and synthesis [32, 33]. Then, the product is designed to serve its environment while the product brings changes to its environment and becomes one of the components in its environment [4]. The design process can be considered as a co-evolutionary process between a product and its environment.

Indeed, EBD is stemmed from the recursive logic that demonstrates a simultaneous and interdependent evolution process among the design problem, design solutions, and design knowledge [2, 32, 33]. The recursive logic implies that 'the generation and evaluation of design solutions depend on design knowledge while the kind of design knowledge that can be used for the current design is determined by the design solutions' [4]. The idea of evolution among the design problem, design solutions, and design knowledge is also reflected in situatedness, 'which emphasizes that the agent's view of a world changes depending on what the agent does' [45]. In line with the statements of the evolving environment, a few researchers view design as a co-evolutionary process between problem and solution spaces [11, 12]. Corne and colleagues thought of design as exploration in that design 'involves the construction and incremental extension of problem statements and associated solutions' [46]. Logan and Smithers stressed the importance of incremental extension of problems and solutions in design creativity [47]. Maher and Poon proposed a computational model of co-evolution using modified genetic algorithms [11].

Findings of protocol analysis support the statement that design is a co-evolutionary process between problem and solution spaces [12, 48]. For instance, Dorst and Corss asked participants to create a concept for a 'litter disposal system' in a new Netherlands train [12]. They observed that designers interpreted the design task quite differently in terms of their own design environment, resources, and capabilities. This different interpretation resulted in different solutions. Some of the solutions may be considered as one of the key features in the subsequent design process, leading to a change in the design task. In addition, Maher and Tang analyzed the protocol data collected from designing new electrical kettles and designing a house for a couple [48]. They segmented protocol data into changes of problem requirements and solutions. The changes of problem requirements included adding new problem requirements, refining problem requirements, searching for new requirements, and re-examining problem requirements. The changes of solutions included generating a creative solution, expressing a solution, and examining a solution. Using this coding scheme, the authors found that designers spent more time thinking about solutions in designing electric kettles and balance time thinking about problems and solutions in designing a house. Also, they observed the transitions between problem and solution spaces in the design process. Therefore, design creativity is not a search process under a fixed design problem for an optimal design solution. Design creativity seems to be a process of formulating a design problem, generating and elaborating design solutions, as well as reformulating and reframing the design problem recursively.

2.2 Design creativity

Creativity has been studied in two folds in the field of design research. One kind of creativity is related to the design process since some special processes underlying the design process are believed to be creative processes. Similarly, Gero indicated this kind of creativity is related to 'developing an understanding of the creativity of designs as a precursor

to improving the generation of designs that are deemed to be creative' [49]. Another kind of creativity is related to the creative product that is a result of the creative process. In this research, we focus on the first kind of creativity that is creativity mechanisms during the design process, namely design creativity.

In the field of psychology, Sternberg and Lubart defined creativity as 'the ability to produce work that is both novel (i.e., original, unexpected) and appropriate (i.e., useful or meets task constraints)' [50]. Similarly, Weisberg defined creativity as 'novel and valuable products, capacity to produce such works and the activity of generating such products' [51]. Simonton added surprising to the definition of creativity except for novel and useful [52].

Guilford proposed that divergent and convergent thinking processes are credited to two fundamental processes underlying creativity [53]. In the divergent thinking process, there are inconclusive and no unique solutions that can be found in many directions. In the convergent thinking process, there is one conclusive and unique solution that can be found in the direction. Finke developed this dual-process model into a 'Geneplore' model that is constituted by generative and exploratory processes [54]. In the generative phase, one constructs an initial idea. In the exploratory phase, the initial idea is interpreted, modified, and regenerated, leading to creative products. The exploratory process can be viewed as interactions among many sub-processes underlying creativity, such as idea interpretation, idea generation, idea evaluation, and overcoming fixation. An integrated dual-process model of creativity has been proposed to systematically describe shifting between idea generation and idea evaluation [55].

Similar efforts were attempted in the field of design. Goel proposed symbol systems to understand design creativity [56]. The first symbol system supports associative processes that benefit lateral transformations, extending the design problem space. The second symbol system supports inference processes that facilitate vertical transformations, deepening

the design problem space. The lateral transformations are associated with divergent thinking, while the vertical transformations are associated with convergent thinking. These two symbol systems align with Guilford's ideas that divergent and convergent thinking are two fundamental processes underlying creativity. These two systems work together, leading to design creativity.

Gero proposed that design creativity may be incubated through adding new variables to perturbate an existing schema or the emergence of new schema [57]. Addition and substitution are two fundamental processes to add new variables based on Stevens' two forms of psychological representational scales. The meaning of additive process is to add variables to the existing variables, while the implication of substitutive process is to delete some of the existing variables and add other variables. In the context of computational analogs, combination, analogy, and mutation are associated with the additive process, while mutation, analogy, and emergence are associated with the substitutive process. For instance, analogy in the additive process refers to that structural knowledge of one problem is transferred to that of another problem. Emergence in the substitutive process facilitates new behaviours and functions, similar to reallocating attention and reinterpreting the results. The interaction between the additive and substitutive process can be modeled as an evolutionary model.

A few scholars suggested that design creativity may be triggered by a co-evolutionary process between problem and solution spaces [11, 12, 48]. The co-evolutionary process illustrates 'developing and refining together both the formulation of a problem and ideas for a solution, which constant iteration of analysis, synthesis and evaluation processes between the two notional design space' [12]. Creative ideas may happen when the unstable co-evolutionary process becomes fixed through an emergent bridge that links the problem and solution spaces.

Nguyen and Zeng proposed that design creativity follows a nonlinear dynamics [58].

The nonlinear dynamics demonstrates that a minor initial state difference may lead to huge state differences after many rounds of evolution. The minor initial state difference may result from formulating the design problem differently, extending knowledge, and changing the sequence of environment decomposition [4]. Some new states may be creative, whereas the other states are inconclusive outcomes. Even if the inconclusive outcomes maybe not creative, the process of exploring the potentially original and useful ideas is still considered a creative process [59]. The nonlinear dynamics implies a mechanism of creativity, which accommodates a degree of flexibility, uncertainty, and unpredictability through a structured and deterministic model of design.

Zeng proposed that design creativity may happen when a designer in a medium level of stress based on Yerkes-Dodson law [4]. The Yerkes-Dodson law shows an inverse U-shape correlation between stress and performance [60]. The following studies of Nguyen and Zeng elaborate stress as perceived workload over mental capacity [58]. Mental capacity is constituted by knowledge, skills, and affect. Knowledge and skills are related to the rational process in dealing with the perceived workload, while affect is associated with the emotional response to the perceived workload.

Howard and Dekoninck described design creativity by the integration of engineering design and cognitive psychology [61]. The authors mapped three creative processes: analysis, generation, and evaluation, into the FBS model. Generation in the creative process is associated with formulation, synthesis, and reformulation, while evaluation in the creative process is associated with analysis and evaluation. In addition, design output can be evaluated based on three criteria, including original, adaptive, and variant. In the context of the FBS model, original design output refers to a creative design output at the behavioural level; adaptive design output refers to a creative design output at the functional level; variant design output refers to a creative design output at the structural level. Therefore, a creative design product should contain at least one creative output at the behaviour, or functional,

or structural level.

2.3 Cognition in design creativity

With the guidance of theoretical models of design creativity, cognition aims to understand the mental processes and representations while engaging in design creativity [13]. Zhao and colleagues mapped cognitive activities of learning process into design activities according to Bloom's taxonomy [15]. The cognitive activities have been classified into six levels: remembering, understanding, applying, analysis, evaluating, and creating [16]. For instance, remembering refers to retrieve relevant knowledge from long-term memory, which includes recognizing and recalling. Creating refers to generating something new, which includes generating, planning, and producing. The design activities have been classified into four levels: physical, perceptual, functional, and conceptual [62]. For example, the physical level refers to activities of physical depictions on paper, which includes making depictions on paper, looking at previous depictions, and moving tools or hands without breaking. The perceptual level refers to activities of attending to visual features of elements and spatial relations among elements, as well as organizing and comparing elements. Thus, one cognitive activity may be associated with many design activities, while many cognitive activities may be associated with one design activity.

Zeng and colleagues classified cognitive activities in the design process into three stages: problem formulation, solution generation, and solution evaluation [32,33]. Problem formulation is to decompose the design problem into components and understand relationships among components. Some skills are required to appropriately formulate the design problem, which includes gathering and structuring information and evaluating the moment to move on to solution generation [63]. A protocol analysis from junior and senior industrial design students revealed that senior students with more creativity due to 'asks less information, processes it instantly, and gives the impression of consciously building up an

image of the problem. They look for and make priorities early on in the process' [64]. In line with this finding in design protocol analysis, senior students paid much attention to the scope of the design problem while freshmen students stuck in problem-definition and did not generate creative solutions [65]. In addition, problem reformulation is critical for designers to generate a potentially creative idea. Problem reformulation can change the structure state space in the FBS model while changing the rules of problem decomposition in the EBD model.

Solution conjectures help designers formulate design problems through exploring and defining problem-and-solution together. A behavioural study revealed that scientists focus on the structure of the problem while architects pay more attention to generate high-quality solutions until they satisfy with them [66]. Once a designer who has specific knowledge and skills for a specific problem type tended to use solution conjectures instead of problem analysis [67].

After formulating a problem, designers need to generate some candidate solutions. Synthesis is to merge various existing components into a new component that does not yet exist. Episodic knowledge, which is formulated from past design experiences, and semantic knowledge, which is formulated from the fact, are involved in the synthesis process. Involving too much past design experience may result in a fixation effect. Jansson and Smith found when engineers faced a design problem with the addition of an illustration of an existing solution resulted in final solutions, they would like to generate solutions that shared many features from the existing solution in design problem [68]. The degrees of fixation may be associated with educational programmers in that designers tended to have less fixation compared to engineers in many cases [69–71]. Another fixation is related to a phenomenon that designers are attachment to early solutions heavily [72]. Rowe observed that initial design ideas have significant impacts on final solutions in that designers were more like to make the initial design ideas work rather than reframing design problems [73].

Ullman and colleagues found that experienced designers pursued a single design solution instead of radically rejecting design solutions to develop a better one [74]. Balle and colleagues observed similar phenomena that once designers developed a poor quality solution, they appeared to improve the solution laboriously by slightly changing the parts of solution [75]. Nguyen and Zeng concluded three paths leading to the fixation: i designers are heavily attached a solution; (ii) designers do not have the right perception of the design problem; (iii) designers evaluate the fitness of the example idea poorly [72].

This fixation has side effects on creative idea generation since designers tend to generate solutions similar to existing design solutions. Smith and Tjandra observed that the quality of a final design solution seemed to depend on a willingness to retake into account early design solutions [76]. Incubation and mind-wandering may help designers overcome fixation due to refreshing memory or forgetting anchors [35, 77]. Such a break during the design process may inhibit memory of inappropriate knowledge and give spaces for emerging appropriate knowledge [78]. Problem reframing is another way to minimize the effects of fixation in that designers can reformulate the design problem from radically distinct perspectives. The components in the design problem and their relationships may be changed, bringing changes to the problem scope and constraints.

Solution evaluation is to assess candidate design solutions' merit and worth based on criteria and standards [79]. The criteria and standards are defined by co-evolutionary spaces of the design problem and design solution. Preferential and aesthetic evaluation have implicit criteria, while permanence and structure evaluation have explicit criteria, which belong to internally guided decision-making and externally guided decision-making, respectively. The externally guided decision-making requires participants to adjust their decisions to fall in with the externally defined single correct answer, while the internally guided decision-making requires participants to evaluate without no correct answer based on external circumstances [80]. After solution evaluation, designers may elaborate the solution

slightly until a solution satisfies with design requirements or may reformulate the design problem, which becomes the input for another solution generation.

2.4 Neurocognition in design creativity

Despite many results brought by protocol analysis in design creativity research, researchers argued that the protocol analysis approaches would interfere with mental activity [81, 82], delay protocol data compared to thinking [83], and be sensitive to subjective factors as the process of coding protocol data into logical and semantic episodes usually depends on experts' knowledge and options. Different from protocol analysis, biometric measures are able to address the limitations of protocol analysis through directly and objectively inferring designers' brain activities in design creativity.

2.4.1 EEG

EEG is a widely used biometric technique for cognitive science through measuring brain activities. EEG is the record of the fluctuation of brain waves generated by the neuron circuit. EEG signals directly measure 'the dynamic, synchronous polarization of spatially aligned neurons in extended grey matter networks, with post synaptic excitatory or inhibitory potentials being the main sources of the signal' [84]. The signals measured in voltage can be seen as a result of 'the process of current flow through the tissues between the electrical generator and the recording electrode, which is called volume conduction' [85]. The two most important effects of volume conduction imply that: (i) an electrode at a given scalp location detects neuronal activity in simultaneously activated areas that far or near the electrode and (ii) a single source activity affects all scalp electrodes simultaneously leading to high correlation among multichannel EEG signals. This implication gives rise to an inverse problem in the EEG source localization that localizes the electrical activity in

the brain according to EEG topographies. The inverse problem is that an EEG topography can be explained by different distributions of neuronal generators. However, the differences in EEG topographies might result from different distributions of activated neuronal generators.

As for the collection of EEG signals, EEG data can be collected through electrodes distributed on the scalp. The position of electrodes on the scalp follows the international 10-20, 10-10, and 10-5 systems. The "10" before "-" and "20" after "-" represent that the distances between adjacent electrodes are either 10% of the total distance between the of nasion and inion, or 20% of the total distance between the left and right of skull. The international 10-20 system has a maximum of 19 electrodes; the international 10-10 system has a maximum of 81 electrodes; the international 10-5 system has a maximum of 300 electrodes.

Each electrode placement is associated with parts of areas of the human cerebral cortex. The human cerebral cortex, which is the outermost layer of the brain, can be divided into four lobes: frontal lobe, parietal lobe, temporal lobe, and occipital lobe [86]. The frontal lobe is the largest lobe in the front of the cerebral hemispheres. The frontal lobe plays an important role in many cognitive functions, such as prospective memory, language, and personality. The posterior frontal lobe is connected to the parietal lobe, which is also located superior to the temporal lobe. The anterior parietal lobe includes the primary sensory cortex, which receives most of the sensory inputs and interprets the simple somatosensory signals. The posterior parietal lobe integrates the simple somatosensory signals into higher-order cognitive functions, such as learning and planning. The temporal lobe is located posterior to the frontal lobe and inferior to the parietal lobe. The temporal lobe has significant roles in phonological representation, sound recognition, and semantic retrieval. The occipital lobe is the smallest lobe, which is located in the most posterior region of the brain. The occipital lobe is mainly responsible for visual processing and interpretation.

Generally, EEG analysis methods can be classified into three domains: time-domain, frequency-domain, and time-frequency domain. Event-related potential (ERP) analysis in the time domain is a measure of that part of a neural response, which is consistently elicited by the stimulus through averaging EEG voltages collected from hundreds and thousands of repeated responses [87]. Two fundamental assumptions are underlying the ERP analysis: (i) the evoked potentials are invariant over trials; (2) the background EEG, such as noise, is random in each trial so that averaging techniques can remove them from EEG signals. The ERP components are key features in an ERP waveform, which are represented by polarity and temporal latency. For instance, 'the P50 component is a positive-going modulation of the ERP amplitude with a maximum voltage at about 50 ms following the onset of an auditory stimulus' [87]. The functional roles of ERP components have been well studied over the last few decades. The N100 component is associated with early stages of attention orienting [88]. The N400 component is associated with language processing and semantic memory [89].

Despite the ERP analysis has made considerable contributions to neurocognitive science, the ERP analysis is appropriate only to measure a controllable, repeatable, and reproducible neural response over an extended period of time due to the assumptions of averaging techniques. In addition, such controllable, repeatable, and reproducible neural responses should be time-locked to exogenous stimuli. For instance, the ERP analysis is appropriate to study the cognitive process of reading a single word while it is inappropriate to research the cognitive process of reading a lengthy sentence [87].

The frequency analysis focuses on event-related oscillations, which are supposed to reflect the coordinated activity of the network in large populations of neuronal [90]. A fundamental assumption underlying the frequency-domain analysis is that EEG signals consist of several oscillatory subcomponents. Each oscillatory subcomponent is thought to reflect a basic cognitive function, such as perception and attention. The integration

of oscillatory subcomponents is believed to reflect higher-order cognitive functions, such as executive functions. These higher-order cognitive functions support human complex and complicate behaviour, such as design and creativity, which is a promising direction in neurocognitive science research.

Spectral decomposition is to decompose EEG signals into evoked event-related oscillations. The evoked event-related oscillations are phase-locked to stimulus onset, meaning that the phase of the oscillation elicited by the onset of a stimulus is consistent across trials at a given time point [87]. Technically, the spectral decomposition can be implemented by computing power spectral density (PSD) of each trial. The PSD is estimates of the distribution of power of a signal over different band frequencies, such as theta band (4-7.5 Hz), alpha band (8-13.5 Hz), beta band (14-29 Hz), and gamma band (30-70 Hz). Welch's method is popularly used to estimate the PSD by applying the discrete Fourier transform (DFT) to each segmented EEG signal and then averaging the results across segments.

Event-related synchronization (ERS) is an increase in EEG power from the periods of baseline to activation, whereas event-related desynchronization (ERD) is a decrease in EEG power from the periods of baseline to activation [91]. Both ERS and ERD are time-locked to the event. The ERS reflects an increase in the synchronicity with which a group of neurons is firing during activation compared to baseline, whereas the ERD reflects a decrease in the synchronicity with which a neuronal assembly is firing during activation compared to baseline. A large number of studies revealed that ERS in alpha band is associated with creativity performance (see Fink and Benedek. 2014 for a comprehensive review [92]) and ERS in theta band is associated with cognitive control and working memory processes(see Sauseng et al., 2010 [93] and Cavanagh and Michael, 2014 for comprehensive reviews [94]).

The time-frequency analysis mainly addresses one of the limitations of frequency analysis in terms of discarding time information of EEG signals. This limitation results from

the basis of the Fourier transform that EEG waveforms in the time domain can be re-represented by a set of sinusoids whose amplitude is constant over time. Short-time Fourier transform (STFT) and discrete wavelet transform (DWT) are two popular time-frequency analysis methods to address this limitation. The STFT is an extension of discrete Fourier transform (DFT) using a Fourier transform in a series of consecutive temporal windows. These consecutive temporal windows can be overlapping or non-overlapping. Once the window size is determined, the same window is used at all times and frequencies, leading to a constant resolution over the time-frequency spectrum. This can be a problem in the case of EEG signals due to low-frequency oscillations in long windows and high-frequency oscillations in short windows [87]. The DWT is able to address some of the limitations of the STFT by 'scaled' and 'shifted' a window function called 'wavelet'(see Allen and MacKinnon, 2010 for a technical review [95]). The temporal and frequency resolution of DWT is no longer fixed by allowing the length of the wavelet to vary. Due to the time-frequency trade-off, the DWT has better temporal resolution but poorer frequency resolution at higher frequencies, as well as better frequency resolution but poorer temporal resolution at lower frequencies.

2.4.2 Neural oscillations in design creativity

With the help of the EEG technique, a large number of studies attempt to uncover brain activities during design creativity. Nguyen and Zeng (2010) preliminarily analyzed the EEG power in the design activity that was segmented into problem analysis, solution generation, solution expression, and solution evaluation [96]. The authors found that solution evaluation was associated with more mental efforts in prefrontal areas compared to other activities. The following study extended the previous work by identifying relationships between mental effort and stress during the conceptual design [97]. That study concluded that mental effort was the lowest at high-stress levels since theta, alpha, and beta power

were lower during high-stress levels compared to low-stress levels. Subsequent studies revealed that subjective rating measure was influenced by mental stress and effort during the conceptual design [98]. The time-course analysis indicated that high levels of mental effort occurred more frequently at the beginning and end of the conceptual design process [99]. Furthermore, the conceptual design process was segmented into a few semantic units, such as reading problem, designing an object on the touchpad, and adding some object to the drawing on the touchpad [100]. Compared to manual segmentation, the EEG microstate-based method have an average deviation of manual segmentations of 2 s. A recent creativity study revealed that idea evolution was associated with smaller decreases in alpha power and more activity in the DMN compared to idea generation and evaluation [39].

In addition, other advanced neuroimaging techniques, such as functional magnetic resonance imaging (fMRI) and functional near-infrared spectroscopy (fNIRS), bring higher spatial resolution of brain activities to neurocognition in design creativity. Early fMRI studies indicated that design and problem-solving tasks activated distinct brain networks being associated with distinct cognitive functions [101, 102]. In particular, compared to problem-solving, design was associated with increased activity in the right dorsolateral prefrontal cortex and recruited a more extensive network of brain areas. These findings suggested that design involves more complex cognitive functions, such as insight, evaluation, and decision-making under uncertainty. Ellamil and colleagues (2012) investigated neural correlates of idea generation and evaluation while designing a book-cover [103], which authors found that idea generation was associated with preferential recruitment of medial temporal lobe regions, while idea evaluation was related to joint recruitment of executive and default mode network regions (DMN). Design ideation was associated with greater activity in the left cingulate and the right superior temporal gyrus [104], while spontaneous ideation was associated with increased activity in the cerebellum, thalamus,

left parietal cortex, right superior frontal, left prefrontal, and paracingulate/cingulate regions [105]. Such creative ideation has been attributed to iterations of two-fold processes: generation and evaluation [106, 107]. Analogical reasoning improved the feasibility, usefulness, and uniqueness of design solutions [108]. Saggar et al. (2017) indicated that a five-week design-thinking training improved participants' improvisation-based creative capacity being associated with the reduced engagement of executive functioning regions [109]. A fNIRS study supported that design was different from problem-solving being associated with distinct brain activations [110]. Researchers also attempted to study the impact of design methodologies on distinct brain regions and coordination between brain regions [111].

2.5 Challenges in design creativity

Challenges with EEG-based design creativity are stemmed from two directions. One is related to the fundamental characteristics of the design process, while another is related to the data analysis approaches. Complexity, recursivity, and non-repetitiveness are three intrinsic characteristics of the design process. The complexity of design lies in the complex relationships among the participating basic design activities and cognitive functions. Several cognitive functions can be simultaneously involved in one basic design activity, whereas one cognitive function may contribute to different design activities. The involved cognitive functions always appear in mixed manners while interacting with each other, which constitute higher-order cognitive functions. Consequently, it is extremely difficult to separate them from each other through experiment design or during data analysis for studying one stimulus-response relationship in strictly controlled settings. The recursivity demonstrates the fact that the design problem, solution, and knowledge keep evolving interdependently and simultaneously [2, 32, 33], which stresses 'an agent's view of a world changes depending on what the agent does' [45] The recursivity implies a nonlinear dynamics process in design in which a minor difference may result in huge differences after

many rounds of evolution among the design problem, design solution, and design knowledge [58]. As a result, the non-repetitiveness of design is related to recursivity in that whatever designers do and whatever changes in the environment will all contribute to updating the initial design problem. This non-repetitiveness defies repetition/averaging based cognitive study techniques.

Protocol analysis is a widely used method to address such non-repetitiveness in design research [12, 48]. Despite a great deal of results brought by protocol analysis in design research, researchers argued that the protocol analysis approaches would interfere with mental activity [81, 82], delay protocol data compared to thinking [83], and be sensitive to subjective factors as the process of coding protocol data into logical and semantic episodes usually depends on experts' knowledge and options. For instance, Lawson found that insights are not elicited by concurrent verbalization since insights occur quickly and unexpectedly with no general rules [82]. Schooler and colleagues indicated that insights in problem-solving involve nonreportable or unconscious processes, which could be disrupted by verbalization [81]. Retrospective data has been challenged with its incompleteness and inaccurateness since one may forget the details of his her decision-making process afterwards [112].

Different from protocol analysis, neuroimaging techniques, such as EEG, could address the limitations of protocol analysis through directly and objectively inferring designers' brain activities. EEG techniques have made considerable contributions to understanding brain activities, which can be borrowed to study neurocognition during design creativity. A strictly controlled experiment is widely used to observe the effects of stimulus on brain response with control of all extraneous variables, which provides a reliable approach to identifying repeatable causal relations between a stimulus and a response [34]. However, such an experiment setting cannot be used to study design creativity since designers need time and freedom to incubate creative solutions, which involves activities such as reframing

and mind wandering [39,113]. In addition, due to design recursivity, strictly controlled settings itself will become a critical independent factor to influence the design results through changing designer's perception of the design problem.

Data analysis approaches can be considered as another challenge in design creativity. The ERP and ERD/ERS analyses, which are widely used methods in neurocognitive science, are not appropriate to analyze EEG signals collected from design creativity. The assumption regarding average and time-lock in the ERP and ERD/ERS can not be satisfied due to the non-repetitiveness of the design process. In addition, the ERP and ERD/ERS analyses have not taken full advantage of multi-channel EEG signals due to neglecting the multivariate characteristics of these measurements, such as the spatial configuration of electric fields at the scalp.

Chapter 3

Loosely controlled experiment supported by EEG microstate analysis

3.1 Loosely controlled experiment

A loosely controlled experiment seems to outperform a strictly controlled experiment by avoiding many controls during the experiment [15]. Table 1 shows comparisons between strictly and loosely controlled experiments. With fewer controls, the design process could be simulated and analyzed in a more natural way compared to strictly controlled experiments. The loosely controlled experiment can be designed by extending response time and integrating thinking and drawing phases. Under this loosely controlled setting, participants are given sufficient freedom to complete the given task in their own way without any interruption or interference. In this way, the characteristics of design creativity could be better modeled as essential to allow participants' naturally exploring possible solutions and generating creative solutions. At the same time, the loosely controlled experiment should main a certain degree of control. A basic principle of loosely controlled experiment for studying design creativity is to 'ensure the emergence of regularities related to the phenomena under observation while applying minimum controls' [15].

The loosely controlled experiment would increase the difficulties of data analysis. EEG signals collected from the loosely controlled experiment are unstructured and not time-locked. The unstructured EEG signals result from not controlling when and where a stimulus and its response happen. As a result, causal relationships between a stimulus and its response are complex and hidden. A stimulus may trigger many responses, while a response may be triggered by many stimuli. Such causal relationships are not always observable since a stimulus may keep changing over time, and its response may be delayed. For instance, an insight moment may be originated before that moment and be influenced by many previous states.

EEG data collection under the loosely controlled experiment is the same as that under the strictly controlled experiment. EEG data are collected under the loosely controlled experiment while designers are asked to solve a design problem, such as solution generation and solution evaluation. Meanwhile, behavioural data are also collected, including sketches, head and body movements, facial expressions.

Table 1: Comparison between strictly and loosely controlled experiments

Experiment name	Stimulus	Causal relation	Completion time	Ecological validity
Strictly controlled experiment	Simple task	Explicit	Fixed to a few seconds	Low
Loosely controlled experiment	Complex task	Implicit	Self-paced	High

3.2 EEG microstate

To support the loosely controlled experiment, EEG microstate analysis appears to be a compelling approach for its capability to segment the unstructured EEG signals into a set of semantic microstates. Different from averaged-based techniques, such as ERP and TRP, the semantic microstates are not time-locked. Each microstate reflects activity in the distributed and large-scale brain networks whose configurations of the scalp potential field remain quasi-stable during successive short time periods [114]. These EEG-defined

large-scale brain networks are closely associated with resting-state networks using fMRI [84]. Particularly, a large number of studies consistently found four EEG microstate classes A, B, C, and D during wakeful rest and sleep. Microstate class A is supposed to reflect verbalization in auditory networks; microstate class B is supposed to reflect visualization in visual networks; microstate class C is supposed to reflect activities in control networks; microstate class D is supposed to reflect activities in dorsal attention networks [115].

Pascual-Marqui and colleagues added several features to K-means to extract EEG microstate classes, namely modified K-means [116]. Considering a 2-D plan in which x- and y-axes represent the electric potential measurements of two electrodes, 'a brain microstate is characterized by the coordinate vector of a point located at unit distance from the origin. All points lying on the line going from the origin toward the microstate belong to the same microstate. The distance from the origin to a point on this line is directly related to the intensity of the neuronal generators corresponding to this microstate, and is also directly related to the global field power (GFP)' [116]. There are a few differences between K-means and modified K-means. On a practical level, the spatial configuration of microstates is polarity invariant since neural oscillations in the brain result in polarity invariant of the scalp potential filed [84]. At a conceptual level, microstate classes are considered as directions in a multi-dimensional topographical space [117].

There are various methods to extract EEG microstate classes, such as atomize and agglomerate hierarchical clustering (AAHC) [118], principle component analysis (PCA) [119], and independent component analysis (ICA) [120]. AAHC is a specialization of hierarchical clustering to extract EEG microstates since it is able to retain short-duration periods of stable topography, which contribute a high global explained variance (GEV). Compared to modified K-means, AAHC is a deterministic algorithm in that its results do not vary from repetitions under the same dataset, while AAHC takes into account GFP. The higher GFP means higher stability of spatial configuration of EEG microstates [84].

AAHC costs a huge amount of time compared to modified K-means. However, Wegner and colleagues indicated that the statistical and information-theoretical properties of EEG microstate sequences are invariant no matter which algorithms are used to extract EEG microstates [121]. These invariant results deliver positive messages: (i) the intrinsic characteristics of EEG microstates do not rely on computations algorithms; (ii) the results obtained from different computations algorithms are comparable.

Once EEG microstate classes are determined, original EEG signals are mapped to EEG microstate classes. A momentary EEG map at a time point is assigned to one of EEG microstate classes when their spatial correlation is the highest compared to other EEG microstate classes. This mapping procedure applies the winner-take-all strategy, which is supported by functional theories. Functional theories assume that only a global functional state occurs at any given moment in time [122, 123]. Under this assumption, it is observed that each microstate class remains quasi-stable from 60 ms to 120 ms before rapidly transitioning to a distinct microstate, which remains quasi-stable again. This observation entails important conclusions in terms of temporal organization of functional brain networks: if brain activity of EEG microstate class is trigged by a network of approximately simultaneously active sources, these different sources must display the approximately same temporal dynamics over a certain duration [84]. Otherwise, the quasi-stable microstate classes would not be observed since differences in the time course of these sources would lead to continuous changes of the spatial configuration of microstate classes [84].

After the fitting-back procedure, a few parameters of EEG microstates can be calculated to reflect activities of neural assemblies. Duration, coverage, and occurrence are typically parameters to describe the temporal properties of EEG microstates. For instance, duration is the average lifespan of EEG microstates that remain stable. This parameter reflects the average amount of time that a set of neural assemblies remains active at the same time. In addition, if EEG microstates represent the atoms of thought, EEG microstate sequences

would reflect the time-course the thought flow. The transitions of microstates are capable of measuring such time-course the thought flow.

3.3 Data analysis approaches

Data pre-processing, task-related power analysis, EEG microstate analysis, and EEG microstate sequences analysis constitute data analysis approaches. Chapters 4 and 5 will use these approaches to analyze the EEG signals collected from loosely controlled experiments of design creativity.

3.3.1 Data pre-processing

The EEGLAB toolbox was used to reduce noise and remove artefacts from the EEG signals [124]. After acquisition, A one-pass zero-phase Hamming windowed-sinc FIR filter between 1 and 40 Hz was applied to the EEG signals. Second, bad global channels of the EEG signals were detected and isolated when one or more criteria were satisfied: a channel was flat for more than 5 seconds; a correlation between a channel and its nearby channels is smaller than 0.8; and a channel's amplitude was greater than 3 standard deviations from the mean. Third, eye-blink, eye-movement, muscle-generated, and other artefacts were removed using the multiple artifact rejection algorithm (MARA) when IC components had more than 40% chance to be labelled as artefacts. Fourth, the EEG signals were segmented into 2-second epochs, with the aim to detect bad segments and bad local channels within segments [125]. Bad local channels in each segment were detected using FASTER [126] criteria (variance, median gradient, amplitude range, and deviation from mean amplitude) when one or more Z scores of four criteria were greater than 3 standard deviations from the mean. The detected bad local channels were interpolated using spherical splines. Next, bad segments were rejected when one or more criteria were satisfied: a channel' amplitude

was higher than ± 100 microvolts; the single electrode probability across segments or the electrode group probability within segments was greater than 3 standard deviations from the mean. Finally, the isolated bad global channels were interpolated using spherical splines. The cleaned EEG signals were re-referenced to average reference and were downsampled to 250 Hz.

3.3.2 Task-related power analysis

The power spectral density ($\mu V^2/Hz$) of EEG signals was estimated by Welch's method with a time window of 500 sample points and 250 sample points overlap between neighbouring time windows. The power ($\mathrm{Pow}, \mu V^2$) of EEG signals was estimated by the composite trapezoidal rule in the theta band (4-7.5 Hz), alpha band (8-13.5 Hz), lower alpha band (8-10 Hz), upper alpha band (10-12Hz), and beta band (14-29 Hz) [127]. The task-related power (TRP) was computed in each channel (i) based on the formula $\mathrm{TRP_i} = \mathrm{Log}(\mathrm{Pow_{i,activation}}) - \mathrm{Log}(\mathrm{Pow_{i,reference}})$. It means that the estimated log-power during the rest was subtracted from the estimated log-power during each design activities [91]. The condition-wise TRP was computed by averaging TRP across runs of the same condition. Positive TRP values reflect power increases from the rest to the design activities, whereas negative TRP values reflect power decreases from the rest to the design activities.

To compare with the previous studies, the condition-wise TRP values at 63 electrodes were grouped into the five cortical areas (frontal, central, temporal, parietal, and occipital) and two hemispheres (left and right) [113]. In the left hemisphere, the areas were defined as follows, frontal: Fp1, AF3, AF7, F1, F3, F5, F7, FC1, FC3; central: FC5, C1, C3, C5; temporal: FT7, T7, TP7, CP5, P5; parietal: CP1, CP3, P1, P3; and occipital: PO3, PO7, P7, O1. In the right hemisphere, the corresponding even-numbered electrodes were included.

Statistical analyses were performed on the design activities considering the selected five

cortical areas in each hemisphere. The TRP changes were analyzed by a repeated measures ANOVA with the three within factors CONDITION, AREA (frontal, central, temporal, parietal, and occipital), and HEMISPHERE (left and right). Post-hoc comparisons of the TRP changes at AREA were performed with the Bonferroni correction between CONDITION. The Greenhouse-Geisser correction was applied in the case of sphericity violations.

3.3.3 EEG microstate analysis

The modified k-means clustering algorithm was applied to identify the microstate classes [116]. Firstly, for each run, each participant, and each condition, the Global Field Power (GFP) of EEG signals was calculated based on Eq. (1). The GFP is the standard deviation of the potentials across all electrodes at a given time point. Secondly, the EEG signals at GFP peaks were submitted to the modified k-means algorithm, which was run 100 times for cluster number $k = 2 \dots 10$. Thirdly, the microstate classes were determined by minimizing the cost function defined in Eq. (2). The optimal microstate classes were selected among 100 repetitions based on minimum cross-validation as shown in Eq. (3). Fourthly, the group-wise microstate classes were determined by the full permutation procedure applied to the subject-wise microstate map across runs, participants, and conditions [128].

$$GFP = \sqrt{\frac{\sum_{i=i}^{N_S}(u_i - \overline{u})^2}{N_S}}, \tag{1}$$

$$F = \frac{1}{N_T(N_S - 1)} \sum_{t=1}^{N_T} ||V_t - \sum_{k=1}^{N_K} a_{kt}\Gamma_k||^2, \tag{2}$$

$$CV = \frac{\sum_{t=1}^{N_T}(V_t' \cdot V_t - (V_t' \cdot \Gamma_k)^2)}{N_T(N_S - 1)} \cdot (\frac{N_S - 1}{N_S - 1 - N_K})^2, \tag{3}$$

In Equations 1-3, u_i is the electric potential of the EEG signals u at the electrode i, $\overline{u}$ is the average electric potential of all electrodes of the EEG signals u and N_S is the number of

electrodes of the EEG signals u. N_T is the sample length . V_t is a $N_S \times 1$ vector consisting of the electric potential at time instant t. N_K is the number of microstate classes. Γ_k, which is a normalized $N_S \times 1$ vector, represents the k-th microstate class. a_{kt} is the intensity of the k-th microstate class at the time instant t. Once the global microstate classes are determined, they were fitted back to the individual EEG signals in the time domain to generate the microstate sequences. Each time point of individual EEG signals was assigned into one of the global microstate classes when they have the highest spatial correlations. In the fitting process, the polarity of global microstate classes was ignored since the same neural generators may result in the inversion of scalp potential field. To avoid modifications of temporal dynamics of microstate sequences, we did not apply any criteria to smooth the microstate sequences, such as the minimum duration of microstates. For each run, for each participant, for each condition, and for each microstate class, the following microstate parameters were calculated:

- mean microstate duration: the average lifespan or duration that a microstate remains stable. The microstate duration can be interpreted as the average amount of time that a set of neural generators remains synchronously active.

- mean microstate occurrence: the average number of times that a microstate occurs per second. The mean microstate occurrence can be interpreted as the average amount of times that a set of neural generators becomes synchronously active.

- mean microstate coverage: the fraction of the total analysis time covered by a microstate. The microstate coverage can be interpreted as the relative rather than absolute presence of a microstate.

3.3.4 EEG microstate sequence analysis

A finite estimate of the entropy rate [129], autoinformation function (AIF) [130], and Hurst exponent estimated by detrended fluctuation analysis (DFA) [131] were applied to measure the short-range, intermediate-range, and long-range temporal dependencies of microstate sequences within each run of conditions.

Firstly, the finite estimate of the entropy rate of microstate sequences was calculated based on Eq. (4)

$$\begin{aligned} h_X(t,k) &= H(X_{t+1}|X_t^{(k)}) \\ &= H(X_{t+1}, X_t^{(k)}) - H(X_t^{(k)}) \\ &= H(X_{t+1}^{(k+1)}) - H(X_t^{(k)}) \end{aligned} \tag{4}$$

where X_{t+1} represents the next symbol of the microstate sequences, while $X_t^{(k)}$ represents the past k values of the microstate sequences. $H(\cdot)$ represents joint entropy, while $H(\cdot|\cdot)$ represents conditional entropy. We used the logarithm to the base 2 for all entropy calculations, resulting in a unit of bits per sample for entropy rates.

Secondly, the AIF of microstate sequences was calculated based on Eq. (5).

$$\begin{aligned} I(\tau) &= H(X_{t+\tau}) - H(X_{t+\tau}|X_t) \\ &= H(X_{t+\tau}) + H(X_t) - H(X_t, X_{t+\tau}) \end{aligned} \tag{5}$$

Thirdly, the Hurst exponent of microstate sequences was estimated by DFA. Microstate sequences were first mapped into the metric space $S_0 = \{-1, +1\}$ [132]. If the number of microstate classes is 7, we can use partitions into one set of 3, and another one containing 4 microstate classes ($\{\{A, B, C\}, \{D, E, F, G\}\}$, for instance). In total, we can obtain 35 different partitions and analyzed the arithmetic average of their DFA estimated Hurst exponent. Each microstate belonging to the first component of the partition was mapped to -1, microstates from the second component to +1, to the effect that each microstate

sequence was mapped to the $\{-1, +1\}$ state space.

Based on the mapped microstate sequence x', the partially integrated sequence $y(t)$ was calculated based on Eq. (6). Then, the partially integrated sequence $y(t)$ was segmented into windows of various sizes $\triangle n$ that were logarithmically spaced on a scale between four samples and N_T samples. In each segmentation with $\triangle n$ samples, the linear trend $y_{\triangle n}(t)$ of integrated $y(t)$ was estimated by a least-squares fit, while the mean-squared residual between $y(t)$ and $y_{\triangle n}(t)$ was calculated based on Eq. (7). The fluctuation was calculated through averaged $F(\triangle n)$ across all identically sized windows. Thus, the Hurst exponent was estimated by the slope of the fluctuations on the various window size.

$$y(t) = \sum_{m=1}^{t} x'(m) - \overline{x}', t \in [1, N_T] \tag{6}$$

$$F(\triangle n) = \sqrt{\frac{1}{\triangle n} \sum_{t=1}^{\triangle n} [y(t) - y_{\triangle n}(t)]^2} \tag{7}$$

Chapter 4

Network oscillations in design creativity

4.1 Introduction

Recent neurocognitive research aims to understand the neurophysiological mechanism of the basic activities underlying design creativity, as reviewed in section 2.4.2. Similar efforts were made in creativity. A recent special issue in a neuroimaging journal published state of the art concerning neurocognitive creativity [133]. Many EEG studies indicated that increases in alpha power over frontal and temporo-parietal sites are associated with idea generation during alternative uses tasks (AUT) (see Fink and Benedek, 2014 [92] for a comprehensive review). The time-course studies indicated that idea generation was characterized as a U-shaped function of alpha power changes [134–136]. Differently, the generation of the first idea was associated with alpha desynchronization, whereas the generation of more ideas was associated with synchronization [113]. In addition, idea evaluation was associated with increases in alpha power, which has positive effects on the originality of idea generation [137]. Beyond idea generation and evaluation, idea elaboration that refines a previously generated idea was associated with increases in upper alpha power over parietal and occipital sites and increases in functional coupling [138, 139].

However, interactions among the basic activities and how they form the complex phenomena comprising design creativity are still unknown. Along with similar thoughts, Fink and Benedek identified three main challenges for creativity research [92]: (i) Conceptual models of creativity need to be clarified to distinguish creativity from classic mental abilities and to decompose the construct of creativity into definable neurocognitive processes; (ii) Integration of structural and functional methods need to be developed to identify the definable neurocognitive processes during creative thinking; and (iii) Studying more complex and real-life creativity.

To investigate such the complex phenomena comprising design creativity, we applied a loosely controlled experiment to simulate the interactions among basic activities in design creativity, including idea generation, idea evolution, and rating idea generation and evolution. Participants were given considerable freedom regarding response time (up to 3 minutes) and response action (integrating thinking and drawing phases) to freely explore and generate potentially creative solutions. To test the effectiveness of loosely controlled experiment, we investigated the regional contribution of brain oscillations in the alpha band through TRP analysis. In addition, we applied EEG microstate analysis to structure and segment unstructured EEG signals collected from the loosely controlled experiment. The structured EEG signals can be represented by a few EEG microstate classes, which are associated with functional brain networks.

During idea generation, participants were expected to use their experience to simultaneously and intuitively generate an idea, which may not invoke creative thinking in participants. During idea evolution, participants were expected to generate novel, useful, and surprising ideas that were radically different from the previous ideas. Idea evolution is a recursive process during which the goal, knowledge, and idea co-evolves through interactive applications of divergent and convergent thinking [2, 3, 32, 33, 58]. Idea evolution is distinct from idea elaboration [138], in which participants are instructed to elaborate and

refine an existing idea to form a part of the final solution. Idea generation and idea evolution can be viewed as two parallel approaches to dealing with a sketch stimulus, which are two independent methods to approaching a creative problem, whereas idea generation and idea elaboration are two steps of creative idea generation. Of note, rating idea generation and evaluation implied an evaluative process in which participants were asked to evaluate the difficulties of those two processes.

We hypothesized that decreases in alpha power would be significantly lower during idea evolution compared to idea generation and rating activity. In addition, we hypothesized that microstate properties would be significantly different between rest and the three modes of thinking, as well as between idea generation, idea evolution, and rating activity.

4.2 Method

4.2.1 Experiment Design

The objective of this experiment was to provide a degree of freedom to simulate the flexible nature of design creativity in three modes of thinking: idea generation, idea evolution, and rating activity. Not only basic design creativity activities but also interactions between them were simulated to form creativity. Adapted from the TTCT-F test and a work regarding sketch evolution [26], the experiment included three conditions: idea generation, idea evolution, and rating activity [140]. A run included idea generation, idea evolution, and rating activity sequentially, which was repeated three times. Three stimuli (see Figure 1A) were given at the beginning of idea generation for the three runs, respectively. Therefore, the experiment consisted of three runs and three conditions within each run.

During idea generation, participants were instructed to complete an incomplete sketch regarding how they had intuitively perceived the image at first sight. During idea evolution, participants were instructed to complete a sketch that was radically distinctive from what

was immediately triggered by the sketch stimulus. During rating activity, participants were instructed to evaluate difficulties of thinking and drawing during idea generation and idea evolution. The duration of each condition was self-paced up to three minutes. Rest was placed at the beginning and end of the experiment, which lasted three minutes. Figure 1B shows an example of the first stimulus of idea generation followed by idea evolution and rating activity.

4.2.2 Participants and experiment procedure

Twenty-nine graduate students participated in this experiment from the Concordia Institute for Information Systems Engineering, Concordia University. Participants were offered a small gift card (a value of CAD$15) to show appreciation for their volunteering in the study after the experiment was completed. Participants were excluded from data analysis in the case of extremely noisy EEG recording. The final sample included 28 participants (4 women, 24 men) aged from 22 to 35, right-handed. All participants had normal or corrected-to-normal vision and did not report any history of medical, psychiatric disorders or treatments that could interfere any of the behavioural and neurophysiological measures. The experimenter helped participants wear EEG cap, ECG belt, respiration rate belt, and GSR finger strap. After being briefed on what to do and the impedances of all the EEG electrodes were below 10 kΩ, the participant completed the experiment by following the experimental procedures specified in the previous subsection. During the experiment, EEG signals were recorded by a 64 channel BrainVision actiCHamp at 500 Hz. EEG was referenced to Cz, and the electrode placement was based on the international 10-10 system. Body movements, the monitor, and the subjects' sketch pad were also captured (Figure 2). This experimental protocol was approved by the Concordia Human Research Ethics Committee. All sections of the experiment were performed in accordance with relevant guidelines and regulations. Informed consent was obtained from all participants.

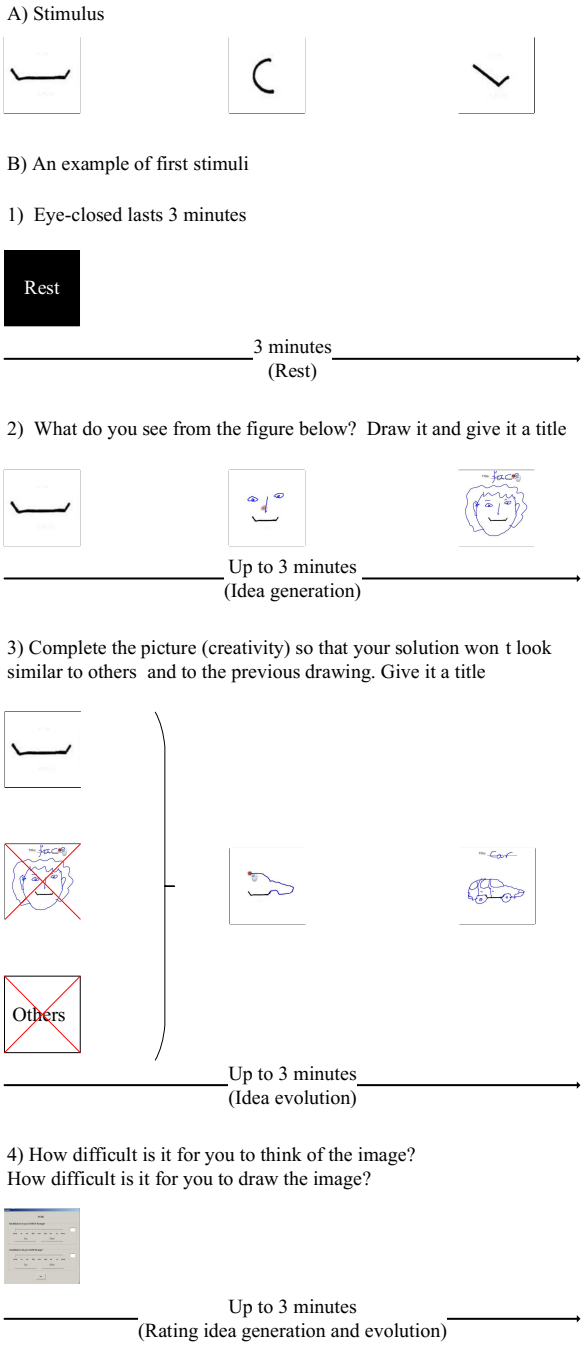

Figure 1: A) Three different stimuli. B) The first stimulus of schematic time courses of the modified TTCT-F. 1) A 3-minute rest period served as the baseline. 2) A maximal 3-minute idea generation period refers to an activation state. 3) A maximal 3-minute idea evolution period refers to an activation state. 4) A maximal 3-minute rating period served as an activation state and a breaking fixation state.

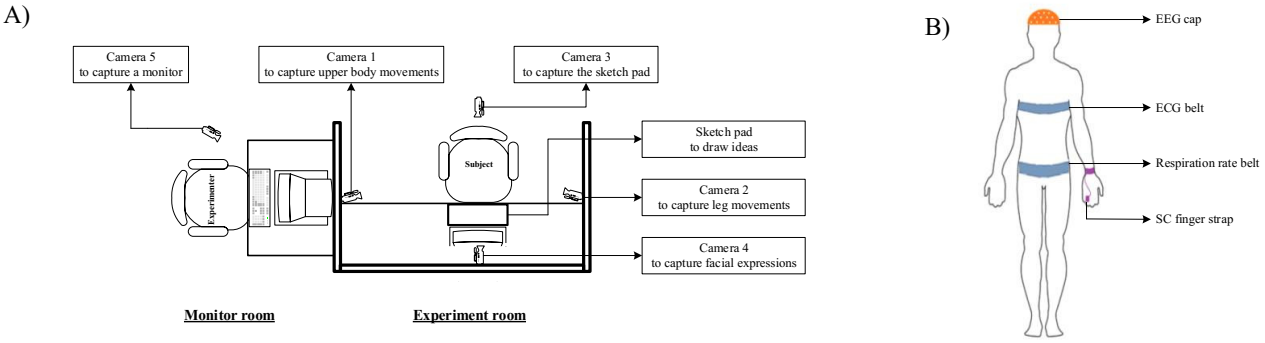

Figure 2: A) View of the experimental configuration adapted from Nguyen and Zeng (2014) with copyright permission from Elsevier. B) Configuration of the devices.

4.3 Results

4.3.1 Behavioural results

Task completion time was 54.047 s (SE=4.441) for idea generation (IG), 92.785 s (SE=5.192) for idea evolution (IEV), and 16.476 s (SE=1.089) for rating idea generation and evolution (RIGE). To test whether task completion time among participants was significantly different for similar tasks, task completion time of each run of similar tasks was normalized. Repeated measures ANOVA indicated that task completion time among participants was significantly different for IEV ($F(2, 54) = 4.762, p = 0.012, \eta_p^2 = 0.150$), but was not significantly different for IG ($F(2, 54) = 2.339, p = 0.106, \eta_p^2 = 0.080$) or RIGE ($F(1.570, 42.398) = 1.286, p = 0.285, \eta_p^2 = 0.045$). A post hoc paired t-test revealed that task completion time decreased significantly from the first run to the second run of IEV ($t(27) = 2.518, p = 0.018, 95\%C = [0.282, 0.277]$), whereas task completion time increased significantly from the second run to the third run of IEV ($t(27) = -2.562, p = 0.016, 95\%C = [-0.292, -0.032]$). However, task completion time was not significantly different between the first and third runs of IEV ($t(27) = -0.185, p = 0.855, 95\%C = [-0.117, 0.980]$).

To test whether task completion time among participants was significantly different for

different tasks, task completion time of all tasks was normalized and averaged within IG, IEV, and RIGE, respectively. Repeated measures ANOVA indicated that task completion time among participants was significantly different amid IG, IEV, and RIGE ($F(2, 54) = 69.554, p < 0.001, \eta_p^2 = 0.720$). A post hoc paired t-test revealed that task completion time decreased significantly from IEV to IG ($t(27) = 5.805, p < 0.001, 95\%C = [25.046, 52.429]$) and RIGE ($t(27) = 11.811, p < 0.001, 95\%C = [63.052, 89.566]$), as well as from IG to RIGE ($t(27) = 5.991, p < 0.001, 95\%C = [24.705, 50.738]$).

4.3.2 EEG results

EEG alpha power

In the lower alpha band (8-10 Hz), the $3 \times 5 \times 2$ repeated measures ANOVA revealed three significant main effects, including CONDITION ($F(1.291, 34.860) = 8.373, p = 0.004, \eta_p^2 = 0.237$), AREA ($F(1.952, 52.693) = 40.390, p < 0.001, \eta_p^2 = 0.599$) and HEMISPHERE ($F(1.000, 27.000) = 5.383, p = 0.028, \eta_p^2 = 0.166$), as well as one significant interaction effect for CONDITION $\times$ AREA ($F(4.358, 117.658) = 3.199, p = 0.013, \eta_p^2 = 0.106$).

A post hoc test with Bonferroni correction on the main effect, CONDITION, indicated that decreases in alpha power were significantly lower during IEV compared to IG ($p < 0.001$) and RIGE ($p = 0.008$). For the main effect HEMISPHERE, decreases in alpha power were significantly lower over left hemispheric sites compared to right hemispheric sites ($p = 0.028$). For the main effect AREA, decreases in alpha power were significantly lower at frontal sites compared to temporal ($p < 0.001$), parietal ($p < 0.001$), and occipital sites ($p < 0.001$). Decreases in alpha power were significantly lower at central sites compared to temporal ($p < 0.001$), parietal ($p < 0.001$), and occipital sites ($p < 0.001$). Decrease in alpha power were significantly lower at temporal sites compared to parietal ($p = 0.017$) and occipital sites ($p < 0.001$). Decreases in alpha power were significantly

lower at parietal sites compared to occipital sites ($p = 0.002$). For the interaction effect CONDITION $\times$ AREA, decreases in alpha power were significantly lower during IEV compared to IG at frontal ($p = 0.017$) central ($p = 0.002$), temporal ($p < 0.001$), parietal ($p = 0.004$), and occipital ($p = 0.006$) sites. Decreased alpha power was significantly lower during IEV compared to RIGE at frontal ($p = 0.005$), central ($p = 0.010$), temporal ($p = 0.002$), and parietal ($p = 0.010$) sites (see Figure 3).

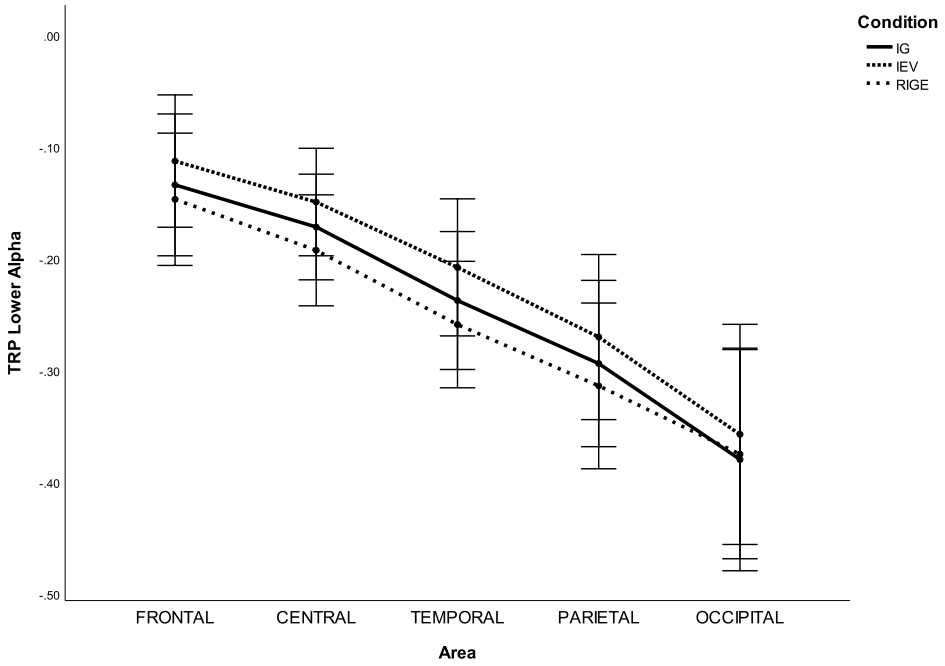

Figure 3: Error bars of task-related alpha power in lower alpha band (8-10 Hz) during idea generation (IG), idea evolution (IE), and rating idea generation and evolution (RIGE).

In the upper alpha band (10-12 Hz), the $3 \times 5 \times 2$ repeated measures ANOVA uncovered one significant main effect, AREA ($F(1.782, 48.111) = 7.733, p = 0.002, \eta_p^2 = 0.223$), as well as one significant interaction effect, CONDITION $\times$ AREA ($F(2.980, 80.470) = 4.139, p = 0.009, \eta_p^2 = 0.133$).

A post hoc test with Bonferroni correction on the main effect AREA indicated that decreases in alpha power were significantly higher at parietal sites compared to frontal ($p = 0.021$), central ($p = 0.040$), and temporal sites ($p < 0.001$). In contrast, decreases

in alpha power were significantly lower at temporal sites compared to occipital sites ($p = 0.012$). For the interaction effect CONDITION $\times$ AREA, decreases in alpha power were significantly lower during IEV compared to RIGE at central sites ($p = 0.086$) (see Figure 4).

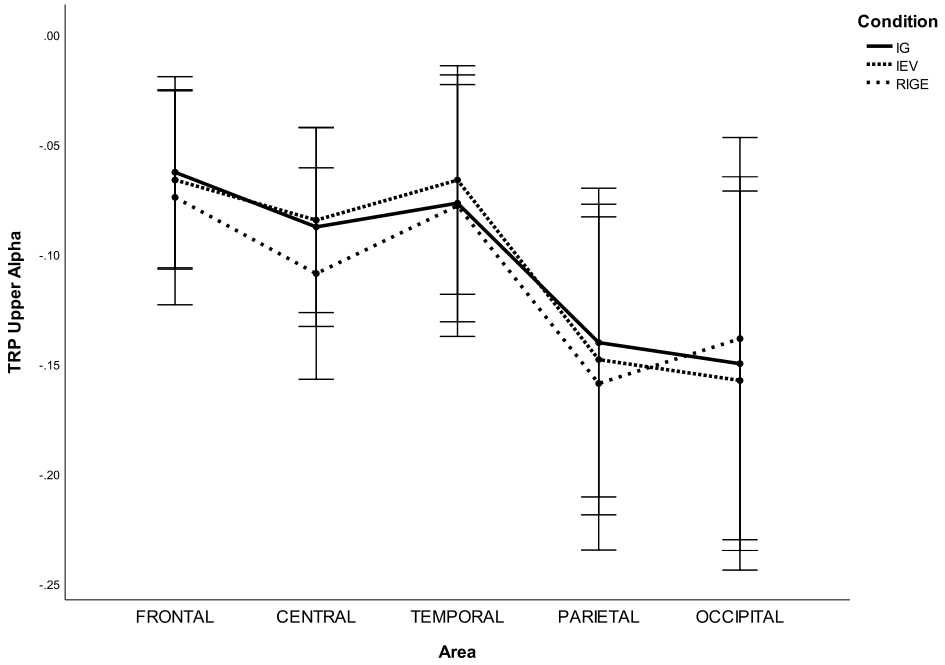

Figure 4: Error bars of task-related alpha power in upper alpha band (10-12 Hz) during idea generation (IG), idea evolution (IE), and rating idea generation and evolution (RIGE).

EEG microstate classes

According to cross validation, the optimal number of individual microstate classes was found to be 6.464 ($SE = 0.166$) for REST, 6.250 ($SE = 0.152$) for IG, 6.285 ($SE = 0.168$) for IEV, and 6.857 ($SE = 0.199$) for RIGE. Therefore, the number of individual microstate classes was defined as six for each run, each condition and each participant due to the comparability and simplicity of statistical analysis.

The six individual microstate classes explained 62.97% ($SE = 1.111$) of the global variance of the original EEG topographies corresponding to peaks of GFP for REST,

60.87% ($SE = 1.150$) for IG, 61.01% ($SE = 1.108$) for IEV, and 61.46% ($SE = 1.129$) for RIGE. Figure 5 showed condition-wise EEG microstate classes and global-wise EEG microstate classes. The microstate classes A, B, C, D, E, and F were labelled and sorted according to the literature [84, 141].

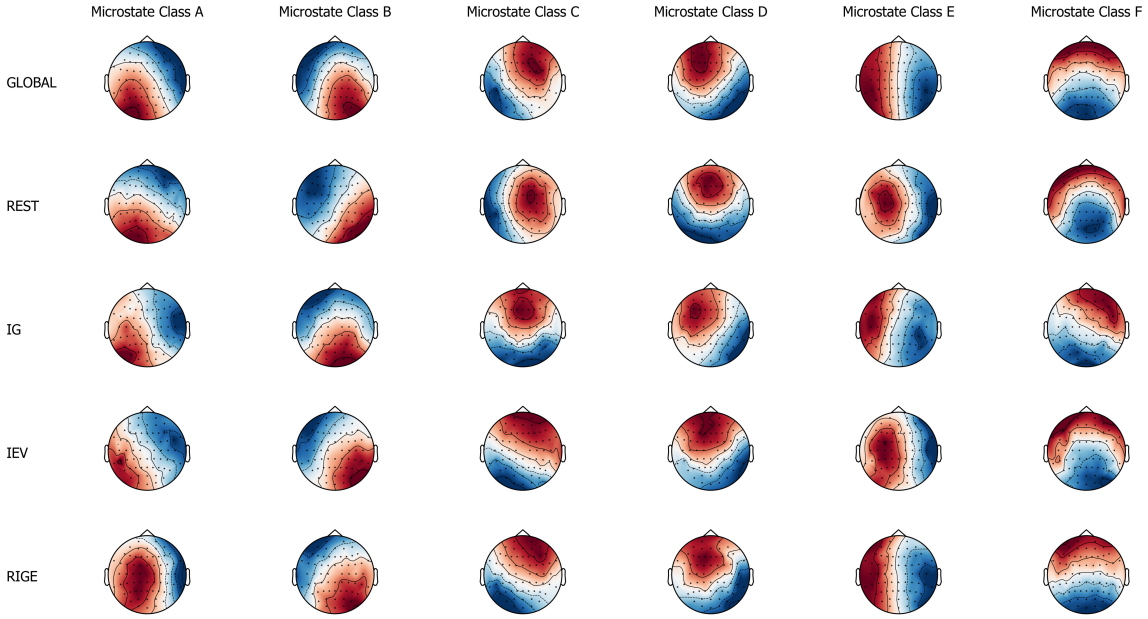

Figure 5: The spatial configuration of the six microstate classes (A, B, C, D, E, and F) for across conditions (global) and within conditions (rest (REST), idea generation (IG), idea evolution (IEV), and rating idea generation and evolution (RIGE)).

EEG microstate topographies

The 4×6 TANOVA revealed a significant main effect, CLASS ($p < 0.001$). Neither the main effect CONDITION ($p = 0.066$) nor the interaction effect CONDITION $\times$ CLASS ($p = 0.804$) were significant.

Class-wise TANOVAs revealed a significant effect, CLASS C ($p = 0.041$). Effects CLASS A ($p = 0.838$), CLASS B ($p = 0.610$), CLASS D ($p = 0.740$), CLASS E ($p = 0.383$) and CLASS F ($p = 0.125$) were not significant.

Paired t-test revealed a significant effect CLASS C between REST and the three modes

of thinking: IG ($p = 0.040$), IEV ($p = 0.041$) and RIGE ($p = 0.025$), as well as a significant effect, CLASS A, between IEV and RIGE ($p = 0.014$) (see Table 2).

Table 2: P-values of pairwise comparison for microstate topography between CLASS (A, B, C, D, E and F) and CONDITION (rest (REST), idea generation (IG), idea evolution (IEV), as well as rating idea generation and evolution (RIGE))

Conditions			Microstate classes					
			Class A	Class B	Class C	Class D	Class E	Class F
REST	Vs.	IG	0.359	0.545	0.040*	0.707	0.137	0.153
REST	Vs.	IEV	0.257	0.317	0.041*	0.438	0.275	0.625
REST	Vs.	RIGE	0.136	0.381	0.025*	0.568	0.157	0.137
IG	Vs.	IEV	0.131	0.747	0.368	0.438	0.749	0.104
IG	Vs.	RIGE	0.733	0.476	0.879	0.800	0.946	0.305
IEV	Vs.	RIGE	0.014*	0.815	0.330	0.664	0.726	0.215

* $\rho < 0.050$, ** $\rho < 0.010$, *** $\rho < 0.005$

EEG microstate parameters

For coverage of microstate classes, the 4×6 repeated measures ANOVA revealed a significant main effect, CLASS ($F(2.609, 70.446) = 19.214, p < 0.001, \eta_p^2 = 0.416$), and a significant interaction effect, CONDITIONS $\times$ CLASS ($F(5.629, 151.984) = 7.081, p < 0.001, \eta_p^2 = 0.208$).

The paired t-test revealed that the coverage of microstate class A was lower during REST compared to IG ($p = 0.017$) and IEV ($p = 0.013$). The coverage of microstate class C was higher during REST compared to IG ($p < 0.005$), IEV ($p < 0.005$), and RIGE ($p < 0.005$). The coverage of microstate class D was higher during REST compared to IG ($p < 0.005$), IEV ($p < 0.005$), and RIGE ($p < 0.05$). The coverage of microstate class E was lower during REST compared to IG ($p < 0.005$), IEV ($p < 0.005$), and RIGE ($p < 0.05$). In particular, the coverage of microstate class C was higher during IEV compared to RIGE ($p = 0.018$). Furthermore, the coverage of microstate class F was lower during IEV compared to IG ($p = 0.015$) and RIGE ($p = 0.019$) (See Table 3 and Figure 6).

Table 3: P-values of pairwise comparison for microstate coverage between CLASS (A, B, C, D, E and F) and CONDITION (rest (REST), idea generation (IG), idea evolution (IEV), as well as rating idea generation and evolution (RIGE))

Conditions			Microstate classes					
			Class A	Class B	Class C	Class D	Class E	Class F
REST	Vs.	IG	0.017^{*}	0.853	0.001^{***}	0.002^{***}	0.001^{***}	0.217
REST	Vs.	IEV	0.013^{*}	0.722	0.001^{***}	0.010^{*}	0.001^{***}	0.845
REST	Vs.	RIGE	0.056	0.815	0.001^{***}	0.013^{**}	0.010^{*}	0.134
IG	Vs.	IEV	0.968	0.842	0.447	0.131	0.378	0.015^{*}
IG	Vs.	RIGE	0.956	0.969	0.057	0.496	0.738	0.317
IEV	Vs.	RIGE	0.976	0.894	0.018^{*}	0.862	0.277	0.019^{*}

* $\rho \leq 0.050$, ** $\rho \leq 0.010$, *** $\rho \leq 0.005$

↗ microstate coverage increases

↘ microstate coverage decreases

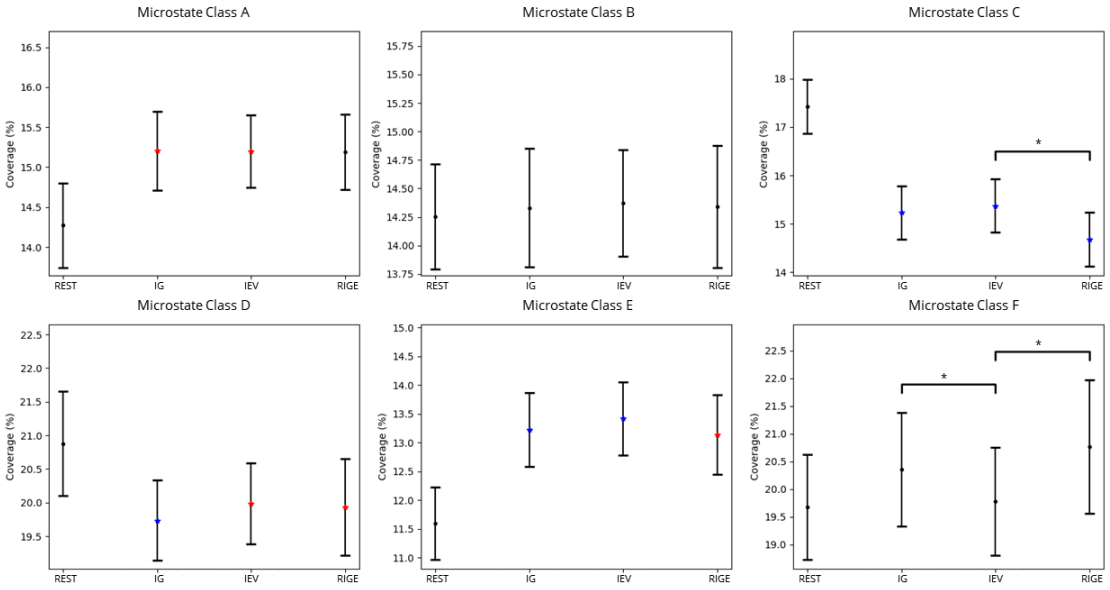

Figure 6: Error bars of microstate coverage during rest (REST), idea generation (IG), idea evolution (IE), and rating idea generation and evolution (RIGE). P-values between rest and other conditions are annotated by black dots ($p > 0.050$), blue dots ($p \leq 0.050$), yellow dots ($p \leq 0.010$), and red dots ($p \leq 0.005$). P-values between conditions are annotated by * ($p \leq 0.050$), ** ($p \leq 0.010$), *** ($p \leq 0.005$).

For duration of microstate classes, the 4×6 repeated measures ANOVA revealed a significant main effect CLASS ($F(2.443, 65.949) = 18.444, p < 0.001, \eta_p^2 = 0.406$) and a significant interaction effect CONDITION $\times$ CLASS ($F(5.967, 161.110) = 4.439, p < 0.001, \eta_p^2 = 0.141$).

The paired t-test revealed a significant effect that the duration of microstate A was lower during REST compared to IG ($p < 0.01$), IEV ($p = 0.004$), and RIGE ($p = 0.038$). The duration of microstate class C was higher during REST compared to IG ($p < 0.01$), IEV ($p < 0.005$), and RIGE ($p < 0.01$). The duration of microstate class D was higher during REST compared to IG ($p = 0.033$). The duration of microstate E was lower during REST compared to IG ($p < 0.005$), IEV ($p < 0.005$), and RIGE ($p = 0.038$). The duration of microstate class F was lower during REST compared to RIGE ($p = 0.023$). In particular, the duration of microstate class F was lower during IEV compared to RIGE ($p = 0.013$) (See Table 4 and Figure 7).

Table 4: P-values of pairwise comparison for microstate duration between CLASS (A, B, C, D, E and F) and CONDITION (rest (REST), idea generation (IG), idea evolution (IEV), as well as rating idea generation and evolution (RIGE))

Conditions			Microstate classes					
			Class A	Class B	Class C	Class D	Class E	Class F
REST	Vs.	IG	0.006^{**}	0.899	0.006^{**}	0.033^{*}	0.001^{***}	0.051
REST	Vs.	IEV	0.004^{***}	0.249	0.002^{***}	0.225	0.001^{***}	0.486
REST	Vs.	RIGE	0.038^{*}	0.904	0.006^{**}	0.780	0.038^{*}	0.023^{*}
IG	Vs.	IEV	0.154	0.213	0.661	0.238	0.533	0.082
IG	Vs.	RIGE	0.705	0.995	0.296	0.051	0.628	0.158
IEV	Vs.	RIGE	0.279	0.303	0.394	0.210	0.377	0.013^{*}

* $\rho \leq 0.050$, ** $\rho \leq 0.010$, *** $\rho \leq 0.005$
↗ microstate duration increases
↘ microstate duration decreases

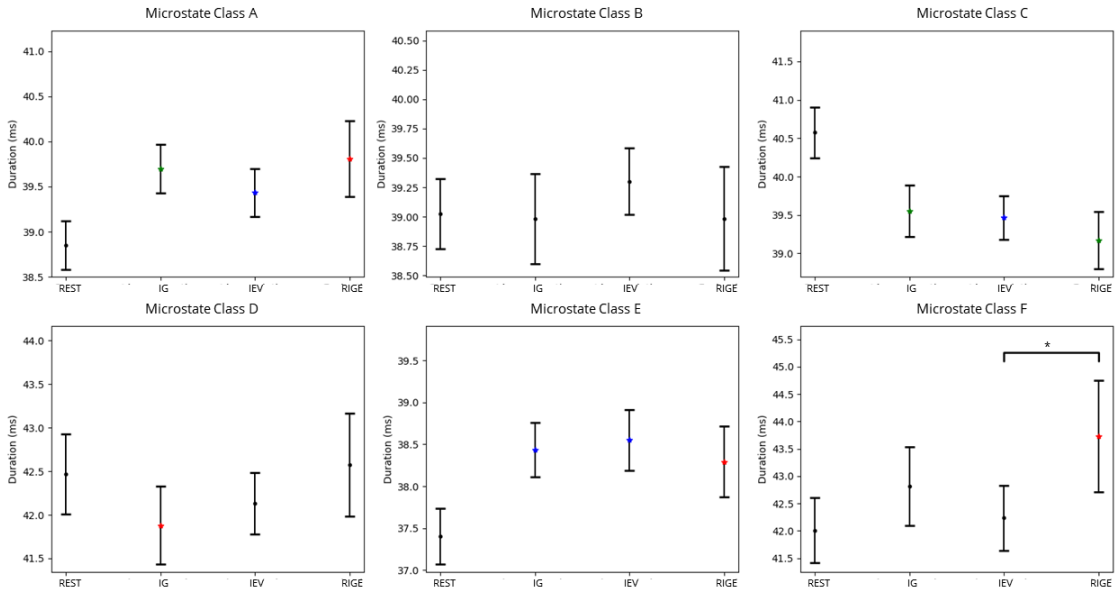

Figure 7: Error bars of microstate duration during rest (REST), idea generation (IG), idea evolution (IE), and rating idea generation and evolution (RIGE). P-values between rest and other conditions are annotated by black dots ($p > 0.050$), blue dots ($p \leq 0.050$), yellow dots ($p \leq 0.010$), and red dots ($p \leq 0.005$). P-values between conditions are annotated by * ($p \leq 0.050$), ** ($p \leq 0.010$), *** ($p \leq 0.005$).

4.4 Discussion

Herein, we present a loosely controlled creativity experiment to uncover the interactions of whole-brain neuronal networks among three modes of thinking in an ecologically valid manner. This experiment provided sufficient flexibility and duration for participants to generate potentially creative ideas while maintaining certain levels of control by structuring the entire experiment into three sections, each of which was anticipated to simulate one of the three modes of thinking. First, we observed that alpha power decreased significantly from rest to the three modes of thinking. This finding is consistent with other more structured experimental studies in that alpha power decreased from rest to visual creativity [142]. Second, microstate topographies were significantly different between rest and the three modes of thinking, as well as between idea evolution and rating activity. Third, it was found that microstate parameters were significantly different between rest and the three modes of thinking, as well as between idea generation and idea evolution and between idea evolution and rating activity. The last two findings benefited from the loose controllability of the adopted experimental design.

Why do we need a loosely controlled creativity experiment?

The behavioural results revealed that task completion time among participants was significantly different within idea evolution but was not significantly different within idea generation or within rating activity. This finding implies that the process of idea evolution is more flexible and unstructured than the processes of idea generation and rating activity. A post hoc paired t-test indicated that task completion time was significantly different between the first and second runs, as well as between the second and third runs of idea evolution. However, task completion time was not significantly different between the first and third runs of idea evolution. This finding implies that the same person may not follow a process in a similar way when generating solutions while solving similar creativity

problems. In addition, a previous experiment on the co-evolutionary creative design process indicated that different people may not arrive at the same result or follow a process similarly when they solve the same creativity problem [12].

Furthermore, task completion time for idea evolution was significantly higher compared to idea generation and rating activity. This result confirms that idea evolution may require more effort and implies more uncertainties due to its opened-ended goals and processes. Experiments reported by other researchers also confirm that a subject needs to spend more time defining and understanding a creativity problem to generate solutions recursively [12, 143].

Indeed, the process of design creativity, which is believed to be unrepeatable, irreproducible, and uncontrollable, is co-evolutionary and follows recursive logic [2, 11, 12, 144]. Recursive logic was first proposed by Zeng and Cheng (1991) to illustrate the nature of design thinking [2]. The logic was further formulated and formalized using set theory into a science-based design process model, which states that design problem, design knowledge, and design solutions evolve simultaneously in a design process [32, 33]. Given a design problem, a designer will identify the relevant knowledge to generate a tentative design solution, which will improve the designer's understanding of the design problem. This improved understanding might lead to a reformulation of the original design problem. The reformulated problem will lead the designer to identify new knowledge and to change the previous solution, which in turn leads to another reformulation of the design problem.

With a similar line of understanding, some scholars have noted the importance of recursion in the sub-phases of creativity [145, 146]. In describing the design process, Gero and Kannengiesser (2004) highlighted that an 'agent's view of the world changes depending on what the agent does' [45]. In describing the creativity process, Corazza (2019) stressed that continued exploration is a primary force driving the recursion underlying the creativity

process, while bidirectional dynamic interaction with the environment influences the recursion underlying the creativity process in terms of dynamic assessment and the emergence of unpredictable new functionalities [147]. Lubart (2001) indicated that initial ideas might interact with the developing work in a dynamic and evolving creative process [145]. Lubart also raised several key questions for future research on creativity, such as 'to what extent is the creative processes recursive?'; 'how exactly this recursion is organized?'; 'what provokes recursion?'; and 'what metacognitive functions control the choice of certain subprocesses and their recursive application?'. Nguyen and Zeng (2012) formulated the recursive design process into a nonlinear dynamic, for which a minor initial state difference may lead to huge state differences after many rounds of evolution [58]. Some of the new states can be credited as creative, whereas others can be identified as inconclusive outcomes that are not creative. The process of exploring the potentially original and effective ideas is still considered a creative process regardless of the originality or conclusiveness of the final outcome. [59]. The nonlinear design dynamics imply a mechanism of creativity, which accommodates a degree of flexibility, uncertainty and unpredictability through a structured and deterministic model of design. Since a design problem often arises from a conflict in the current environment, which includes nature, human and artefacts, design knowledge is retrieved from a subset of relationships among environment components, and a design solution is always generated by synthesizing existing objects in the environment. Therefore, the nonlinear recursive design process can be naturally viewed as an environment-evolving process. The environment evolutionary process, termed Environment-Based Design (EBD), continues until the designer determines that a design solution is satisfactory [3].

It is obvious from both the experimental and theoretical observations described above that flexibility/freedom is a fundamental need to incubate creativity through sufficient duration and open-ended tasks. The sufficient duration might induce a period of incubation and

mind wondering that could facilitate creative problem solving through relaxation, overcoming fixation, and mental set-shifting [35–38]. Open-ended tasks offer unlimited potential for participants to explore solutions without predefined solutions or strategies. The ill-defined nature of this method, which is the most important characteristic of open-ended tasks, provides a degree of uncertainty of solutions in that an intermediate solution may redefine the original task from which new tasks may emerge. Different emergent tasks will induce different knowledge and solutions, which will, in turn, redefine the original tasks.

In order to achieve statistically significant results, conventional creativity tests, which are strictly controlled, limit participants' flexibility/freedom. Dietrich (2019) observed that conventional creative tests do not have sufficient ecological validity due to the lack of considerations of multifaceted creativity [148]. Agnoli et al. (2020) also indicated that insufficient duration (15 s) might inhibit the search for originality such that a less constrained experimental setting is needed in future research [113]. Moreover, conventional creativity tests are focused on a single phenomenon of a creative process that includes idea generation, idea elaboration or idea evaluation. Zeng et al. (2011) indicated that the lack of understanding of interactions between the phenomena of a creative process is a major shortcoming of conventional creativity tests [146].

Therefore, both behavioural findings and theoretical findings have suggested that creativity needs to be studied through a loosely controlled creativity experiment. The purpose of loosely controlled creativity experiments is to encourage participants' natural characteristics of creativity in ways that can be analysed using a statistically reliable and significant approach. The loosely controlled creativity experiment concentrates on complex creativity activities, during each of which different creative phenomena are involved since it is believed that these phenomena are interdependent. Idea generation, idea evaluation, and idea elaboration, as suggested by Ellamil et al(2012) [103], Hao et al. (2016) [137], and Rominger et al. (2018) [138], might occur at a different time during idea evolution.

Idea generation could be generally associated with a bottom-up and spontaneous process, whereas idea evaluation could be related to a top-down and controlled process. Idea elaboration cannot continue without a recursive implementation of idea generation and idea evaluation. Recently, complex creativity activities gradually attracted the attention of scholars in the field of design. For instance, Alexiou et al. (2009) designed an open-ended task that required not only solution generation but also problem understanding and solution evaluation [101].

Nevertheless, loosely controlled creativity experiments increase the difficulty of data analysis since it triggers complex pairs of stimuli and response underlying the unstructured EEG data. Nguyen and Zeng (2014) conducted a preliminary analysis of the EEG spectrogram of a single subject from the loosely controlled creativity experiment, which is further analysed in the present paper [140]. The authors' lab has been identifying the regularities underlying the unstructured data from the loosely controlled creative process. Nguyen et al. (2019) proposed microstate- and frequency-based methods to segment unstructured EEG data produced from complex design activities [100]. It was found that the best segmentation algorithm, which is the microstate-based method, has an average deviation of 2-s from manual segmentation. Each structured segment can be associated with a primitive design activity. Moreover, EEG microstate analysis has been used to structure unstructured data in the goal-free and goal-directed tasks by different authors [115, 141, 149–154]. Each microstate class could be associated with a specific whole-brain network, which has been effectively studied through fMRI. Accordingly, the loosely controlled creativity experiment with the support of EEG microstate analysis, known as a task-related EEG (tEEG) framework [15], appears to offer an effective approach for studying real-world complex creativity activities. This study further refines and validates the tEEG framework by investigating the three modes of thinking in an ecologically valid manner.

Is a loosely controlled creativity experiment valid?

The validity of the loosely controlled creativity experiment was verified by comparing its findings on phenomena that have been effectively studied by validated experimental research. It was found that alpha power decreased significantly from rest to the three modes of thinking. These findings are consistent with those from ERD/ERS- and TRP-based research on visual creativity (see Pidgeion et al. (2016) for a comprehensive review) [142]. Both of ERD/ERS and TRP revealed characteristics of neural oscillations in specific frequency bands among different conditions. These frequency features were independent of task completion time. That is, significant differences in task completion time did not affect the results that were analysed by the ERD/ERS or TRP. Therefore, it is reasonable and feasible to compare findings based on ERD/ERS and TRP to verify the validity of the loosely controlled creativity experiment.

It was found that alpha power changes were more sensitive during the three modes of thinking in the lower alpha frequency band (8-10 Hz) than that in the upper alpha frequency band (10-12 Hz). This finding is in line with alpha power in the sub-frequency bands potentially being associated with different functional roles [155]. In the lower alpha band, alpha power decreased significantly over almost the entire scalp from idea evolution to idea generation and rating activity, as shown in Figure 3. This finding is consistent with the figural divergent production task being associated with power decreases in the lower alpha band over almost the entire cortical sites [156]. Moreover, in line with decreases in alpha power more likely being associated with general attention demands, such as alertness and arousal [157, 158], these findings indicate heightened general attention demands during idea generation and rating activity. The less general attention demands might result from participants frequently switching their focus to connect more objects or to overcome fixation, leading to creativity during idea evolution. Similarly, alpha power desynchronized approximately 1-s before the onset of an imperative stimulus, reflecting expectancy [159].

We speculate that participants might follow their intuition to generate a solution without overcoming fixations during idea generation.

In the upper alpha band, the power differences between areas did not exhibit a general trend for the lower alpha band in the three modes of thinking, as shown in Figure 4. It was found that alpha power decreased more strongly in the three modes of thinking at parietal sites compared to frontal, central, and temporal sites. This finding is in agreement with findings from conventional experimental approaches in that stronger decreases in alpha power are associated with figural creative ideation at parietal and occipital sites [138, 156]. In addition, this finding is consistent with that alpha power desynchronization being associated with the generation of first responses of four alternative uses [113]. Similarly, alpha power desynchronization was also observed during the verbal creative tasks fulfillment with and without overcoming self-inducted stereotypes, which lasted a few minutes [160]. Moreover, alpha power decreased significantly over temporal sites during rating activity compared to during idea evolution. Of note, differences in alpha power changes between idea generation and idea evolution were insignificant. However, this finding is inconsistent with verbal divergent thinking being associated with increases in alpha power over frontal and temporo-parietal sites (see Fink and Benedek (2014) for a comprehensive review). Recent time-course studies of divergent thinking have indicated alpha power increases at the end of the creative thinking process [113,134,135,161]. The insignificant differences might result from the loosely controlled creativity experiment in which idea generation might be embedded in idea evolution, which is the fundamental nature of an open-ended design process [2, 12, 32, 162]. Alternatively, the insignificant differences might result from the adopted reference interval that was placed at the beginning of the experiment rather than the beginning of each run of the experiment. More research is needed to understand the inconsistency since little evidence is available regarding the time-course of alpha activity during the creative process in the figural domain. Indeed, previous findings have indicated

that alpha power desynchronization was associated with semantic memory performance, perceptual performance, and intelligence [163–165]. Intelligence has been categorized as fluid intelligence (Gf) and crystallized intelligence (Gc), where Gf refers to the measurement of reasoning ability while Gc refers to the measurement of abilities of gaining, retaining, structuring, and conceptualizing information [166]. These findings indicated that the rating activity involved more task-specific demands such as memory and fluid intelligence since participants need to recall idea generation and idea evolution processes and evaluate their difficulty regarding thinking and drawing. Therefore, on the one hand, the loosely controlled creativity experiment appears to be valid due to consistent findings between our experiment and validated experiments at a macro level. On the other hand, the loosely controlled creativity experiment might induce some critical features of creativity, which could lead to inconsistent findings at a micro level.

What added value is obtained from a loosely controlled creativity experiment?

EEG microstate results revealed that multiple brain networks were activated in a different manner amid rest and the three modes of thinking. The motivation for applying EEG microstate analysis was to decompose the complex creativity activity into several primitive sub-activities through structuring the unstructured EEG data collected from the loosely controlled creativity experiment. Each primitive sub-activity was associated with a sub-phase of a creative process. The interactions between sub-activities were investigated through temporal properties of microstate classes, such as coverage and duration. Combined EEG-fMRI and EEG source localization studies have indicated that microstate classes are closely associated with the resting-state networks [115, 141, 149]. Along a similar line of thought, Benedek and Fink (2019) proposed a theoretical neurocognitive framework of creative cognition that would also need to decompose the complex cognitive

capacity into different basic cognitive functions such as memory, attention, and cognitive control [167]. Benedek and Fink's theoretical framework and the presented framework of loosely controlled creativity experiment share the same philosophy. Naturally, the new findings summarized above benefited from the loose controllability of the adopted experimental design with the support of EEG microstate analysis.

The results reported in the section 'EEG microstate classes' revealed six optimal microstate classes, as shown in Figure 5. This finding supports the argument that the optimal number of microstate classes should be estimated for each individual rather than for a group by directly aggregating each individual's EEG data [84]. Microstate classes were labelled from A to F according to the study of Custo et al. (2017), who reported seven microstate classes in the analysis of 164 subjects during rest [141]. Microstate A exhibits an asymmetric left-right orientation; microstate B exhibits a right-left orientation; microstate C exhibits an anterior-posterior orientation; microstate D exhibits a fronto-central maximum; microstate E exhibits a likely symmetric left-right orientation; and microstate F exhibits an anterior-posterior orientation. It must be noted that microstates C and F have high spatial correlations, which could lead to incorrect microstate labels between them. However, microstates C and F have negative temporal correlations compared to rest and the three modes of thinking, which could provide distinguishable information to assign their labels. This phenomenon was also observed in another study when the number of microstate classes was larger than four [141], according to which microstate F was associated with the normative microstate C described in the study of Britz et al. (2010), while microstate C was newly generated and assigned [115]. Therefore, these findings agree with the argument that not only spatial characteristics but also temporal characteristics are necessary for assigning maps with the most appropriate microstate class [84].

The results reported in the section 'EEG microstate topographies' revealed that the topographies of microstates A, B, D, E, and F were not significantly different among rest and

the three modes of thinking, as shown in Table 2. These findings are in line with observations that a few resting state microstates persisted in goal-directed tasks [151], supporting the notion that the brain might be activated in an organized manner instead of remaining inactive during rest [168, 169]. Moreover, the topography of microstate C was significantly different among rest and the three modes of thinking. Microstate C has been associated with the activity in the posterior cingulate cortex (PCC), which is a central part of the default mode network (DMN) [141]. The functions of PCC appear to be associated with internally directed cognition and unconstrained rest [170]. This finding implies that activity in the DMN plays an important role during rest and the three modes of thinking. Tasks for the three modes of thinking could change the activation of DMN topology.

The results reported in the section 'EEG microstate parameters', revealed that the coverage and duration of microstate A increased significantly from rest to the three modes of thinking, as shown in Figure 6 and Figure 7. These findings are in line with the association of microstate A with visual processing since the loosely controlled creativity experiment triggers increased visual activity during idea generation and idea evolution [150, 154]. However, microstate A has been associated with verbal processing at rest in a study from Britz et al. (2010) [115]. The inconsistent findings may indicate that microstate A does indeed reflect the activity in a left-posterior hub, which inhibits connections to left-hemispheric areas that are activated during verbal processing [150]. We speculate that the functional significance of EEG microstates might be distinct between goal-free and goal-directed tasks. Since little evidence is available regarding the functions of EEG microstates in task-specific conditions, more studies are needed to shed light on this issue through establishing standard databases that could record the functions of EEG microstates for each goal-free and goal-directed task.

It was found that the coverage of microstate D decreased significantly from rest to the

three modes of thinking. These findings support that microstate D is associated with reflexive aspects of attention, focus switching, and reorientation, which likely occur more frequently during rest than during the goal-directed tasks [150]. Moreover, the coverage of microstate D was not significant among the three modes of thinking. Similar to this observation, the coverage of microstate D was not significantly different between fluid reasoning tasks [154]. These findings did not support another report in which microstate D was associated with the dorsal attention network, which plays an important role in spatial attention and working memory [115, 171]. However, memory might be relevant for idea generation process, which is involved in recalling ideas from the memory and newly creating ideas during the tasks [172, 173]. Thus, further studies are needed to better understand the functional role of microstate D and how they might be associated with memory.

Finally, the coverage of microstate C decreased significantly from idea evolution to rating activity, whereas the coverage of microstate F increased significantly from idea evolution to idea generation and rating activity. Furthermore, the duration of microstate F increased significantly from idea evolution to rating activity. As mentioned earlier, microstate C has been associated with activity in the DMN that is more active during rest. In contrast, microstate F has been primarily associated with activity in the dorsal anterior cingulate cortex (dACC), which is more active during the cognitive control tasks [115, 174]. These findings support that the default mode network and cognitive control network play central roles in creativity [38,175,176]. The more active DMN indicated that idea evolution might be more associated with irrational cognitive process, such as relaxation or incubation. This irrational cognitive process might help participants overcome their fixation and redefine the open-ended problem, which is necessary for generating creative ideas. The more active control network indicated that idea generation and rating activity might be associated with rational cognitive process, such as decision-making. This rational cognitive process might help participants to determine the most appropriate solutions from several

tentative solutions.

4.5 Conclusion

The present study investigated different brain responses to idea generation, idea evolution, and rating activity through a loosely controlled creativity experiment. The loosely controlled creativity experiment was designed to offer a degree of flexibility/freedom for participants to incubate the genesis of their creative ideas. The validity of the loosely controlled creativity experiment was verified through comparing its findings on the phenomena that have been effectively studied by validated experimental research. It was found that alpha power decreased significantly from rest to the three modes of thinking. These findings are in line with those from visual creativity research based on ERD/ERS and TRP. The findings of alpha power changes between three modes of thinking revealed that idea evolution required less general attention, while rating activity involved more task-specific demands, such as memory and intelligence. In addition, EEG microstate analysis revealed that microstate C was more active during idea evolution compared to during the other two modes of thinking; microstate F was less active during idea evolution compared to during the other two modes of thinking. These findings indicate that the default mode network plays a central role during idea evolution while the cognitive control network plays an important role during idea generation and rating activity. These new findings were obtained since the loosely controlled creativity experiment activates multiple brain networks to accomplish tasks involving the three modes of thinking. Taken together, the loosely controlled creativity experiment with the support of EEG microstate analysis appears to offer an effective approach to investigating real-world complex creativity activity.

Chapter 5

Temporal dynamics of network oscillations in design creativity

5.1 Introduction

Recent research attempts to associate microstates with different cognitive components such as modalities of thinking [150] and fluid reasoning [154]. Temporal dynamics of EEG microstate sequences increasingly attract the attention of scholars, reflecting the need to quantify the temporal structure and complexity of microstate sequences, running in parallel to, and thus representing the ongoing flow of thoughts and cognitive processes, such as self-reported spontaneous [177] and task-initiated thoughts [178, 179]. A few studies revealed key characterises of temporal dynamics underlying resting EEG microstate sequences, such as scale-free dynamics [132], short- and long-range correlations [180], and non-Markovianity [130]. In contrast to resting-state EEG microstate sequences, temporal dynamics of EEG microstate sequences are still unknown for design creativity.

Besides, identifying the involvement of higher-order cognitive functions, namely cognitive workload and cognitive control, during design creativity could lead to a better understanding of design thinking and designers' cognitive activities. Cognitive workload could

be interpreted as the increasing utilization of brain resources under an increasing demand of the confronted task [88]. The fronto-parietal network activation was highlighted in the literature when cognitive workload is high [181]. Alpha desynchronization reflects general attention demands in the lower alpha band and semantic memory performance in the upper alpha band [155]. Additionally, decreases in alpha power have been observed under increased cognitive workload [182, 183]. Cognitive control refers to'the ability to coordinate thoughts and actions in relation with internal goals' [184], which supports goal-directed human behaviour through engaging and coordinating a variety of brain activities [185]. Theta synchronization has been linked to cognitive control and working memory processes [186–188] (see Sauseng et al., 2010 [93] and Cavanagh and Michael 2014 [94] for comprehensive reviews). Research findings identified the active involvement of certain brain areas, medial prefrontal cortex (mPFC) in particular, during tasks requiring cognitive control [189]. Further research indicated that theta power over medial frontal cortex is positively related to the cognitive control demands [190, 191].

We applied a loosely controlled experiment to simulate the nature of design creativity, including problem understanding, idea generation, rating idea generation, idea evaluation, and rating idea evaluation. Participants were given considerable freedom regarding response time (self-paced) and response action (integrating thinking and drawing phases) to comprehend design problems, generate and evaluate solutions through taking into account creativity, structure, and performance. To align our findings with other validated evidence, we investigated the regional contribution of brain oscillations in the classical frequency bands (theta, alpha, and beta) to the different cognitive tasks studied through TRP analysis. In addition, we identified EEG-defined large-scale brain networks and uncovered their temporal dynamics regarding short- and long-range correlations during the conceptual design process through EEG microstate analysis.

During problem understanding, participants read the given problem to comprehend the

design requirements. Information related to problem description keeps being encoded during such reading and understanding processes, where participants' cognitive workload may increase along the time course. During idea generation, participants need to generate and express their ideas, which is the most 'unstructured' activity where designers are confronted with incomplete and imprecise information. It is during idea generation that participants have the least instructions and constraints to express their ideas, suggesting that cognitive control mechanisms may be relaxed. In the meantime, given the least instruction but the most freedom participants are most likely to unconsciously conduct different design activities in a recursive way, which resembles an entire-design process. Higher cognitive workload may be expected during idea generation when compared with the other four design activities, which seems like a comparison between the entire process and its individual components. Following the same direction, idea generation may embody more characteristics of the conceptual design process than the other activities so that idea generation is sometimes viewed as a bottom-up, spontaneous, and unstructured activity [192]. During idea evaluation, participants need to compare two design solutions and make their preferential evaluations. Rating idea generation and evaluation share a considerable similarity especially when the same rating form is used for the two rating stages in the current experimental settings. The rating activity is the most 'structured' and well-defined process among the studied design activities, which may indicate an opposite expectation on cognitive control and cognitive workload compared to idea generation.

We hypothesized that idea generation would be associated with the highest cognitive workload but the lowest cognitive control among the studied five design activities. Higher cognitive workload would be associated with more pronounced decreases in alpha power, while lower cognitive control would be associated with decreases in theta and beta power. In addition, we expected that task-negative microstate classes would be more prevalent during idea generation while idea generation would be associated with shorter correlation

times.

5.2 Method

5.2.1 Experiment Design

The experiment consists of six runs corresponding to six different design problems: design a birthday cake, design a recycle bin, design a toothbrush, design a wheelchair, design a workspace, and design a drinking fountain [98], as listed in Table 5. Figure 8A) shows the sequence of six design problems presented to the participants. Each run consists of five successive design activities: problem understanding, idea generation, rating idea generation, idea evaluation, and rating idea evaluation. Figure 8B) shows an example of schematic time courses of designing a birthday cake.

During problem understanding, participants were asked to read and understand a design problem. During idea generation, participants were asked to sketch a solution that satisfied the requirements of design problem. During idea evaluation, participants were asked to evaluate the performance or preference of two given solutions. NASA Task Load Index was placed at the end of idea generation and evaluation, namely rating idea generation and rating idea evaluation respectively. During rating activity, participants were asked to rate their mental demand, time demand, performance, effort, and stress level. The rests were placed at the begin and end of this experiment. By dividing the experiment into the above mentioned five design activities, we aimed at a reduced difficulty in investigating such a complex design process and adding certain 'structure' to the unstructured data. Such segmentation was the main control applied in the experiment, meaning that despite the task description showing on the screen from the beginning of each design activity, any additional control including time limit, oral instructions, or 'think-aloud' related control, was avoided during the experiment. In the meanwhile, the presented experiment was loosely controlled

as participants were given unlimited response time during each design activity and they were given sufficient freedom to complete the given task in their own way without any interruption or interference. In this way, the characteristics of design process could be better modelled as sufficient time and freedom could be essential to allow participants' naturally exploring possible solutions and completing the given task recursively.

Table 5: Six design problems

Design Problem	Description
Design a birthday cake	Make a birthday cake for a five year old kid. How should it look like?
Design a recycle bin	Sometimes, we do not know which items should be recycled. Create a recycle bin that helps people recycle correctly.
Design a toothbrush	Create a toothbrush that incorporates toothpaste. (Incorporate = include, combine)
Design a wheelchair	In Montreal, people on wheelchair cannot use metro safely because most of metros have only stairs or escalators. Elevator is not an option because it is too costly to build one. You are asked to create the most efficient solution to solve this problem.
Design a workspace	Employees in an IT company are sitting too much. The company wants their employees to stay healthy and work efficiently at the same time. You are asked to create a workspace that can help the employee to work and exercise at the same time.
Design a drinking fountain	Two problems with standard drinking fountain: (a) Filling up water bottle is not easy; (b) People too short cannot use the fountain and people too tall has to bend over too much. Create a new drinking fountain that solves these problems.

5.2.2 Participants and experiment procedure

A total of 42 participants took part in this experiment, who were graduate students in the Gina Cody School of Engineering and Computer Science, Concordia University. A gift card of CAD$100 was given as compensation to the best design. Three participants were excluded from data analysis since they have not completed all the experiments. 11

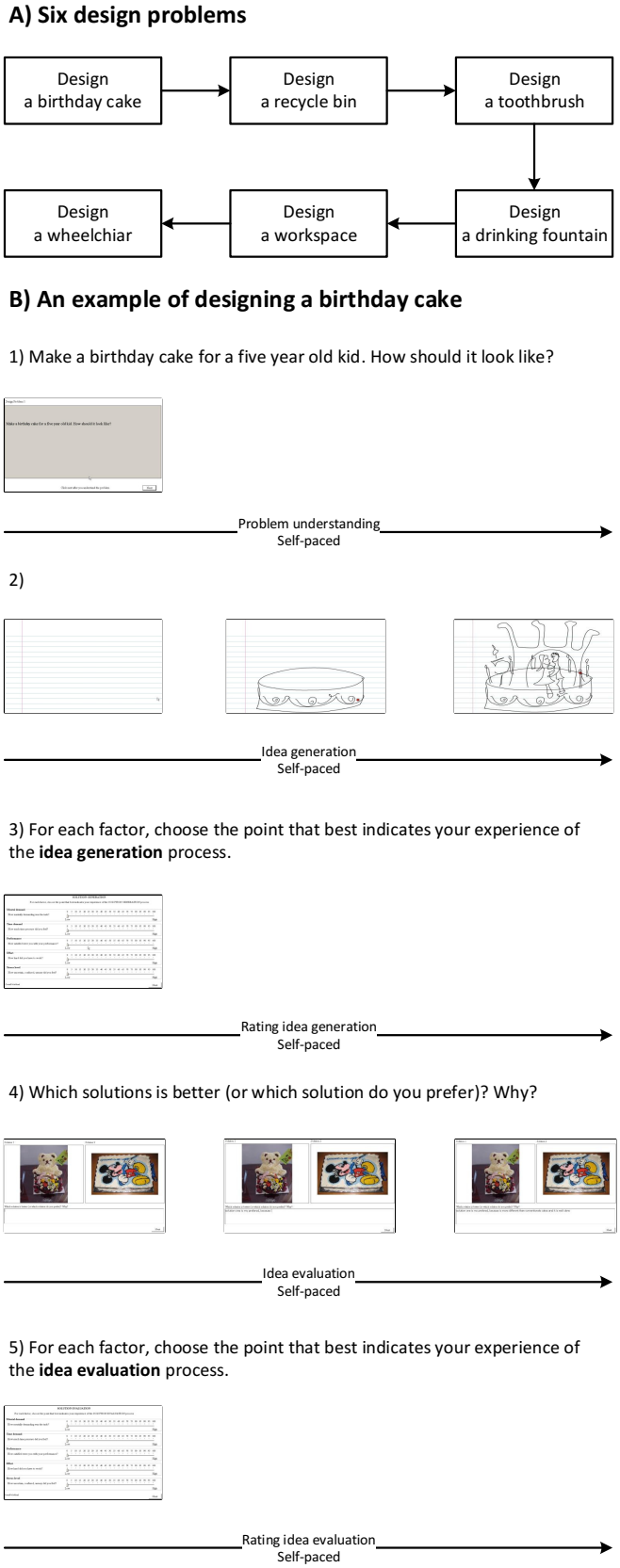

Figure 8: A) The sequence of six design problems. B) An example of schematic time courses of designing a birthday cake. 1) Self-paced problem understanding. 2) Self-paced idea generation. 3) Self-paced workload rating for the idea generation. 4) Self-paced idea evaluation. 5) Self-paced workload rating for the idea evaluation

participants were excluded from data analysis due to technical errors such as missing markers. One participant was excluded from data analysis due to large electrode impedances and poor data quality. The final samples included 27 participants (8 women, 19 men) aged from 24 to 39. All the participants had normal or corrected-to-normal vision. The experimenters helped subjects wear the HRV chest strap, GSR finger strap, respiration rate belt and EEG cap. The experimenters briefed each participant the experimental tasks; impedances of all the EEG electrodes were below 10 kΩ; participants completed the experiment by following the experimental procedures specified in the experimental design. EEG signals were recorded by a 64 channel BrainVision actiCHamp at 500 Hz during the experiment. The EEG was referenced to Cz and the electrode placement was based on the international 10-10 system. The experimental protocol was approved by the Concordia Human Research Ethics Committee. All sections of the experiment were performed in accordance with relevant guidelines and regulations. All subjects signed the informed consent form before taking the experiment.

5.3 Results

5.3.1 Behavioural results

In rating idea generation, self-rated mental demand was 49.01 (SE=3.25); self-rated time demand was 39.79 (SE=3.68); self-rated performance was 54.23 (SE=3.08); self-rated effort was 42.38 (SE=3.60); and self-rated stress was 41.84 (SE=3.59). In rating idea evaluation, self-rated mental demand was 39.38 (SE=3.13); self-rated time demand was 32.14 (SE=3.60); self-rated performance was 61.66 (SE=3.04); self-rated effort was 36.29 (SE=3.22); and self-rated stress was 32.45 (SE=3.82).

Post hoc paired t tests revealed significant decreases in self-rated mental demand ($p = 0.000$), self-rated time demand ($p = 0.001$), self-rated effort ($p = 0.007$), and self-rated

stress ($p = 0.003$) from idea generation to idea evaluation, as well as significant increases in self-rated performance ($p = 0.010$).

5.3.2 EEG results

EEG theta power

In the theta band, the $5 \times 5 \times 2$ repeated measures ANOVA revealed two significant main effects of CONDITION ($F(4, 104) = 31.838, p = 0.000, \eta^2 = 0.550$) and AREA ($F(2.528, 65.733) = 25.767, p = 0.000, \eta^2 = 0.498$), as well as three significant interaction effects of CONDITION $\times$ AREA ($F(5.994, 155.848) = 26.820, p = 0.000, \eta^2 = 0.508$), CONDITION $\times$ HEMISPHERE ($F(4, 104) = 5.299, p = 0.001, \eta^2 = 0.169$), and CONDITION $\times$ AREA $\times$ HEMISPHERE ($F(6.340, 164.833) = 3.756, p = 0.001, \eta^2 = 0.126$).

Table 6 lists the p-values of pairwise comparisons of TRP theta with Bonferroni correction between CONDITION on each AREA, while Figure 9 shows grand average topographical maps and error bars of task-related theta power between conditions. It was found that theta power was lower over frontal, central, temporal, parietal, and occipital sites during IG than during PU ($ps < 0.036$), RIG ($ps < 0.016$), IE ($ps < 0.007$), and RIE ($ps < 0.001$). Theta power was significantly lower over central sites during PU than during RIG ($p = 0.015$), and over central and temporal sites during PU than during RIE ($ps < 0.004$), whereas it was significantly higher over central sites during PU than during IE ($p = 0.036$). Theta power was significantly lower over central and temporal sites during IE than during RIG ($ps < 0.022$), as well as over frontal, central, temporal sites during IE than during RIE ($ps < 0.005$).

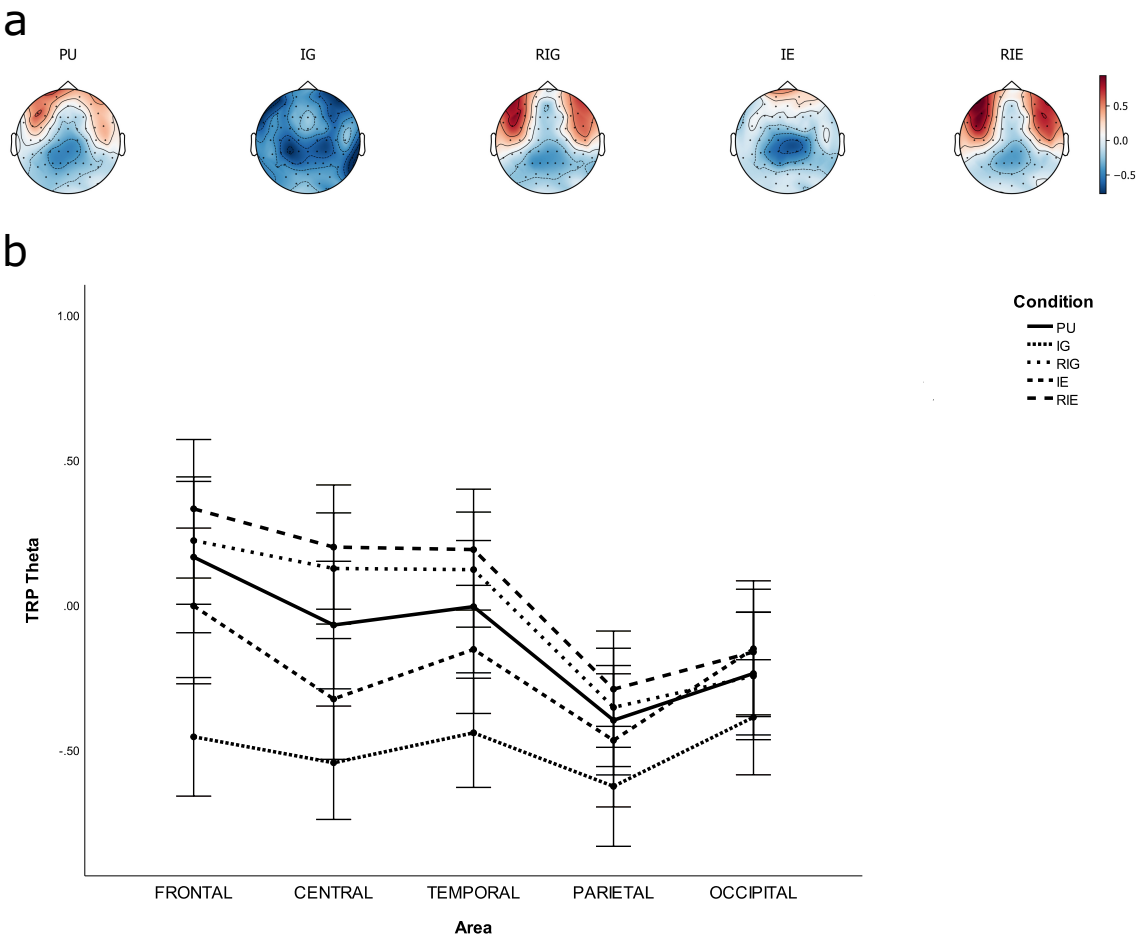

Figure 9: Task-related power in theta band during problem understanding, idea generation, rating idea generation, idea evaluation, and rating idea evaluation. a Grand average topographical maps of task-related beta power. b Error bars of task-related theta power.

Table 6: P-values of pairwise comparisons with Bonferroni correction of TRP theta between AREA and CONDITION, including problem understanding (PU), idea generation (IG), rating idea generation (RIG), idea evaluation (IE), and rating idea evaluation (RIE).

Activity			Area									
			Frontal		Central		Temporal		Parietal		Occipital	
PU	Vs.	IG	0.0^{***}	↘	0.0^{***}	↘	0.0^{***}	↘	0.002^{***}	↘	0.036^{*}	↘
PU	Vs.	RIG	1.0		0.015^{*}	↗	0.239		1.0		1.0	
PU	Vs.	IE	0.556		0.036^{*}	↘	0.45		1.0		1.0	
PU	Vs.	RIE	0.067		0.001^{***}	↗	0.004^{***}	↗	0.12		0.608	
IG	Vs.	RIG	0.0^{***}	↗	0.0^{***}	↗	0.0^{***}	↗	0.001^{***}	↗	0.016^{*}	↗
IG	Vs.	IE	0.0^{***}	↗	0.001^{***}	↗	0.0^{***}	↗	0.007^{**}	↗	0.001^{***}	↗
IG	Vs.	RIE	0.0^{***}	↗	0.0^{***}	↗	0.0^{***}	↗	0.0^{***}	↗	0.001^{***}	↗
RIG	Vs.	IE	0.074		0.001^{***}	↘	0.022^{*}	↘	0.558		0.431	
RIG	Vs.	RIE	0.335		1.0		1.0		1.0		0.414	
IE	Vs.	RIE	0.005^{***}	↗	0.0^{***}	↗	0.002^{***}	↗	0.08		1.0	

* $\rho \leq 0.050$, ** $\rho \leq 0.010$, *** $\rho \leq 0.005$
↗ TRP theta increases
↘ TRP theta decreases

EEG alpha power

In the alpha band, the $5 \times 5 \times 2$ repeated measures ANOVA revealed two significant main effects of CONDITION ($F(4, 104) = 26.880, p = 0.000, \eta^2 = 0.508$) and AREA ($F(2.735, 71.105) = 51.801, p = 0.000, \eta^2 = 0.666$), as well as two significant interaction effects of CONDITION $\times$ AREA ($F(6.153, 159.978) = 21.723, p = 0.000, \eta^2 = 0.455$) and CONDITION $\times$ AREA $\times$ HEMISPHERE ($F(6.512, 169.299) = 3.700, p = 0.001, \eta^2 = 0.125$).

Table 7 lists the p-values of pairwise comparisons of TRP alpha with Bonferroni correction between CONDITION on each AREA, while Figure 10 shows grand average topographical maps and error bars of task-related alpha power between conditions. It was found that decreases in alpha power were significantly smaller over frontal, central temporal, parietal, and occipital sites during PU compared to IG ($ps < 0.001$), as well as over occipital sites during PU compared to RIG ($p = 0.039$), as well as over frontal, central, temporal, and parietal sites during PU compared to IE ($ps < 0.006$). Decreases in alpha power were significantly larger over frontal, central, temporal, and parietal sites during IG

compared to during RIG ($ps < 0.002$), as well as over frontal and temporal sites during IG compared to during IE ($ps < 0.001$), as well as over frontal, central, temporal, parietal, and occipital sites during IG compared to during RIE ($ps < 0.017$). In addition, decreases in alpha power were significantly larger over central and temporal sites during IE compared to during RIG ($ps < 0.015$), as well as over frontal, central, and temporal sites during IE compared to RIE ($ps < 0.015$).

Table 7: P-values of pairwise comparisons of TRP alpha with Bonferroni correction between AREA and CONDITION, including problem understanding (PU), idea generation (IG), rating idea generation (RIG), idea evaluation (IE), and rating idea evaluation (RIE).

Activity			Area									
			Frontal		Central		Temporal		Parietal		Occipital	
PU	Vs.	IG	0.0^{***}	↘	0.0^{***}	↘	0.0^{***}	↘	0.001^{***}	↘	0.001^{***}	↘
PU	Vs.	RIG	0.297		1.0		1.0		0.246		0.039^{*}	↘
PU	Vs.	IE	0.004^{***}	↘	0.001^{***}	↘	0.004^{***}	↘	0.006^{**}	↘	0.401	
PU	Vs.	RIE	1.0		1.0		1.0		0.484		0.102	
IG	Vs.	RIG	0.0^{***}	↗	0.0^{***}	↗	0.0^{***}	↗	0.002^{***}	↗	0.367	
IG	Vs.	IE	0.0^{***}	↗	0.052		0.01^{**}	↗	0.138		0.082	
IG	Vs.	RIE	0.0^{***}	↗	0.0^{***}	↗	0.0^{***}	↗	0.0^{***}	↗	0.017^{*}	↗
RIG	Vs.	IE	0.088		0.001^{***}	↘	0.015^{*}	↘	1.0		1.0	
RIG	Vs.	RIE	0.89		1.0		1.0		1.0		1.0	
IE	Vs.	RIE	0.015^{*}	↗	0.001^{***}	↗	0.01^{**}	↗	0.431		1.0	

* $\rho \leq 0.050$, ** $\rho \leq 0.010$, *** $\rho \leq 0.005$
↗ TRP alpha increases
↘ TRP alpha decreases

EEG beta power

In the beta band, the $5 \times 5 \times 2$ repeated measures ANOVA revealed two significant main effects of CONDITION ($F(2.864, 74.459) = 41.769, p = 0.000, \eta^2 = 0.616$) and AREA ($F(4, 104) = 43.514, p = 0.000, \eta^2 = 0.626$), as well as two significant interaction effects of CONDITION $\times$ AREA ($F(6.372, 165.660) = 30.607, p = 0.000, \eta^2 = 0.541$) and CONDITION $\times$ AREA $\times$ HEMISPHERE ($F(6.241, 162.265) = 3.425, p = 0.003, \eta^2 = 0.116$).

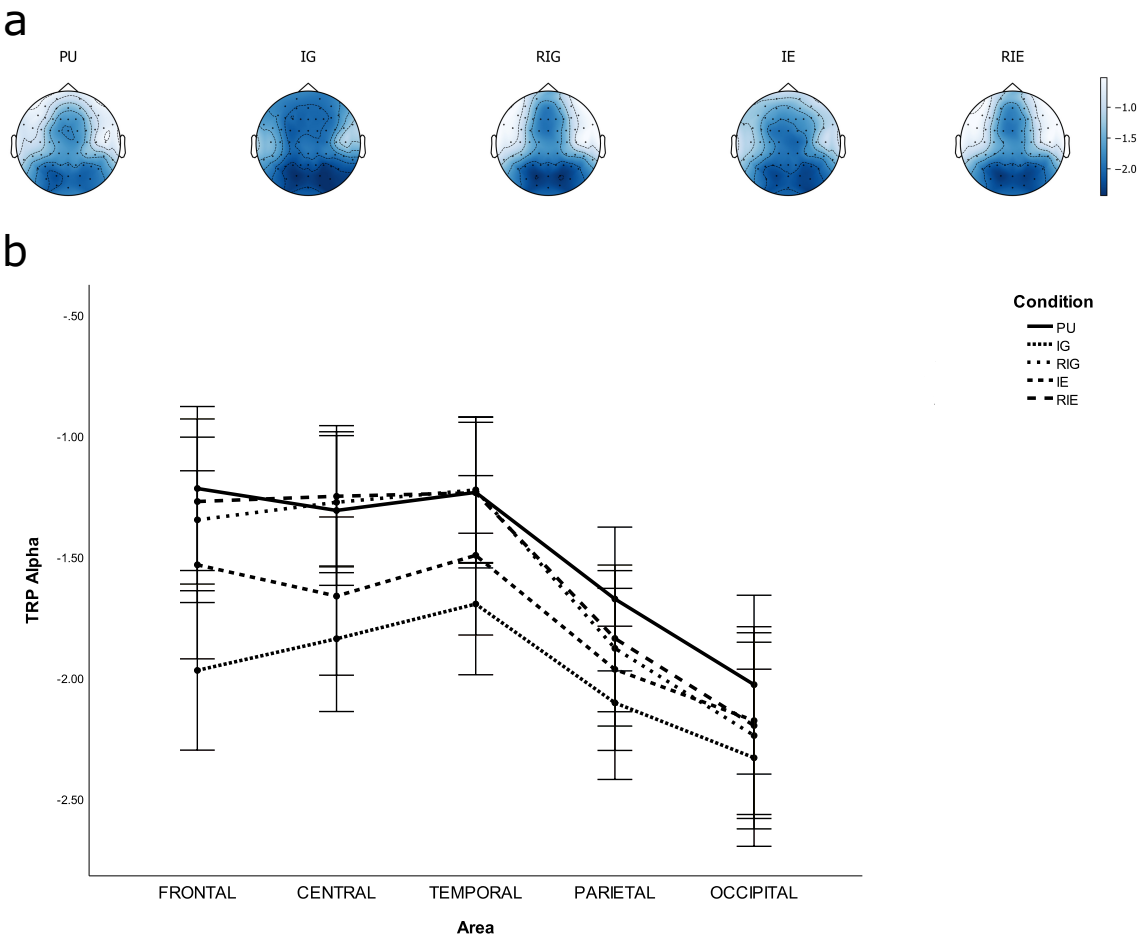

Figure 10: Task-related power in alpha band during problem understanding, idea generation, rating idea generation, idea evaluation, and rating idea evaluation. a Grand average topographical maps of task-related alpha power. b Error bars of task-related alpha power.

Table 8 lists the p-values of pairwise comparisons of TRP beta with Bonferroni correction between CONDITION on each AREA, while Figure 11 shows grand average topographical maps and error bars of task-related beta power between conditions. It was found that beta power increased significantly over frontal, central, temporal, parietal, and occipital sites from IG to PU ($ps < 0.001$), RIG ($ps < 0.041$), and RIE ($ps < 0.001$), as well as over frontal, central, temporal and parietal sites from IG to IE ($ps < 0.001$). The beta power increased significantly over frontal, central and temporal from IE to RIG ($ps < 0.029$) and RIE ($ps < 0.008$), as well as over frontal, central, temporal, and parietal sites from IE to PU ($ps < 0.031$).

Table 8: P-values of pairwise comparisons of TRP beta with Bonferroni correction between AREA and CONDITION, including problem understanding (PU), idea generation (IG), rating idea generation (RIG), idea evaluation (IE), and rating idea evaluation (RIE).

Activity			Area									
			Frontal		Central		Temporal		Parietal		Occipital	
PU	Vs.	IG	0.0^{***}	↘	0.0^{***}	↘	0.0^{***}	↘	0.0^{***}	↘	0.001^{***}	↘
PU	Vs.	RIG	1.0		0.945		0.463		0.412		0.547	
PU	Vs.	IE	0.012^{*}	↘	0.002^{***}	↘	0.031^{*}	↘	0.007^{**}	↘	0.988	
PU	Vs.	RIE	1.0		0.264		0.711		1.0		0.751	
IG	Vs.	RIG	0.0^{***}	↗	0.0^{***}	↗	0.0^{***}	↗	0.0^{***}	↗	0.041^{*}	↗
IG	Vs.	IE	0.0^{***}	↗	0.001^{***}	↗	0.001^{***}	↗	0.001^{***}	↗	0.135	
IG	Vs.	RIE	0.0^{***}	↗	0.0^{***}	↗	0.0^{***}	↗	0.0^{***}	↗	0.001^{***}	↗
RIG	Vs.	IE	0.029^{*}	↘	0.001^{***}	↘	0.006^{**}	↘	1.0		1.0	
RIG	Vs.	RIE	1.0		1.0		1.0		1.0		1.0	
IE	Vs.	RIE	0.008^{**}	↗	0.001^{***}	↗	0.007^{**}	↗	0.147		1.0	

* $\rho \leq 0.050$, ** $\rho \leq 0.010$, *** $\rho \leq 0.005$
↗ TRP beta increases
↘ TRP beta decreases

EEG microstate classes

Based on cross validation as shown in Eq. (3), the optimal number of individual microstate classes was found to be equal to 7.109 (SE=0.134) for rest, 7.370 (SE=0.079) for problem understanding, 7.547 (SE=0.080) for idea generation, 7.849 (SE=0.089) for rating idea generation, 7.458 (SE=0.087) for idea evaluation, and 7.156 (SE=0.302) for rating

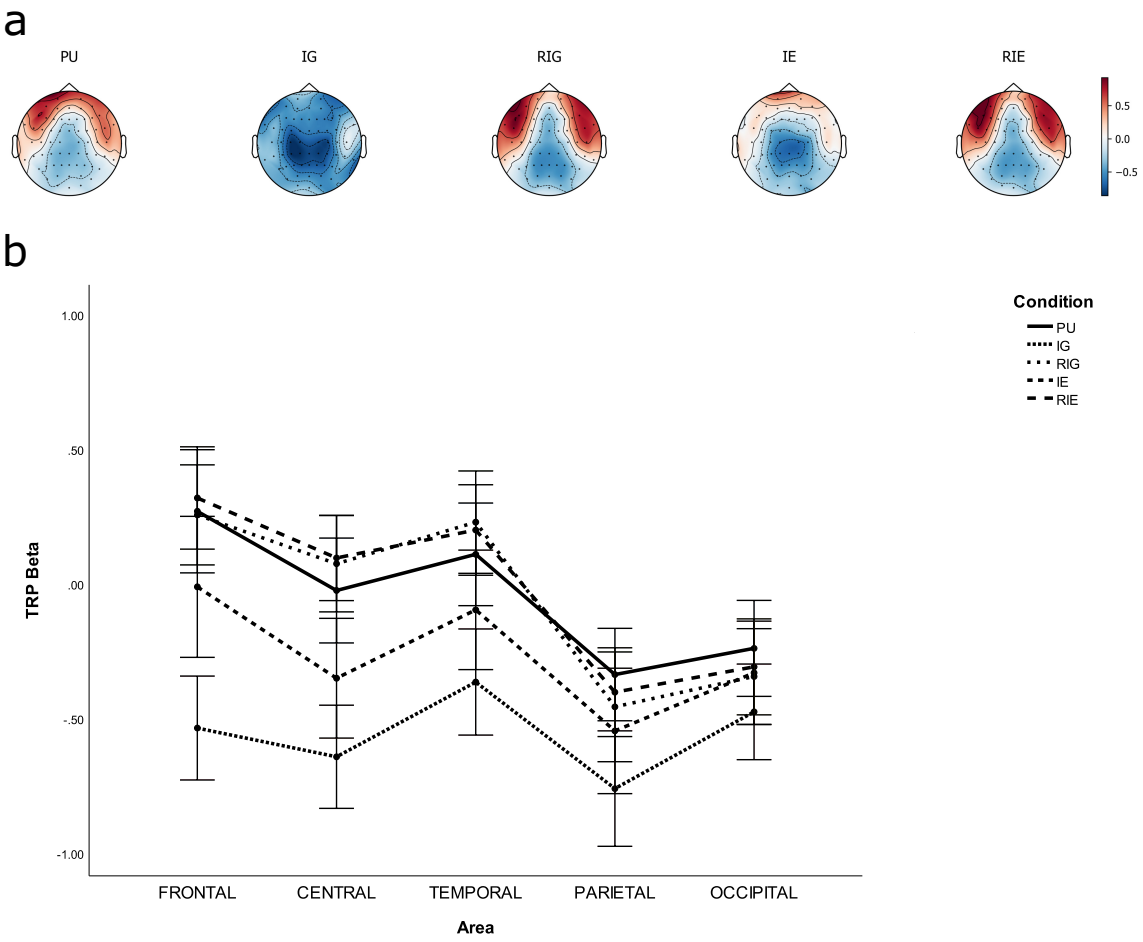

Figure 11: Task-related power in beta band during problem understanding, idea generation, rating idea generation, idea evaluation, and rating idea evaluation. a Grand average topographical maps of task-related beta power. b Error bars of task-related beta power.

idea evaluation. Figure 12 shows the topographic maps of seven microstate classes across and within conditions, which include rest, problem understanding, idea generation, rating idea generation, idea evaluation, and rating idea evaluation. The seven microstate classes were labelled as A, B, C, D, E, F, and G according to the studies of Michel and Koenig (2018) [84] and Custo et al. (2017) [141]. The number of individual microstate classes was defined as seven for each run, each condition and each participant because of comparability and simplicity of statistical analysis.

The seven individual microstate classes explained 68.6% (SE=0.7) of the global variance of the original EEG topographies corresponding to peaks of GFP for rest, 67.1% (SE=0.4) for problem understanding, 67.4% (SE=0.3) for idea generation, 65.8% (SE=0.4) for rating idea generation, 67.3% (SE=0.4) for idea evaluation, and 66.4% (SE=0.4) for the rating idea evaluation.

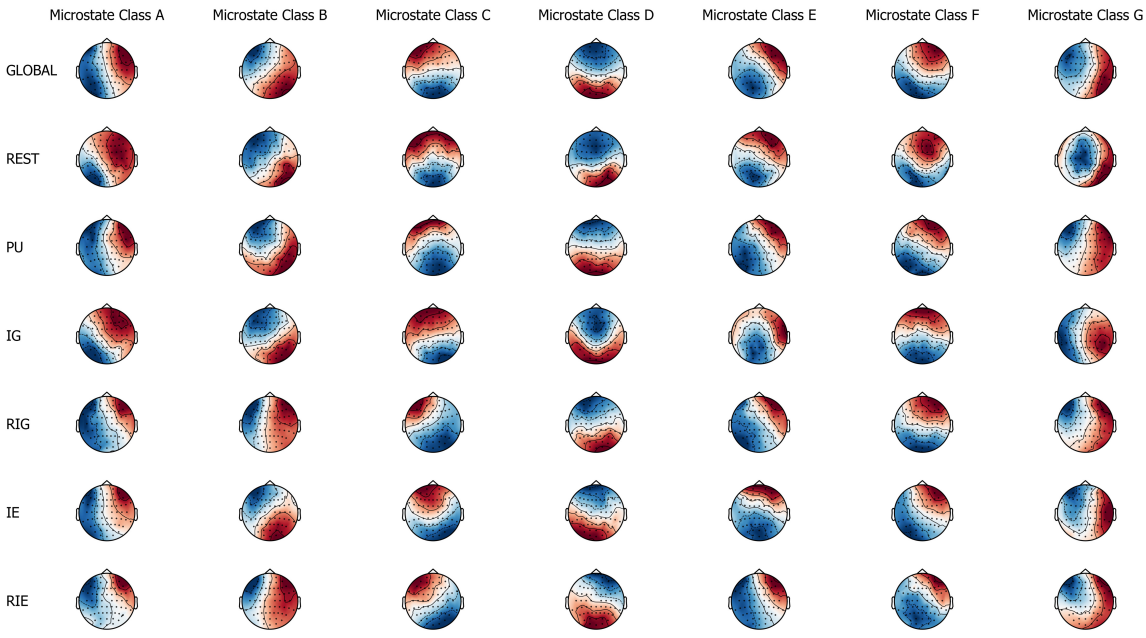

Figure 12: The spatial configuration of the seven microstate classes (A, B, C, D, E, F, and G) for across conditions (global) and within conditions (rest, problem understanding, idea generation, rating idea generation, idea evaluation, and rating idea evaluation).

EEG microstate parameters

For EEG microstate coverage, the 6 $\times$ 7 repeated measures ANOVA revealed a significant main effect CLASS ($F(3.737,, 97.159) = 4.498, p = 0.003, \eta^2 = 0.147$) and a significant interaction effect CONDITION $\times$ CLASS ($F(7.378, 191.837) = 37.213, p = 0.000, \eta^2 = 0.589$).

Table 9 lists p-values of post hoc paired t tests with Bonferroni correction on microstate coverage, while Figure 13 shows error bars of microstate coverage in each condition. In particular, the coverage of microstate class A was the lowest during REST compared to during PU, IG, RIG, IE, and RIE ($ps = 0.000$), while the coverage of microstate class B was the lowest during REST compared to PU, RIG, IE, and RIE ($ps < 0.005$). Similarly, the coverage of microstate class G was the lowest during REST compared to during PU, IG, RIG, and RIE ($ps < 0.040$). On the contrary, the coverage of microstate class C was the highest during REST compared to during PU, RIG, IE, and RIE ($ps < 0.001$), while the coverage of microstate class D was the highest during REST compared to PU, IG, RIG, and RIE ($ps < 0.009$). The coverage of microstate class F was higher during REST compared to during RIG and RIE ($ps < 0.021$).

In addition, the coverage of microstate class A decreased significantly from RIG and RIE to PU, IG, and IE ($ps < 0.001$), as well as from PU to IG ($p = 0.001$). The coverage of microstate class B increased significantly from IG and IE to PU, RIG, and RIE ($ps < 0.001$). The coverage of microstate class C decreased significantly from IG to RIG, RIE, and IE ($ps < 0.003$), as well as from PU to RIG and RIE ($ps < 0.002$). The coverage of microstate class D decreased significantly from IG and IE to PU, RIG, and RIE ($ps < 0.002$), as well as from PU to RIG and RIE ($ps < 0.001$). The coverage of microstate class E increased significantly from PU to RIE ($p = 0.028$). The coverage of microstate class F decreased significantly from IG and IE to PU, RIG, and RIE ($ps < 0.003$). The coverage of microstate class G decreased significantly from RIG and RIE to IG and IE ($ps < 0.002$).

Table 9: P-values of pairwise comparisons for microstate coverage with Bonferroni correction between CLASS (A, B, C, D, E, F, G) and CONDITION (rest (REST), problem understanding (PU), idea generation (IG), rating idea generation (RIG), idea evaluation (IE), and rating idea evaluation (RIE)).

Condition			Microstate classes													
			Class A		Class B		Class C		Class D		Class E		Class F		Class G	
REST	Vs.	PU	0.0^{***}	↗	0.0^{***}	↗	0.001^{***}	↘	0.0^{***}	↘	1.0		0.91		0.008^{**}	↗
REST	Vs.	IG	0.0^{***}	↗	0.064		0.734		0.009^{**}	↘	1.0		1.0		0.04^{*}	↗
REST	Vs.	RIG	0.0^{***}	↗	0.0^{***}	↗	0.0^{***}	↘	0.0^{***}	↘	1.0		0.021^{*}	↘	0.0^{***}	↗
REST	Vs.	IE	0.0^{***}	↗	0.005^{***}	↗	0.001^{***}	↘	0.071		1.0		0.054		0.394	
REST	Vs.	RIE	0.0^{***}	↗	0.0^{***}	↗	0.0^{***}	↘	0.0^{***}	↘	1.0		0.009^{**}	↘	0.0^{***}	↗
PU	Vs.	IG	0.001^{***}	↘	0.0^{***}	↘	0.056		0.0^{***}	↗	1.0		0.002^{***}	↗	0.962	
PU	Vs.	RIG	0.001^{***}	↗	1.0		0.002^{***}	↘	0.001^{***}	↘	0.881		0.272		0.379	
PU	Vs.	IE	0.223		0.001^{***}	↘	1.0		0.002^{***}	↗	1.0		0.003^{***}	↗	0.271	
PU	Vs.	RIE	0.001^{***}	↗	1.0		0.001^{***}	↘	0.001^{***}	↘	0.028^{*}	↗	0.335		0.488	
IG	Vs.	RIG	0.0^{***}	↗	0.0^{***}	↗	0.0^{***}	↘	0.0^{***}	↘	1.0		0.001^{***}	↘	0.001^{***}	↗
IG	Vs.	IE	0.492		1.0		0.003^{***}	↘	1.0		1.0		0.628		1.0	
IG	Vs.	RIE	0.0^{***}	↗	0.0^{***}	↗	0.0^{***}	↘	0.0^{***}	↘	1.0		0.002^{***}	↘	0.002^{***}	↗
RIG	Vs.	IE	0.0^{***}	↘	0.001^{***}	↘	0.1		0.0^{***}	↗	0.727		0.001^{***}	↗	0.002^{***}	↘
RIG	Vs.	RIE	1.0		1.0		1.0		1.0		1.0		1.0		1.0	
IE	Vs.	RIE	0.0^{***}	↗	0.0^{***}	↗	0.055		0.0^{***}	↘	0.388		0.001^{***}	↘	0.001^{***}	↗

* $\rho \leq 0.050$, ** $\rho \leq 0.010$, *** $\rho \leq 0.005$
↗ microstate coverage increases
↘ microstate coverage decreases

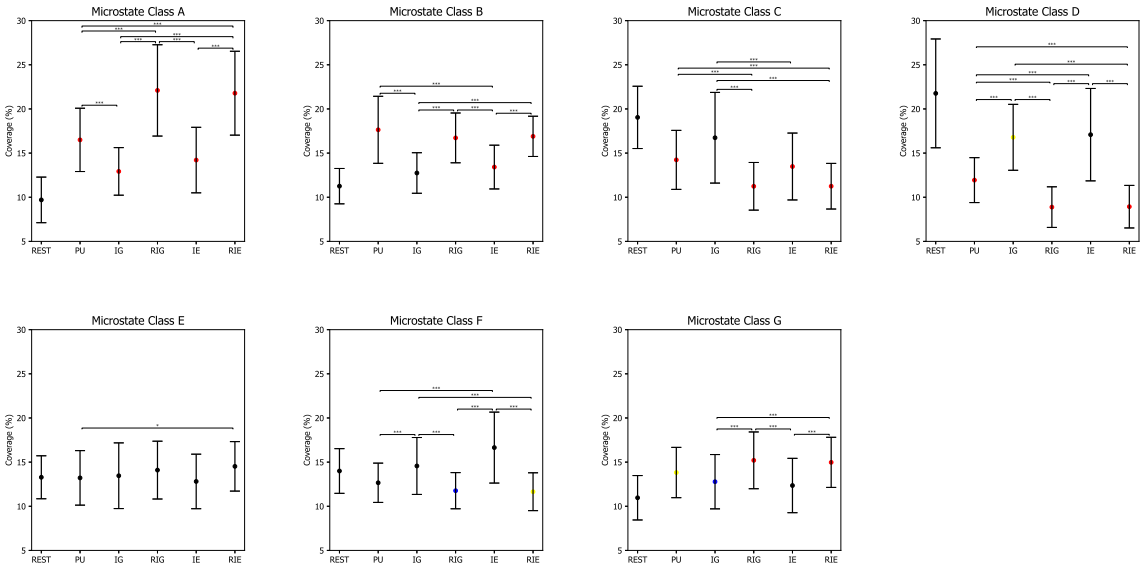

Figure 13: Error bars of microstate coverage during rest (REST), problem understanding (PU), idea generation (IG), rating idea generation (IE), idea evaluation (IE), and rating idea evaluation (RIE). P-values between rest and other conditions are annotated by black dots ($p > 0.050$), blue dots ($p \leq 0.050$), yellow dots ($p \leq 0.010$), and red dots ($p \leq 0.005$). P-values between conditions are annotated by * ($p \leq 0.050$), ** ($p \leq 0.010$), *** ($p \leq 0.005$).

For EEG microstate duration, the 6 $\times$ 7 repeated measures ANOVA revealed two significant main effects CONDITION ($F(3.099.80.585) = 48.401, p = 0.000, \eta^2 = 0.651$) and CLASS ($F(3.616, 94.017) = 5.896, p = 0.000, \eta^2 = 0.185$), as well as a significant interaction effect CONDITION $\times$ CLASS ($F(6.911, 179.685) = 41.691, p = 0.000, \eta^2 = 0.616$).

Table 10 lists p-values of post hoc paired t tests with Bonferroni correction on microstate duration, while Figure 14 shows error bars of microstate duration in each condition. In particular, the duration of microstate class A was lower during REST compared to during RIG and RIE ($ps = 0.000$). The duration of microstate class B was lower during REST compared to during PU ($p = 0.044$), whereas it was higher during REST compared to during IG ($p = 0.007$). The duration of microstate classes C, D and E was the lowest during REST compared to PU, IG, RIG, IE, and RIE ($ps < 0.002$). The duration of microstate class F was higher during REST compared to during PU, IG, RIG, and RIE ($ps < 0.004$). The duration of microstate class G was higher during REST compared to during IG ($p = 0.027$).

Besides, the duration of microstate class A decreased significantly from RIG and RIE to PU, IG, and IE ($ps < 0.001$), as well as from PU to IG ($p = 0.001$). The duration of microstate class B increased significantly from IG and IE to PU, RIG, and RIE ($ps < 0.001$). The duration of microstate class C decreased significantly from PU to RIG and RIE ($ps < 0.007$), as well as from IG to RIG, IE, and RIE ($ps < 0.006$). The duration of microstate class D decreased from PU to RIG and RIE ($ps < 0.002$), as well as from IG and IE to PU, RIG, and RIE ($ps < 0.001$). The duration of microstate class E decreased significantly from RIE to PU ($p = 0.018$). The duration of microstate class F decreased significantly from IE to PU, RIG, and RIE ($ps < 0.034$). The duration of microstate class G decreased significantly from RIG and RIE to IG and IE ($ps < 0.001$).

For EEG microstate occurrence, the 6 $\times$ 7 repeated measures ANOVA revealed two

Table 10: P-values of pairwise comparisons with Bonferroni correction for microstate duration between CLASS (A, B, C, D, E, F, G) and CONDITION (rest (REST), problem understanding (PU), idea generation (IG), rating idea generation (RIG), idea evaluation (IE), and rating idea evaluation (RIE)).

Condition			Microstate classes													
			Class A		Class B		Class C		Class D		Class E		Class F		Class G	
REST	Vs.	PU	0.079		0.044^{*}	↗	0.0^{***}	↘	0.0^{***}	↘	0.001^{***}	↘	0.0^{***}	↘	1.0	
REST	Vs.	IG	1.0		0.007^{**}	↘	0.0^{***}	↘	0.0^{***}	↘	0.0^{***}	↘	0.004^{***}	↘	0.027^{*}	↘
REST	Vs.	RIG	0.0^{***}	↗	0.113		0.0^{***}	↘	0.0^{***}	↘	0.001^{***}	↘	0.0^{***}	↘	1.0	
REST	Vs.	IE	1.0		0.123		0.0^{***}	↘	0.0^{***}	↘	0.001^{***}	↘	1.0		0.069	
REST	Vs.	RIE	0.0^{***}	↗	0.005^{***}	↗	0.0^{***}	↘	0.0^{***}	↘	0.02^{*}	↘	0.0^{***}	↘	1.0	
PU	Vs.	IG	0.001^{***}	↘	0.0^{***}	↘	0.081		0.0^{***}	↗	1.0		0.409		0.419	
PU	Vs.	RIG	0.001^{***}	↗	1.0		0.001^{***}	↘	0.001^{***}	↘	1.0		0.787		0.918	
PU	Vs.	IE	0.062		0.001^{***}	↘	1.0		0.01^{**}	↗	1.0		0.034^{*}	↗	0.108	
PU	Vs.	RIE	0.001^{***}	↗	1.0		0.007^{**}	↘	0.002^{***}	↘	0.018^{*}	↗	1.0		0.17	
IG	Vs.	RIG	0.0^{***}	↗	0.0^{***}	↗	0.0^{***}	↘	0.0^{***}	↘	1.0		0.077		0.001^{***}	↗
IG	Vs.	IE	1.0		1.0		0.006^{**}	↘	1.0		1.0		0.741		1.0	
IG	Vs.	RIE	0.0^{***}	↗	0.0^{***}	↗	0.0^{***}	↘	0.0^{***}	↘	0.381		0.282		0.0^{***}	↗
RIG	Vs.	IE	0.0^{***}	↘	0.001^{***}	↘	0.455		0.0^{***}	↗	1.0		0.003^{***}	↗	0.001^{***}	↘
RIG	Vs.	RIE	1.0		1.0		1.0		1.0		0.526		1.0		1.0	
IE	Vs.	RIE	0.0^{***}	↗	0.0^{***}	↗	1.0		0.0^{***}	↘	0.209		0.004^{***}	↘	0.0^{***}	↗

* $\rho \leq 0.050$, ** $\rho \leq 0.010$, *** $\rho \leq 0.005$
↗ microstate duration increases
↘ microstate duration decreases

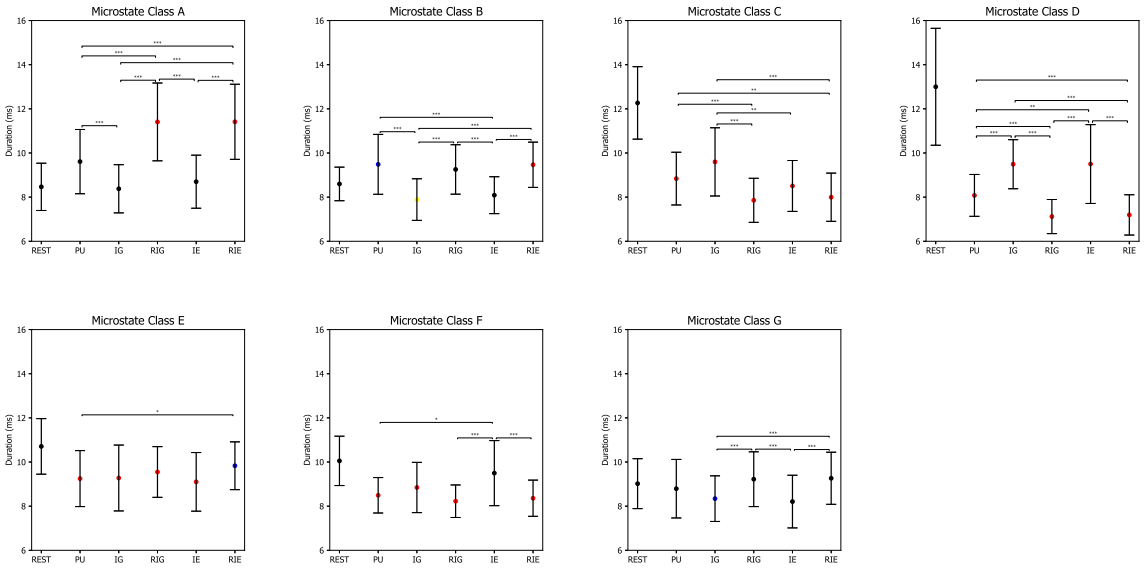

Figure 14: Error bars of microstate duration during rest (REST), problem understanding (PU), idea generation (IG), rating idea generation (IE), idea evaluation (IE), and rating idea evaluation (RIE). P-values between rest and other conditions are annotated by black dots ($p > 0.050$), blue dots ($p \leq 0.050$), yellow dots ($p \leq 0.010$), and red dots ($p \leq 0.005$). P-values between conditions are annotated by * ($p \leq 0.050$), ** ($p \leq 0.010$), *** ($p \leq 0.005$).

significant main effects CONDITION ($F(3.393.88.230) = 34.593, p = 0.000, \eta^2 = 0.571$) and CLASS ($F(3.707, 96.380) = 10.582, p = 0.000, \eta^2 = 0.289$), as well as a significant interaction effect CONDITION $\times$ CLASS ($F(7.618, 198.068) = 33.086, p = 0.000, \eta^2 = 0.560$).

Table 11 lists p-values of post hoc paired t tests with Bonferroni correction on microstate occurrence, while Figure 15 shows error bars of microstate occurrence in each condition. In particular, the occurrence of microstate classes A, B, and G increased significantly from REST to PU, IG, RIG, IE, and RIE ($ps = 0.000$). Similarly, the occurrence of microstate class E increased significantly from REST to IG, RIG, and RIE ($ps < 0.043$), while the occurrence of microstate class F increased significantly from REST to IG and IE ($ps = 0.000$). On the contrary. the occurrence of microstate class D decreased significantly from REST to PU, RIG, and RIE ($ps < 0.011$).

In addition, the occurrence of microstate class A decreased significantly from RIG and RIE to PU, IG, and IE ($ps < 0.003$), as well as from PU to IG ($p = 0.014$). The occurrence of microstate class B increased significantly from IG and IE to PU, RIG, and RIE ($ps < 0.011$). The occurrence of microstate class C decreased significantly from PU to RIG and RIE ($ps < 0.014$), from IG to RIG, IE, and RIE($ps < 0.002$), as well as from IE to RIE ($p = 0.016$). The occurrence of microstate class D decreased significantly from PU to RIG and RIE ($ps < 0.001$), as well as from IG and IE to PU, RIG, and RIE ($ps < 0.001$). The occurrence of microstate class F decreased significantly from IG and IE to PU, RIG, and RIE ($ps < 0.001$). The occurrence of microstate class G increased significantly from IE to RIG and RIE ($ps < 0.047$).

EEG microstate sequences

The finite entropy rate was 1.633 bits/sample (SE=0.021) for REST, 1.663 bits/sample (SE=0.016) for PU, 1.826 bits/sample (SE=0.018) for IG, 1.623 bits/sample (SE=0.017)

Table 11: P-values of pairwise comparisons with Bonferroni correction for microstate occurrence between CLASS (A, B, C, D, E, F, G) and CONDITION (rest (REST), problem understanding (PU), idea generation (IG), rating idea generation (RIG), idea evaluation (IE), and rating idea evaluation (RIE)).

Condition			Microstate classes												
			Class A		Class B		Class C		Class D		Class E		Class F		Class G	
REST	Vs.	PU	0.0^{***}	↗	0.0^{***}	↗	1.0		0.011^{*}	↘	0.162		1.0		0.0^{***}	↗
REST	Vs.	IG	0.0^{***}	↗	0.0^{***}	↗	0.406		0.387		0.043^{*}	↗	0.0^{***}	↗	0.0^{***}	↗
REST	Vs.	RIG	0.0^{***}	↗	0.0^{***}	↗	0.332		0.0^{***}	↘	0.015^{*}	↗	1.0		0.0^{***}	↗
REST	Vs.	IE	0.0^{***}	↗	0.0^{***}	↗	1.0		1.0		0.116		0.0^{***}	↗	0.0^{***}	↗
REST	Vs.	RIE	0.0^{***}	↗	0.0^{***}	↗	0.169		0.0^{***}	↘	0.012^{*}	↗	1.0		0.0^{***}	↗
PU	Vs.	IG	0.014^{*}	↘	0.0^{***}	↘	0.229		0.001^{***}	↗	1.0		0.001^{***}	↗	1.0	
PU	Vs.	RIG	0.001^{***}	↗	1.0		0.014^{*}	↘	0.001^{***}	↘	1.0		1.0		0.462	
PU	Vs.	IE	0.999		0.003^{***}	↘	1.0		0.001^{***}	↗	1.0		0.001^{***}	↗	0.997	
PU	Vs.	RIE	0.003^{***}	↗	1.0		0.002^{***}	↘	0.001^{***}	↘	0.335		0.404		1.0	
IG	Vs.	RIG	0.0^{***}	↗	0.001^{***}	↗	0.0^{***}	↘	0.0^{***}	↘	1.0		0.0^{***}	↘	0.084	
IG	Vs.	IE	1.0		1.0		0.002^{***}	↘	1.0		1.0		0.915		1.0	
IG	Vs.	RIE	0.0^{***}	↗	0.001^{***}	↗	0.0^{***}	↘	0.0^{***}	↘	1.0		0.001^{***}	↘	0.378	
RIG	Vs.	IE	0.001^{***}	↘	0.011^{*}	↘	0.11		0.0^{***}	↗	0.554		0.001^{***}	↗	0.028^{*}	↘
RIG	Vs.	RIE	1.0		1.0		1.0		1.0		1.0		1.0		1.0	
IE	Vs.	RIE	0.001^{***}	↗	0.006^{**}	↗	0.016^{*}	↘	0.0^{***}	↘	0.751		0.0^{***}	↘	0.047^{*}	↗

* $\rho \leq 0.050$, ** $\rho \leq 0.010$, *** $\rho \leq 0.005$
↗ microstate occurrence increases
↘ microstate occurrence decreases

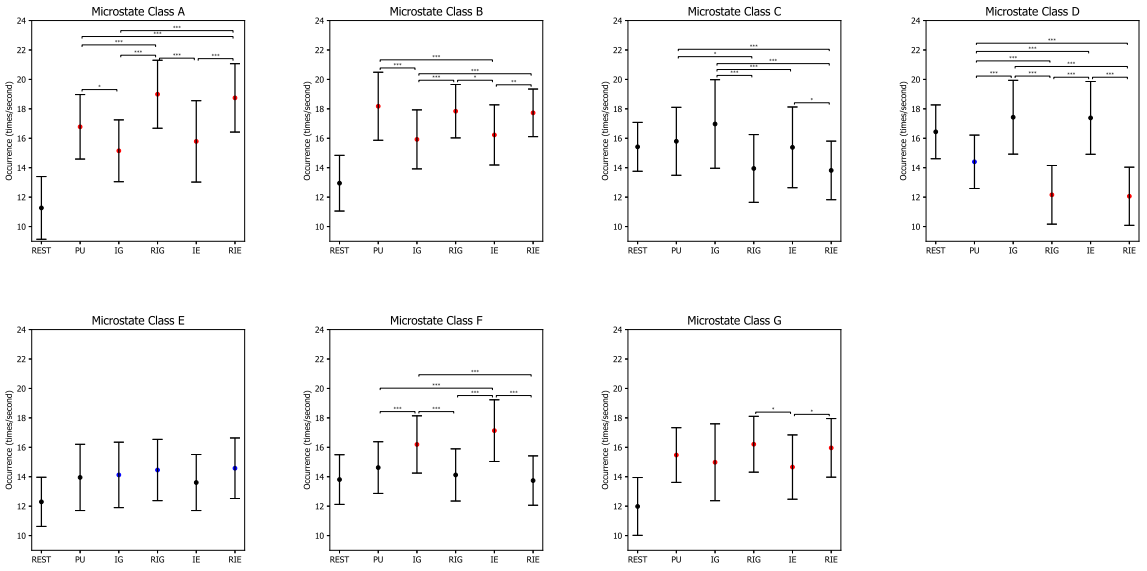

Figure 15: Error bars of microstate occurrence during rest (REST), problem understanding (PU), idea generation (IG), rating idea generation (IE), idea evaluation (IE), and rating idea evaluation (RIE). P-values between rest and other conditions are annotated by black dots ($p > 0.050$), blue dots ($p \leq 0.050$), yellow dots ($p \leq 0.010$), and red dots ($p \leq 0.005$). P-values between conditions are annotated by * ($p \leq 0.050$), ** ($p \leq 0.010$), *** ($p \leq 0.005$).

for RIG, 1.782 bits/sample (SE=0.017) for IE, and 1.595 bits/sample (SE=0.017) for RIE, when considering the previous 6 microstate labels. The repeated measures ANOVA revealed a significant effect CONDITION ($F(3.237, 84.153) = 40.629, p = 0.000, \eta^2 = 0.610$). Post hoc paired t tests with Bonferroni correction as shown in Figure 16 indicated that the entropy rate was higher during IG and IE compared to during REST, PU, RIG, and RIE ($ps < 0.001$), while the entropy rate was higher during PU compared to during RIE ($p = 0.006$).

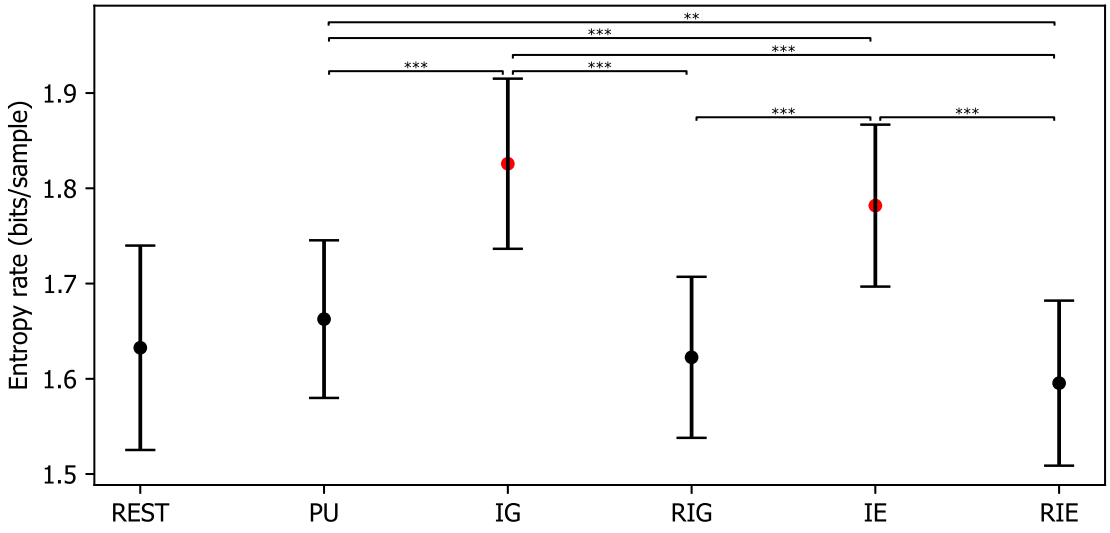

Figure 16: Error bars of entropy rate of microstate sequences during rest (REST), problem understanding (PU), idea generation (IG), rating idea generation (IE), idea evaluation (IE), and rating idea evaluation (RIE). P-values between rest and other conditions are annotated by black dots ($p > 0.050$), blue dots ($p \leq 0.050$), yellow dots ($p \leq 0.010$), and red dots ($p \leq 0.005$). P-values between conditions are annotated by * ($p \leq 0.050$), ** ($p \leq 0.010$), *** ($p \leq 0.005$).

The first-peak latencies in milliseconds of AIF was 50 (SE=1.6) for REST, 36 (SE=1.1) for PU, 42 (SE=1.6) for IG, 33 (SE=0.9) for RIG, 36 (SE=1.1) for IE, and 35 (SE=1.1) for RIE, when time lags were considered up to 200 ms. Figure 17 shows the mean and 95% confidence interval of AIF for each condition.

In addition, the Hurst exponent averaged from 35 partitions was 0.628 (SE=0.005) for

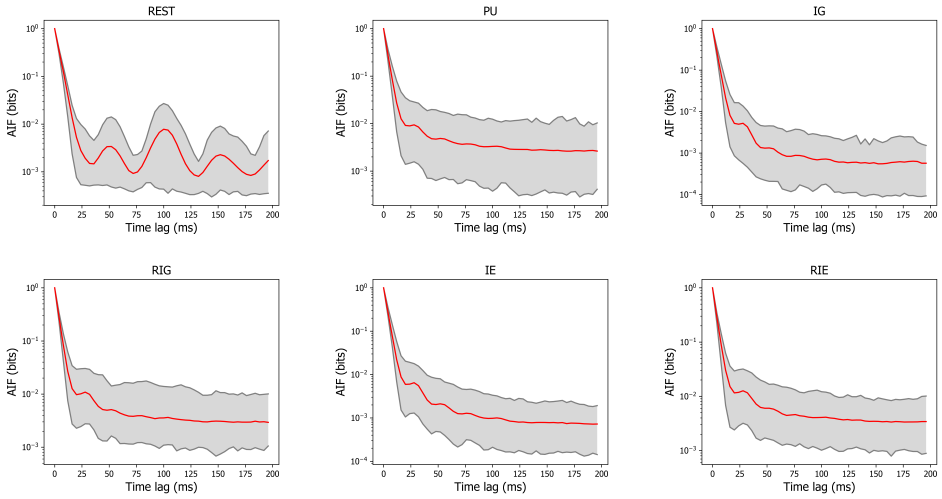

Figure 17: The autoinformation function for each condition. The red line represents the mean of autoinformation function across subjects for each condition, while the shaded area represents 95% confidence interval for each condition.

REST, 0.628 (SE=0.004) for PU, 0.594 (SE=0.003) for IG, 0.637 (SE=0.005) for RIG, 0.604 (SE=0.003) for IE, and 0.644 (SE=0.005) for RIE. The repeated measures ANOVA revealed a significant effect CONDITION ($F(3.276, 85.182) = 24.696, p = 0.000, \eta^2 = 0.487$). Post hoc paired t tests with Bonferroni correction as shown in Figure 18 revealed that the Hurst exponent was significantly lower during IG and IE compared to during REST, PU, RIG, and RIE ($ps < 0.041$), while the Hurst exponent was significantly lower during PU compared to during RIE ($p = 0.025$).

5.4 Discussion

Herein, we investigated the temporal dynamics of EEG-defined whole-brain neuronal networks during the conceptual design process in a loosely controlled setting. First, the loosely controlled setting simulated the natural design process to facilitate an ecologically valid neurocognitive study. The experiment setting provides sufficient response time to

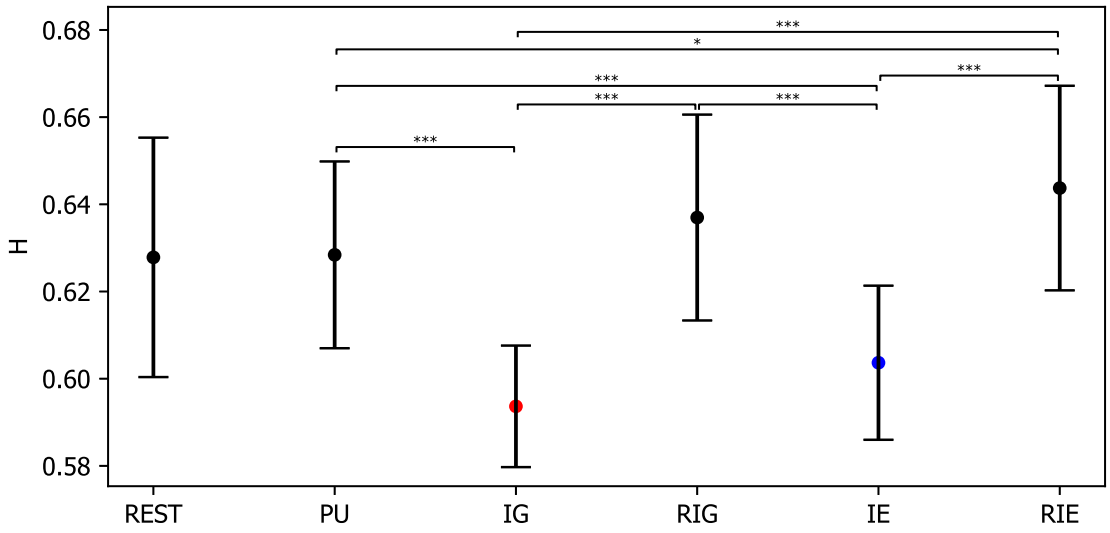

Figure 18: Error bars of Hurst exponent of microstate sequences averaged from 35 partitions during rest (REST), problem understanding (PU), idea generation (IG), rating idea generation (IE), idea evaluation (IE), and rating idea evaluation (RIE). P-values between rest and other conditions are annotated by black dots ($p > 0.050$), blue dots ($p \leq 0.050$), yellow dots ($p \leq 0.010$), and red dots ($p \leq 0.005$). P-values between conditions are annotated by * ($p \leq 0.050$), ** ($p \leq 0.010$), *** ($p \leq 0.005$).

accommodate the flexibility and freedom necessary for participants to explore potentially creative ideas. Simultaneously, the loosely controlled setting maintained certain degrees of control over the experiment by dividing the experiment into three main sub-design activities, which are problem understanding (PU), idea generation (IG), and idea evaluation (IE). NASA Task Load Index was added after IG and IE, namely rating idea generation (RIG) and rating idea evaluation (RIE), to subjectively measure participants' mental demand, time demand, performance, effort, and stress level. Secondly, the TRP analysis revealed that IG was associated with significant decreases in theta, alpha, and beta power, suggesting the highest cognitive workload and lowest cognitive control. Finally, the EEG microstate analysis indicated that microstate class C was more prevalent during IG while IG was associated with the shortest correlation times, supporting the lowest cognitive control in IG.

How are different conceptual design activities associated with cognitive workload?

The alpha band TRP analysis suggests differences among three groups of experimental conditions, which are IG, IE, and PU/RIG/RIE. It was found that IG, IE, and PU/RIG/RIE were associated with decreases in alpha power while the degrees of decreases in alpha power were the largest over almost all sites during IG, followed by during IE and PU/RIG/RIE. Decreased alpha power is considered as a reliable indicator of cognitive workload for ecologically valid tasks [193–195]. In addition, decreases in alpha power were associated with task difficulty [156,196,197], semantic memory [155,198], and attention [199], when these were manipulated to induce different levels of cognitive workload [200, 201]. These findings indicated that the IG task triggered the highest cognitive workload, followed by IE and PU/RIG/RIE.

Recent studies in the field of neurocognitive creativity demonstrated the functional role of changes in alpha power. Some studies indicated that alpha power decreased from rest to creativity-related tasks [39, 142, 156, 160] while others reported that alpha power increased from rest to creativity related tasks following a U-shaped curve [92, 134–136]. The former is in line with the finding that a reduction of alpha power is associated with a more complex and ill-defined problem, especially in ecologically valid settings where a higher cognitive workload is triggered [39, 156, 195]. In more ecologically valid settings such as design, not only functional but also performance factors need to be considered at the same time. The more factors are considered, the more task-relevant information would be processed and maintained in working memory. Such increased maintenance of task-relevant information is associated with alpha desynchronization [202]. The latter demonstrates an inhibitory top-down control process that inhibits task-irrelevant information to generate creative solutions [203–205]. Therefore, IG would maintain the greatest amount of task-relevant information

to generate solutions that meet design requirements, while IE would involve more task-relevant information to make preferential evaluations.

Besides, the obtained NASA-TLX results indicated that mental demand, time demand, effort, and stress decreased significantly from IG to IE, supporting the hypothesis that IG would trigger the highest cognitive workload. The degrees of cognitive workload may be affected by varying task difficulty and complexity, semantic process, and attention. The higher cognitive workload is associated with ill-defined problems compared to well-defined problems [156], as well as increases in task difficulty [196, 197]. Along the same line, the degrees of ill-definedness and task difficulty are the highest during IG, the lowest during PU/RIG/RIE, and at an intermediate level during IE. More specifically, participants are confronted with the most well-defined problems during RIG and RIE, and read/comprehend/decompose design requirements during PU. During IG, on the contrary, participants are dealing with ill-defined problems, synthesising and evaluating knowledge recursively to generate/detail/elaborate solutions, which in turn reformulate design requirements. IE is not as complex or ill-defined as IG, but is more complex than PU/RIG/RIE in that participants apply the knowledge generated in PU and IG to judge the existing solutions without pre-defined judging criteria/constraints. In sum, not only EEG but also behavioural findings suggest that IG would be associated with the highest cognitive workload.

Indeed, cognitive workload and mental stress in conceptual design could be triggered by uncertainty and recursivity, which are two fundamental characteristics of design. Uncertainty inherits from ill-defined design statements and would last throughout the conceptual design process due to recursivity. Incomplete and imprecise information collected from design statements may heighten the degrees of uncertainty and unpredictability, which could be linked to mental stress such that Mental Stress = Perceived Workload / ((Knowledge + Skills) * Affect) as defined in Nguyen and Zeng (2012) [58]. Designer's affect could be

very low when uncertainty becomes high, as Grupe and Nitschke (2013) stated that 'uncertainty diminishes how efficiently and effectively we can prepare for the future and thus contributes to anxiety' [206]. Consequently, the mental stress would increase and more knowledge and skills are required to compensate for the decreasing affect in designer's effort to complete the task. Such variations in designer's mental stress, affect, knowldge, and skills, indicate that cognitive workload may increase with increasing uncertainty, which is supported by a meta-analysis of fMRI studies showing that the brain is more active under conditions of uncertainty, compared to certainty [207]. From this viewpoint, participants tend to experience the most uncertainty during IG whereas they are more certain about their solutions during RIG/RIE. Therefore, the higher cognitive workload would be induced in IG due to its greater degrees of uncertainty.

Furthermore, recursivity demonstrates continuous evolution during the conceptual design process in which goals, solutions, and knowledge evolve simultaneously [2, 32, 33]. The newly generated solutions will not only improve the designe's understanding but also help reformulate the design problem. The reformulated design problem will trigger the designer to identify new knowledge to elaborate the previous solutions or regenerate different tentative solutions, which in turn updates the design problem. High cognitive workload would be triggered during such a recursive process as designers need to maintain a large amount of multidimensional information and their relationships with goals, solutions, and knowledge. IG seems to share the most features of the recursive design process whereas PU/RIG/RIE share the most similarity with well-defined problem solving. Therefore, higher cognitive workload would be induced during IG compared to IE and PU/RIG/RIE.

How are different conceptual design activities associated with cognitive control?

The TRP analysis in theta and beta bands suggests differences among three groups of experimental conditions, which are IG, IE, and PU/RIG/RIE. It was found that theta and beta power increased over frontal sites from REST to PU/RIG/RIE and IE, whereas they decreased over all sites from REST to IG. A comparison within design activities indicated that theta and beta power increased significantly over almost all sites from IG to IE, and PU/RIG/RIE, as well as from IE to PU/RIG/RIE, while theta and beta power did not show significant differences over almost all sites in PU/RIG/RIE. Increased theta power over the frontal sites has been viewed as a function of working memory and cognitive control. Generally, increased frontal theta activity has been interpreted as a need for increased cognitive control in response to conflict [94, 208], encoding and retrieval of information from working memory [93, 127], while increased beta activity is associated with the maintenance of intended status quo [209]. These findings indicated that IG, IE, PU/RIG/RIE triggered cognitive control with the lowest to the highest intensities, respectively.

Higher cognitive control is beneficial to goal-directed contexts, whereas lower cognitive control is helpful to learning and creative problem-solving contexts [192]. The heightened cognitive control in the PU/RIG/RIE group may result from ignoring distractors in the reading activity, which could improve reading speed and comprehension [210, 211]. Alternatively, the increased cognitive control in the PU/RIG/RIE group may result from the "structured" process, which could narrow the focus of attention on a well-defined target. Besides, increases in theta power over frontal sites from IE and RIG/RIE to REST indicated the involvement of more cognitive control during IE and RIG/RIE, which is in line with increases in theta power being associated with heightened cognitive control during the complex decision-making [186]. Interestingly, IE involved less cognitive control compared

to RIG/RIE due to the smaller increases in theta power, even if IE and RIG/RIE shared similar evaluative process. This difference in cognitive control may be ascribed to the properties of evaluative criteria, such as abstractness and quantity. Riddle and colleagues reported that a higher level of abstraction rules is linked to decreased beta amplitude while a larger number of rules is associated with increased theta amplitude [188]. Our analysis indicated the same findings in that beta power decreased significantly over frontal, central, and temporal sites from RIG/RIE to IE while theta power increased significantly over frontal, central, and temporal sites from IE to RIG/RIE. Indeed, IE involved higher level of abstraction rules compared to RIG/RIE in that participants needed to express their preferences without an explicit criterion. IE could be categorized as internally guided decision-making whereas RIG/RIE could be categorized as externally guided decision-making. The internally guided decision-making would involve less cognitive control compared to externally guided decision-making [80]. These findings suggest that higher cognitive control results from the heightened attention during more "structured" processes such as PU/RIG/RIE, while less cognitive control results from internally oriented processes, such as IE.

Furthermore, the lowest cognitive control was associated with IG compared to IE and PU/RIG/RIE. IG is typically viewed as a mixed process between self-generated and task-initiated thoughts [192]. A study of the role of inhibition in creativity revealed that lower cognitive control enhanced the frequency and originality of ideas [212]. In the same vein, lower cognitive control may incubate a few critical activities, such as mind wandering [77] and hypofrontality [213, 214], to improve creative performance. In addition, a study of musical improvisation indicated that creative improvisation was characterized by a dissociated pattern of activity in the prefrontal cortex [215]. Less activation in the prefrontal cortex could reduce cognitive control, which may help participants overcome fixation or associate objects that are semantically less similar to reinterpret the design problem [72]. In the same lines, neuroimaging studies indicated that creative idea generation is associated

with activation of the DMN resulting from reduced cognitive control [38, 103]. However, a recent study reported interactions between the DMN and the cognitive control network underlying creativity [216], suggesting that the balance between the DMN and cognitive control network may benefit flexible regulation for creative performance [175, 217]. Our findings regarding decreased alpha and theta power in IG support the argument that IG involves not only increased cognitive workload but also reduced cognitive control. Further study is needed to shed light on the temporal dynamics of brain networks during the conceptual design process.

How are different conceptual design activities associated with the range of temporal correlations?

Our analysis of microstate parameters and temporal correlations within microstate sequences suggests differences between two groups of experimental conditions, IG and IE on one side, and PU, RIG, RIE on the other side.

Summarizing the microstate parameters coverage, duration and occurrence, we found a prevalence of microstate classes A and B during the conditions PU/RIG/RIE, whereas microstate classes C and D were more prominent during REST, IG and IE. An increased coverage and occurrence of classes C and D during rest is probably related to the fact that their topography reflects the parieto-occipital dominance of resting-state alpha oscillations. The relation with conditions IG and IE is less clear. One explanation is that all design tasks involved visuo-spatial imagery, which would activate occipital (visual) and parieto-occipital cortices. Combining EEG microstate analysis and source reconstruction, microstate class C has been found to correlate with activity in the precuneus [141], which is involved in visuospatial processing and introspection, both of which may play a role during IG. In regard to cognitive control, the microstate literature has not reached a consensus so far. As reviewed by Michel and Koenig [84], positive as well as negative correlations

of microstate class C with cognitive control mechanisms have been reported. Assuming that the RIG/RIE conditions correspond to a higher level of cognitive control, our results suggest that microstate class C is negatively correlated with cognitive control, and that microstate classes A and B indicate more control. This interpretation would agree with the results found in the studies of cognitive processes that microstate C reflects activity in the DMN [178, 179].

The microstate classes (E,F,G) showed less pronounced differences between the experimental conditions. Microstate class F was more prominent during IE, and microstate class G was more pronounced during RIG/RIE.

The current literature on the relationship between individual microstate classes and cognitive functions still contains open discussions [84]. Moreover, the assignment of topographies obtained from clustering algorithms to specific microstate classes (A-G) can be challenging, especially when more than four microstate classes are used. For this reason, and hypothesizing that cognitive activities might be better captured by dynamic microstate properties, we analyzed temporal correlations of microstate sequences and found marked differences between our experimental conditions.

We analyzed temporal microstate correlations for short, intermediate and long time scales, and observed the following patterns. Short- and long-range correlations, as measured by the finite entropy rate and Hurst exponents respectively, gave consistent results. The finite entropy rate in IG and IE was significantly larger than in the PU/RIG/RIE group. This indicates a faster decorrelation, or a lower predictability, in the former group. Thus, a short sequence of IG/IE microstates ($k = 6$ samples in our case) encodes much less information about which network will activate next, compared to PU/RIE/RIG. A matching observation was made via Hurst exponent analysis for time scales approximately 100 times longer compared to the scale assessed by the entropy rate. Conditions IG and IE showed Hurst exponents closer to $H = 0.5$, which indicates uncorrelated activity, and therefore less

long-range correlated activity than found in the PU/RIG/RIE conditions. Taken together, these findings suggest that functional brain networks, as measured by EEG microstates, retain less memory about their previous trajectory during IG and IE.

In terms of our cognitive control hypothesis, we conclude that during problem understanding (PU) and rating (RIG,RIE) the brain exerts a stronger cognitive control over network transitions, and that this control is reflected by a more deterministic brain state trajectory, eventually producing a more predictable microstate sequence. During IG and IE, the interplay of functional networks appears less restricted. Interpreting the microstate sequence as a process of stochastic transitions between functional brain networks, a larger entropy rate means that the brain has more degrees of freedom in choosing the next network configuration. In relation to the performed tasks, this less restricted mode of operation might reflect the creativity component of the task, especially during IG, which shows the maximum entropy rate and the lowest Hurst exponent. In our framework, the increasing entropy rate is mediated by a relaxation of cognitive control mechanisms.

In this context, it is interesting to look at intermediate time scales, where oscillatory brain activity becomes apparent. Microstate frequency analysis has been developed only recently, where periodic microstate patterns linked to alpha oscillations were described during the resting state [130]. Our AIF analysis (Figure 17) shows that the alpha frequency linked microstate oscillations (time lag 100 ms) of the resting state are substituted by higher frequencies as soon as the brain engages in the cognitive tasks. The conditions PU/RIG/RIE show the highest microstate frequencies (AIF peaks at the lowest time lags), corresponding to the lower beta frequency band around 14 Hz. These findings match the TRP analysis where beta and theta frequencies appear during PU/RIG/RIE over bilateral fronto-temporal areas. Likewise, TRP analysis for IG showed a decrease in theta and beta oscillatory activity, explaining why the AIF during IG shows peaks at longer time lags, i.e. less beta frequency contributions. As cognitive control mechanisms are known to be mediated by

theta frequencies [93], we conclude that our cognitive control model is consistent not only with the TRP results, but also with the temporal microstate analysis across all time scales. The added value of microstate frequency analysis is that the identified frequencies indicate periodic behaviour of entire large-scale brain networks, rather than analyzing oscillations at the single sensor level. Our data suggest that cognitive control is associated with periodic activity of large-scale networks in the beta frequency band.

Of note, entropy rates, Hurst exponents and AIF coefficients are independent of how the microstate label assignment to the microstate maps is chosen. As seen in Figure 12, in the case of seven microstate classes the assignment of the k-means output to the labels A-G reported in the literature can be ambiguous. As the entropy-based quantities (entropy rate, AIF) reported in this study would be the same for any label assignment, this methodology adds further robustness to our results.

5.5 Conclusion

This present study was designed to investigate temporal dynamics of brain activity in response to distinct design activities during the conceptual design process through a loosely controlled setting. The loosely controlled setting simulated the natural design process to facilitate an ecologically valid neurocognitive study, which offered sufficient response time for participants to freely explore potentially creative solutions while maintaining certain degrees of control through segmenting the conceptual design process into sub-design activities, including problem understanding, idea generation, rating idea generation, idea evaluation, and rating idea evaluation. Aligning our findings with those of other validated evidence, the TRP analysis revealed that idea generation was associated with significant decreases in theta, alpha, and beta power, suggesting the highest cognitive workload and lowest cognitive control. In the same vein, the EEG microstate analysis indicated that microstate class C was more prominent during idea generation. Further temporal dynamics

analysis found that idea generation was consistently associated with the shortest correlation times, as measured by the finite entropy rate, AIF, and Hurst exponent. This finding suggests that the interplay of functional brain networks is less restricted during idea generation, supporting the idea that the brain has more degrees of freedom during tasks involving creativity. Taken together, we conclude that idea generation is associated with the highest cognitive workload and lowest cognitive control, consistently supported by TRP and microstate analysis.

Chapter 6

Capturing temporal dynamics of network oscillations in design creativity

6.1 Introduction

The results in Chapter 5 indicated that cognitive activities in design creativity have long-range temporal correlations. This study further investigates temporal dynamics of network oscillations in design creativity through answering three questions: (i) can we capture temporal dynamics of network oscillations in design creativity? (ii) how far can we predict from current temporal dynamics of network oscillations in design creativity; (iii) can we use temporal dynamics of network oscillations to classify different cognitive activities in design creativity?

G*ä*rtner and colleagues modeled EEG microstate sequences using a first-order Markov chain in which the current microstate state depends on only one previous microstate state [218]. The following studies applied the first-order microstate transition matrix to demonstrate the temporal dynamics of microstates during rest [219, 220] and cognitive processes, such as mental calculation [178], self-reported/self-generated thoughts [177, 179]. However, Gschwind and colleagues challenged the approach of low-order Markov chain due to

ignoring the long-range dependency [221].

Recurrent neural network (RNN) shows its own superiority in processing time series or sequential data [222], which can be borrowed to implicitly model EEG microstate sequences. In RNN's hidden state, the output from the previous time step is fed as input to the current time step. This typical recurrent connection enables RNN to update the current state based on past states and current input data. Hence, RNN performs well in capturing temporal dynamics of sequential data, with the capability of memorizing previous information. However, the standard RNN fails to explore long-term dependencies because of the gradient vanishing problem [223]. Two improved versions of RNN, i.e., long-short term memory (LSTM) [224] and gated recurrent unit (GRU) [225] are then proposed better to analyze the temporal information of the input sequence.

LSTM has been shown to be capable of storing and accessing information over a very long timespan by introducing a memory cell to control the previous information [226]. LSTM can update existing memory at each time step through three introduced gates: input gate, forget gate, and output gate. These gates determine whether the input is significant enough to remember, whether it should continue to keep or forget the value and whether it should output the value, respectively. LSTM can migrate the gradient vanishing problem using explicit gating mechanisms and carry important information over a long-range. Therefore, LSTM is widely used in a variety of tasks to capture potential long-term temporal dependencies [227–230].

GRU is recently proposed as a simpler alternative to the LSTM that can capture dependencies of different time steps by modulating the information flow inside the unit. GRU does not have memory cells and uses hidden states to transfer the long-term information directly with only two gates: reset gate and update gate. The simpler structure makes GRU's training process is faster than LSTM's. However, it is difficult to conclude which types of improved RNNs would perform better in general

Therefore, this research will use LSTM and GRU to test (i) whether temporal dynamics of network oscillations can be captured in design creativity by reconstructing EEG microstate sequences reproducibly; (ii) whether temporal dynamics of network oscillations can be predicted in design creativity by lagging certain time points; (iii) whether different cognitive activities can be classified in design creativity by considering their temporal dynamics of network oscillations.

6.2 Method

Figure 19 shows the overview framework for reconstruction, predication, and classification of EEG microstate sequences. The encoder and decoder were made up of the autoencoder architecture for two subtasks: the reconstruction and prediction of EEG microstate sequences, while the encoder and classifier formed the framework for the classification task.

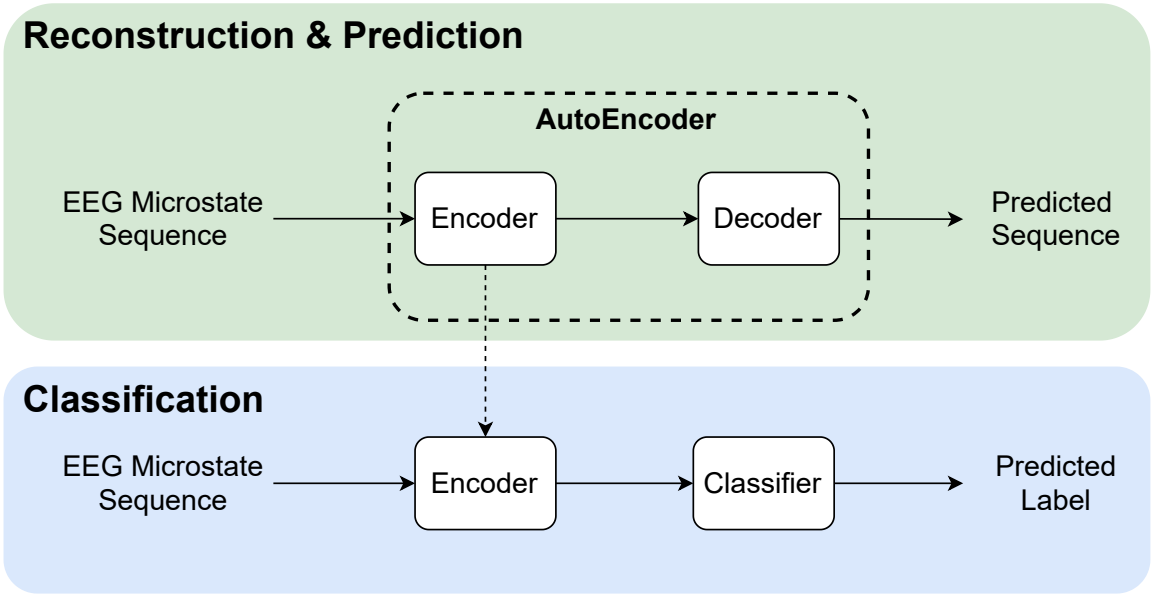

Figure 19: The overview of encoder-decoder architecture for reconstruction, prediction, and classification of EEG microstate sequences.

6.2.1 Reconstruction of EEG microstate sequences

The goal of the reconstruction task was to approximate the output to the input as closely as possible with a sequence-to-sequence (Seq2Seq) AE, which was divided into two main parts as shown in Figure 20. At first, the encoding block, which comprised the one-hot layer and encoder, transformed a variable-length EEG microstate sequence into a vector representation that contained latent information of the input sequence. Then, the decoding block, which consisted of the decoder and *argmax* operation, was followed to convert the vector representation back to the original EEG microstate sequence.

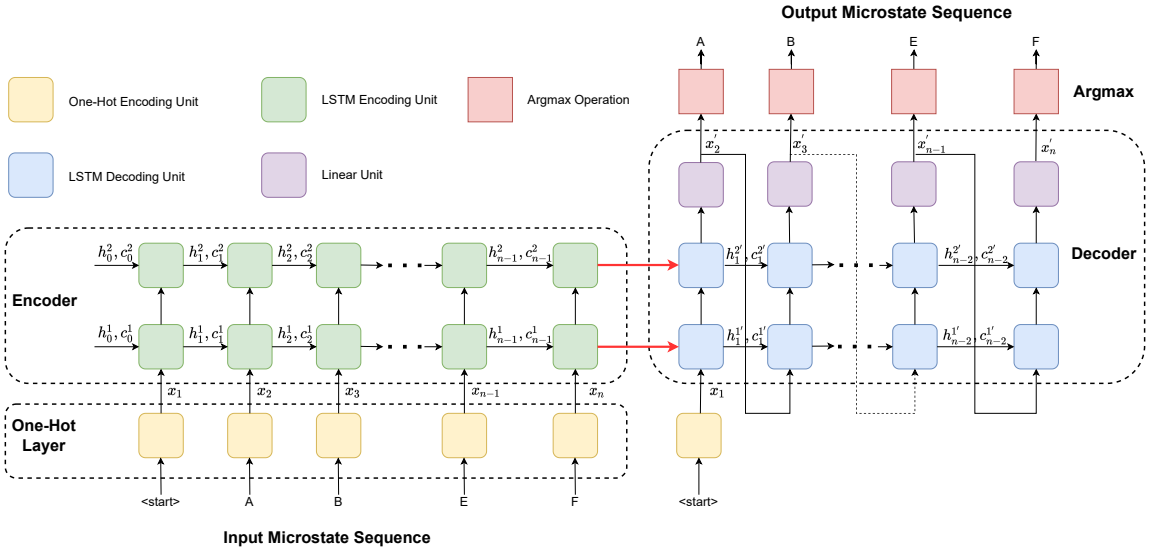

Figure 20: The detail of encoder-decoder architecture along with LSTM network for reconstruction and prediction of EEG microstate sequences.

Encoding block

The encoding block included an one-hot layer and an encoder. The one-hot layer was to convert EEG microstate sequences from categorical variables to numerical variables. For instance, $\mathbf{l} = \{l_0, l_2, \cdots, l_N\}$ represents a EEG microstate sequence, in which l_0 represents a start token while $l_n\,(n > 0)$ represents a categorical variable with one of EEG

microstate classes from A to G. For each element in an EEG microstate sequence, An one-hot layer was to map a categorical variable (A to G) to a numerical vector ($(1, 0, \cdots, 0, 0)$ to $(0, 0, \cdots, 1, 0)$), as well as a start token into a numerical vector $(0, 0, \cdots, 0, 1)$. The obtained numerical microstate sequence $\mathbf{x} = \{x_0, \cdots, x_N\}$ was then set as the input of the encoder.

Next, the encoder was to extract latent representations of $\mathbf{x}$, which contains information of temporary dynamics of EEG microstate sequence. A LSTM and GRU networks were implemented as the encoder to extract such information, respectively. The left parts in Figure 20 shows the architecture of encoder containing of two-layer LSTM network as an example. Equation 8 represents the inputs and outputs of encoder at each time step, where h_n^* is a hidden state at time step n for the *-th layer of LSTM network while c_n^* is a cell state at time step n for the *-th layer of LSTM network. Note that the initial hidden state h_n^0 and cell state c_n^0 were set as zeros, which were default values generally.

$$\begin{aligned} (h_n^1, c_n^1) &= \text{EncoderLSTM}^1(x_n, (h_{n-1}^1, c_{n-1}^1)) \\ (h_n^2, c_n^2) &= \text{EncoderLSTM}^2(h_n^1, (h_{n-1}^2, c_{n-1}^2)) \end{aligned} \tag{8}$$

Once the final EEG microstate x_N has been passed into the LSTM encoder, the (h_N^1, c_N^1) and (h_N^2, c_N^2) are considered as the latent representations of the entire EEG microstate sequence.

Decoding block

The decoding block included a decoder and an argmax operation. The decoder was to convert the extracted latent representations to an estimated numerical EEG microstate sequence $\mathbf{x}'$. The LSTM and GRU network was implemented as the decoder, respectively. The right parts in Figure 20 shows the architecture of decoder containing of two-layer LSTM network as an example. Equation 9 represents the inputs and outputs of decoder

and argmax operation at each time step, where $o_n^{2'}$ is an output at time step n for the second layer of LSTM network while $f(\cdot)$ was to transfer the $o_n^{2'}$ into the EEG microstate numerical vector ${x'}_{n+1}$. Note that the initial hidden and cell states of the decoder were the latent representations that were extracted from the encoder. Finally, the reconstructed EEG microstate l' was obtained by employing an argmax operation to estimate the label of the ${x'}_n$ from the output layer at each time step.

$$
\begin{aligned}
o_n^{1'}, (h_n^{1'}, c_n^{1'}) &= \text{DecoderLSTM}^1({x'}_n, (h_{n-1}^{1'}, c_{n-1}^{1'})) \\
o_n^{2'}, (h_n^{2'}, c_n^{2'}) &= \text{DecoderLSTM}^2(h_n^{1'}, (h_{n-1}^{2'}, c_{n-1}^{2'})) \\
{x'}_{n+1} &= f(o_n^{2'})
\end{aligned}
\tag{9}
$$

6.2.2 Prediction of EEG microstate sequences

Prediction of EEG microstate sequences has the same architecture with reconstruction of EEG microstate sequences, but with different inputs of the decoder. The input of encoder was the EEG microstate sequence l while the input of decoder was the EEG microstate sequence with k time steps lagging $\hat{\mathrm{l}} = \{l_0, l_{k+1}, l_{k+2}, \cdots, l_{k+N}\}$ and the hidden and cell states extracted from the encoder.

6.2.3 Classification of EEG microstate sequences

Researchers have proved that the alterations of temporal dynamics of EEG microstate sequences are related to the disturbances of mental processes under neurological and psychiatric conditions [229]. Based on these findings, our task in this section was to explore whether the latent representation of EEG microstate sequence can be used as features in the classification of cognitive activities in design creativity. As shown in the bottom part of Figure 19, the classification framework can be divided into two main blocks: encoder (feature extractor) and classifier. The details of each block are given as Figure 21, which

will be described as following.

The encoder has been trained in the task of reconstruction of EEG microstate sequences to extract the latent representations, which include temporary dynamics of EEG microstate sequences. There were six independently trained encoders for EEG microstate sequences collected from rest, problem understanding, idea generation, rating idea generation, idea evaluation, and rating idea evaluation, which were named as EncoderRest, EncoderPu, EncoderIG, EncoderRIG, EncoderIE, and EncoderRIE. The six encoders were used to encode an EEG microstate sequence independently, which would output six independent vectors. Such the six independent vectors would be concatenated to one vector as an input feature vector for a classifier. Next, different classifiers were used to distinguish EEG microstate sequences from different activities, which included naive Bayes (NB), support vector machine (SVM), fully-connected neural network (FNN), and conventional neural network (CNN).

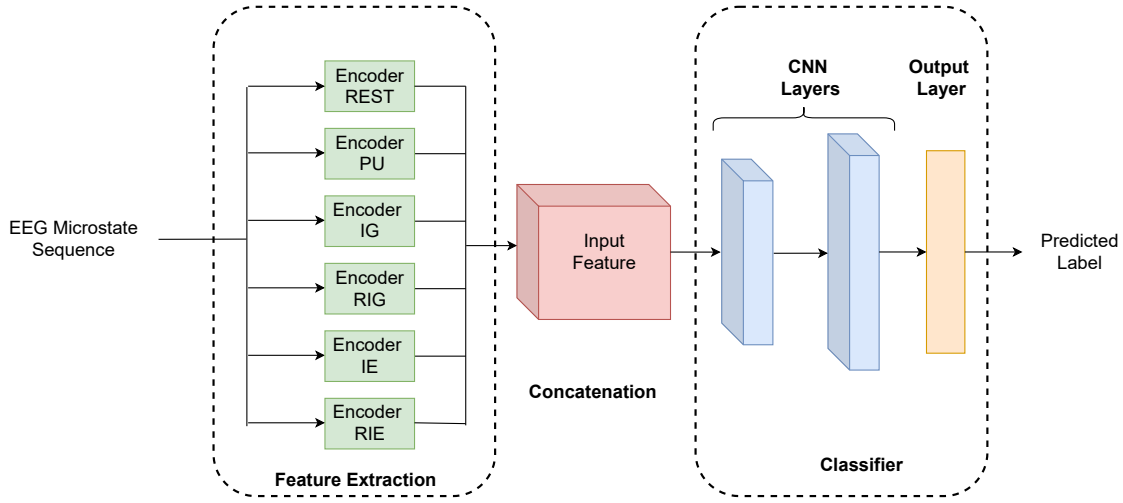

Figure 21: The detail of encoder-decoder architecture along with CNN network for classification of EEG microstate sequences.

6.2.4 Network configuration

The encoder and decoder could be implemented by LSTM or GRU networks. The details of LSTM network configuration would be described as follows while the GRU network has similar configuration but without the cell state. The inputs of encoder included three components: data, initial hidden and cell states. The data input had a dimension of $(\text{frame\_length}, \text{batch\_size}, \text{feature\_size})$, where frame_length represented the length of frame of EEG microstate sequences; batch_size represented the number of frames in each batch, that was 8; feature_size represented the number of EEG microstate classes adding start token, that was 8. For the reconstruction and classification tasks, the frame length of EEG microstate sequences varied among 100 ms, 200 ms, 400 ms, 800 ms. For the predication task, the frame length of EEG microstate sequences was 200 ms. The initial hidden and cell states of encoder had the same dimensions of $(\text{layer\_number}, \text{batch\_size}, \text{hidden\_size})$, where layer_size represented the number of layers, that was 2; hidden_size represented the number of features in the hidden state, that was 64. The inputs of decoder had the same dimensions with encoder while the initial hidden and cell states of the decoder were the final hidden and cell states of encoder.

In addition, two-layers CNN and a linear output layer constituted a CNN-based classifier. The input of the first CNN layer has a dimension of $(\text{batch\_size}, \text{in\_channels}, \text{in\_length})$, where batch_size was 32; in_channels represented the number of channels in the input sequences, that was 6 obtained from the number of trained encoders; in_length represented the length of input sequences, that was 64 obtained from trained encoder. The number of channels of the first layer was 64. As such, the input dimension of the second CNN layer was $(32, 64, 64)$ while the output dimension was $(32, 128, 64)$. The output of the second CNN layer was flattened and then passed to the output layer whose input dimension and output dimension were $64 \times 128 = 8192$ and 6, respectively.

6.2.5 Evaluation metrics on reconstruction, prediction, and classification of EEG microstate sequences

The performance of the reconstruction and predication of EEG microstate sequences was measured by accuracy in Eq. 10, for each condition and each participant. The overall performance of the reconstruction and predication was measured by mean accuracy and its standard error across conditions and participants.

$$\text{Accuracy} = \frac{\text{number of correctly predicted microstates}}{\text{length of microstate sequence}}, \tag{10}$$

The performance of classification of EEG microstate sequences was measured by sensitivity/recall, specificity, precision, and F-measure. Theses measures were typically used in binary classification. Therefore, generalizations of these measures were needed in this multiclass classification by dividing the multiclass classification into several binary classification [231]. The overall performance of the multiclass classification were measured by mean accuracy and its standard error across conditions and participants. For each class, the sensitivity/recall, specificity, precision, and F-measure are listed as follows:

$$\begin{aligned}
\text{Sensitivity} &= \frac{\text{TP}}{\text{TP+FN}}, && (11)\\
\text{Specificity} &= \frac{\text{TN}}{\text{TN+FP}}, && (12)\\
\text{Precision} &= \frac{\text{TP}}{\text{TP+FP}}, && (13)\\
\text{F-measure} &= 2 \cdot \frac{\text{precision} \cdot \text{recall}}{\text{precision+recall}}, && (14)
\end{aligned}$$

where TP is the number of true positive predictions; TN is the number of true negative predictions; FP is number of false positive predictions; and FN is the number of false negative predictions.

6.3 Results

6.3.1 Reconstruction of EEG microstate sequences

Table 12 shows accuracy results of reconstruction of EEG microstate sequences considering different frame length, overlap rate, RNN type, and tasks condition. The reconstruction accuracy was the most sensitive to the frame lengths. The frame lengths of 100 ms and 200 ms resulted in significantly higher reconstruction accuracy compared to the frame lengths of 400 ms and 800 ms. The 75% overlap rate between neighbouring frames resulted in significantly higher reconstruction accuracy compared to the 50% and 0% overlap rate between neighbouring frames. In most case, GRU performed well than LSTM in terms of reconstruction accuracy.

For each task condition, the highest and lowest reconstruction accuracies were demonstrated as follows. For REST, 99.65% reconstruction accuracy resulted from the frame length of 100 ms, 75% overlap rate between neighbouring frames, and LSTM. 27.41% reconstruction accuracy resulted from the frame length of 800 ms, 0% overlap rate between neighbouring frames, and GRU. For PU, 99.88% reconstruction accuracy resulted from the frame length of 100 ms, 75% overlap rate between neighbouring frames, and LSTM. 31.99% reconstruction accuracy resulted from the frame length of 800 ms, 0% overlap rate between neighbouring frames, and GRU. For IG, 99.99% reconstruction accuracy resulted from the frame length of 100 ms, 75% overlap rate between neighbouring frames, and LSTM. 38.85% reconstruction accuracy resulted from the frame length of 800 ms, 0% overlap rate between neighbouring frames, and LSTM. For RIG, 99.87% reconstruction accuracy resulted from the frame length of 100 ms, 75% overlap rate between neighbouring frames, and GRU. 31.31% reconstruction accuracy resulted from the frame length of 800

ms, 0% overlap rate between neighbouring frames, and GRU. For IE, 99.97% reconstruction accuracy resulted from the frame length of 100 ms, 75% overlap rate between neighbouring frames, and GRU. 39.03% reconstruction accuracy resulted from the frame length of 800 ms, 0% overlap rate between neighbouring frames, and LSTM. For RIE, 99.81% reconstruction accuracy resulted from the frame length of 100 ms, 75% overlap rate between neighbouring frames, and GRU. 31.45% reconstruction accuracy resulted from the frame length of 800 ms, 0% overlap rate between neighbouring frames, and GRU.

Generally, the reconstruction accuracy was higher for shorter frame lengths, larger overlap rate between neighbouring frames, and GRU. Once the frame lengths were larger than 200 ms, the reconstruction accuracy decreased significantly. Regardless of overlap rate and RNN type, around 93% reconstruction accuracy were for shorter frame lengths of 100 ms and 200 ms. A recent study of EEG microstate sequences revealed that around 90% reconstruction accuracy were for shorter frame lengths of 200 ms and 400 ms using LSTM during rest [229]. This study also found that the reconstruction accuracy of random sequences were around 25% for frame lengths of 200 ms and 400 ms. These results indicated that RNN techniques are capable of capturing the temporal dynamics of EEG microstate sequences in design creativity.

Additionally, significantly low reconstruction accuracy for longer frame lengths of 400 ms and 800 ms corroborates the nonstationary nature of EEG signals in design creativity. This approximation has a little bit different from previous studies that estimate the long-range memory effects of EEG microstate sequences last up to 2000 ms during rest [180, 221, 229]. This difference may result from design creativity that involves complex and high-order cognitive activities, such decision-making and incubation. Such complex and high-order cognitive activities have less restrictions on brain networks, leading to rapid and irregular changes of EEG microstate sequences.

Table 12: Accuracy results for reconstruction of EEG microstate sequences considering frame length, overlap rate, RNN type, and task condition. The results are presented as Mean ± S.E. across subjects, while the best results are marked by bold font.

Frame Length	Overlap Rate	RNN Type	Task Condition						
			REST	PU	IG	RIG	IE	RIE	AVG
100 ms	0 %	LSTM	93.08±0.47	96.18±0.71	99.88±0.03	95.92±0.59	99.71±0.07	94.90±0.66	96.61±0.28
		GRU	**95.08±0.35**	**97.78±0.39**	**99.93±0.01**	**97.71±0.35**	**99.83±0.04**	**96.78±0.53**	**97.85±0.19**
	50 %	LSTM	97.91±0.16	99.08±0.19	99.95±0.01	99.16±0.12	99.93±0.01	98.69±0.22	99.12±0.08
		GRU	**98.74±0.11**	**99.47±0.09**	**99.97±0.00**	**99.52±0.07**	**99.94±0.01**	**99.30±0.13**	**99.49±0.05**
	75 %	LSTM	**99.65±0.04**	**99.88±0.02**	**99.99±0.00**	99.87±0.02	99.97±0.02	99.81±0.04	**99.86±0.01**
		GRU	99.61±0.03	99.85±0.02	99.98±0.00	99.87±0.02	**99.97±0.01**	**99.81±0.02**	99.85±0.01
200 ms	0 %	LSTM	71.79±1.27	77.66±1.21	92.38±1.13	**79.11±0.84**	87.19±1.28	**78.73±0.89**	81.14±0.70
		GRU	**75.88±0.89**	**78.82±1.76**	**94.20±0.87**	77.66±1.17	**92.63±0.77**	74.42±1.31	**82.27±0.79**
	50 %	LSTM	80.82±1.21	82.42±1.22	92.84±1.05	82.01±0.93	90.55±1.15	81.33±1.11	84.99±0.59
		GRU	**84.53±0.90**	**87.76±1.11**	**97.91±0.30**	**84.89±1.00**	**96.64±0.46**	**83.87±1.02**	**89.27±0.57**
	75 %	LSTM	86.65±0.95	88.11±1.23	95.00±0.78	86.91±1.06	92.96±0.96	85.99±0.83	89.27±0.48
		GRU	**92.16±0.53**	**92.99±0.83**	**98.96±0.14**	**92.47±0.87**	**98.29±0.26**	**91.98±0.68**	**94.47±0.34**
400 ms	0 %	LSTM	36.98±1.26	46.75±1.06	55.83±1.62	**48.62±0.77**	55.22±1.17	**49.52±0.79**	48.82±0.68
		GRU	**42.05±1.30**	**48.16±1.32**	**63.61±1.26**	47.93±0.99	**60.27±1.21**	46.16±0.96	**51.36±0.78**
	50 %	LSTM	45.26±1.24	51.03±1.07	62.34±1.56	52.04±0.73	59.59±1.34	50.87±0.85	53.52±0.65
		GRU	**51.79±0.99**	**55.66±1.15**	**69.43±1.11**	**54.39±0.84**	**65.94±1.16**	**54.46±0.96**	**58.61±0.67**
	75 %	LSTM	53.43±1.21	55.84±1.31	68.30±1.68	55.07±0.81	63.73±1.37	54.50±0.72	58.48±0.66
		GRU	**60.72±1.30**	**60.97±1.04**	**74.09±1.05**	**60.47±0.78**	**69.03±0.93**	**60.11±0.95**	**64.23±0.59**
800 ms	0 %	LSTM	**28.00±0.99**	**35.73±0.65**	38.85±0.88	**37.47±0.64**	39.34±0.82	**36.92±0.54**	**36.05±0.43**
		GRU	27.41±1.06	31.99±0.83	**41.59±0.75**	31.31±0.76	**40.11±0.74**	31.45±0.61	33.98±0.52
	50 %	LSTM	28.45±1.06	34.36±0.78	38.85±1.05	35.77±0.56	39.02±0.81	35.03±0.68	35.24±0.44
		GRU	**31.68±1.30**	**36.75±0.91**	**44.46±0.84**	**36.48±0.76**	**43.16±0.88**	**35.88±0.75**	**38.07±0.51**
	75 %	LSTM	32.51±1.15	37.89±0.98	42.56±0.90	37.66±0.67	42.40±0.80	**37.10±0.68**	38.35±0.44
		GRU	**33.49±1.39**	**38.62±0.72**	**45.63±0.83**	**37.87±0.74**	**43.93±0.74**	36.53±0.83	**39.34±0.49**

6.3.2 Prediction of EEG microstate sequences

Once temporal dynamics of EEG microstate sequences are captured with high reconstruction accuracy for shorter frame lengths, it is worth to investigate how far we can predict from a fixed frame length of EEG microstate sequences. The frame length of 200 ms was used to predict the next 48 ms, 100 ms, and 200 ms through GRU under different conditions, as shown in Table 13.

Under the frame length of 200 ms, the prediction accuracy was around 82% when predicting next 48 ms, around 67% when predicting next 100 ms, and around 39% when predicting next 200 ms. These results indicated that predication accuracy was significantly decreased when forecast lags beyond 100 ms. In addition, these results indicated that the overlap rate between neighbouring frames is a key parameters to capture temporal dynamics of EEG microstate sequences in that they may share more temporal information and increase sample sizes.

Table 13: Accuracy results for prediction of EEG microstate sequences considering lag and task condition. The results are presented as Mean ± S.E. across subjects, while the best results are marked by bold font.

Lag	**Task Condition**						
	REST	PU	IG	RIG	IE	RIE	AVG
48 ms	79.18±0.35	82.31±0.30	82.54±0.16	83.01±0.27	81.95±1.30	81.19±1.56	81.70±0.36
100 ms	62.44±0.38	67.67±0.42	63.72±0.37	70.20±0.34	65.78±0.47	70.37±0.38	66.70±0.29
200 ms	31.42±0.81	41.57±0.82	30.29±0.78	46.42±0.82	35.22±0.94	47.33±0.81	38.71±0.63

6.3.3 Classification of EEG microstate sequences

Sensitivity, specificity, precision, and F-measure were used to evaluate the classifier performance under different parameters. Sensitivity (also known as recall) measures the proportion of positive predictions, which can be used to evaluate the performance of a classifier on instances of the positive classes.

Table 14 shows the sensitivity results when various methods with different parameters were used to classify cognitive activities in design creativity. For each task condition, the highest and lowest sensitivity were demonstrated as follows. For REST, the highest sensitivity was 51.20% using the frame length of 800 ms with the CNN-based classifier while the lowest sensitivity was 1.70% using the frame length of 100 ms with the SVM-based classifier. For PU, the highest sensitivity was 82.75% using the frame length of 800 ms with the CNN-based classifier while the lowest sensitivity was 2.48% using the frame length of 100 ms with the SVM-based classifier. For IG, the highest sensitivity was 96.86% using the frame length of 800 ms with the CNN-based classifier while the lowest sensitivity was 24.80% using the frame length of 100 ms with the NB-based classifier. For RIG, the highest sensitivity was 93.16% using the frame length of 800 ms with the CNN-based classifier while the lowest sensitivity was 3.21% using the frame length of 100 ms with the SVM-based classifier. For IE, the highest sensitivity was 93.16% using the frame length of 800 ms with the CNN-based classifier while the lowest sensitivity was 28.20% using the frame length of 100 ms with the NB-based classifier. For RIE, the highest sensitivity was 93.66% using the frame length of 800 ms with the CNN-based classifier while the lowest sensitivity was 2.47% using the frame length of 100 ms with the SVM-based classifier.

Therefore, these results indicated a clear trend of increasing sensitivity with increasing frame lengths no matter what kinds of algorithms were used. This trending implies the long-range correlations of network oscillations in design creativity. In addition, the CNN-based classifier has good performance than other classifiers for the longer frame lengths. This may result from the conventional structure in CNN that can capture the correlations in the time and spatial spaces.

Specificity is used to evaluate the performance of a classifier on instances of the negative classes. Table 15 shows the specificity results when various methods with different parameters were used to classify cognitive activities in design creativity. Generally, these

Table 14: Sensitivity and recall results for classification of EEG microstate sequences considering frame length and method. The results are presented as Mean ± S.E. across subjects, while the best results are marked by bold font.

Frame Length	Method	Task Condition						
		REST	PU	IG	RIG	IE	RIE	AVG
100 ms	NB	**38.89±3.61**	**20.72±2.31**	24.80±1.97	**26.40±2.87**	28.20±3.11	**26.22±2.87**	27.54±1.22
	SVM	1.70±0.90	2.48±0.85	82.73±3.06	3.21±1.20	35.24±4.20	2.47±0.95	21.30±2.53
	FNN	4.40±1.71	12.82±2.55	85.60±2.78	22.96±4.04	**58.87±4.12**	19.18±3.63	**33.97±2.61**
	CNN	4.86±1.10	13.23±2.14	**89.07±2.72**	20.80±3.51	46.40±4.77	17.02±2.99	31.90±2.57
200 ms	NB	**41.61±3.54**	22.18±2.37	28.73±2.28	28.98±2.82	31.25±3.21	29.70±3.01	30.41±1.25
	SVM	4.00±1.74	4.60±1.37	83.28±2.68	6.31±1.65	40.02±4.25	4.81±1.53	23.84±2.52
	FNN	18.27±3.52	39.48±5.49	**92.57±1.37**	54.06±6.29	71.90±4.64	49.64±6.52	54.32±2.72
	CNN	22.37±3.01	**44.47±4.56**	91.38±1.61	**55.99±5.75**	**68.38±4.32**	**52.27±5.62**	**55.81±2.43**
400 ms	NB	47.20±3.51	26.16±2.27	36.17±2.32	34.60±3.27	35.60±3.25	31.45±2.64	35.20±1.27
	SVM	13.97±3.28	9.80±2.02	84.43±2.38	15.08±2.78	48.34±4.43	11.08±2.30	30.45±2.48
	FNN	39.55±4.94	63.92±5.94	94.84±1.09	70.81±5.57	83.87±3.93	69.32±5.76	70.38±2.37
	CNN	**47.91±3.46**	**75.81±3.33**	**94.94±0.72**	**87.07±1.85**	**90.85±1.47**	**87.90±2.07**	**80.75±1.57**
800 ms	NB	47.84±4.17	28.45±2.97	40.96±2.77	35.84±2.96	40.77±3.57	36.38±2.65	38.37±1.38
	SVM	20.16±4.24	19.92±3.07	85.81±2.06	28.37±3.78	57.14±4.34	22.61±3.53	39.00±2.41
	FNN	29.37±4.96	57.18±5.85	95.45±1.15	65.66±5.99	80.13±4.31	63.36±5.11	65.19±2.52
	CNN	**51.20±3.97**	**82.75±2.60**	**96.86±0.35**	**93.67±0.81**	**93.16±1.58**	**93.66±0.55**	**85.22±1.50**

results indicated relatively high specificity regardless of different classifiers and parameters. The averaged specificity were around 93%.

For each task condition, the highest and lowest specificity were demonstrated as follows. For REST, the highest specificity was 99.88% using the frame length of 100 ms with the SVM-based classifier while the lowest specificity was 82.26% using the frame length of 100 ms with the NB-based classifier. For PU, the highest specificity was 99.38% using the frame length of 100 ms with the SVM-based classifier while the lowest specificity was 88.26% using the frame length of 100 ms with the NB-based classifier. For IG, the highest specificity was 92.78% using the frame length of 800 ms with the CNN-based classifier while the lowest specificity was 32.44% using the frame length of 100 ms with the SVM-based classifier. For RIG, the highest specificity was 99.55% using the frame length of 100 ms with the SVM-based classifier while the lowest sensitivity was 86.84% using the frame length of 100 ms with the NB-based classifier. For IE, the highest specificity was 97.30% using the frame length of 800 ms with the CNN-based classifier while the lowest specificity was 81.50% using the frame length of 200 ms with the SVM-based classifier. For RIE, the

highest specificity was 99.74% using the frame length of 100 ms with the SVM-based classifier while the lowest specificity was 86.07% using the frame length of 200 ms with the NB-based classifier.

Table 15: Specificity results for classification of EEG microstate sequences considering frame length and method. The results are presented as Mean ± S.E. across subjects, while the best results are marked by bold font.

Frame Length	**Method**	**Task Condition**						
		REST	PU	IG	RIG	IE	RIE	AVG
100 ms	NB	82.26±1.62	88.26±1.16	**83.67±1.19**	86.84±1.26	82.84±1.57	86.20±1.62	85.01±0.60
	SVM	**99.88±0.07**	**99.38±0.27**	32.44±4.05	**99.55±0.22**	81.22±3.08	**99.74±0.11**	85.37±2.11
	FNN	99.81±0.07	98.50±0.36	55.83±3.85	98.74±0.21	83.07±2.94	98.87±0.27	**89.14±1.49**
	CNN	99.69±0.07	98.63±0.37	44.70±4.69	98.79±0.25	**87.40±2.67**	99.27±0.14	88.08±1.80
200 ms	NB	84.52±1.35	89.24±0.94	**83.21±1.27**	87.47±1.06	82.83±1.37	86.07±1.77	85.56±0.56
	SVM	**99.80±0.11**	**99.08±0.33**	37.67±3.97	**99.34±0.23**	81.50±2.71	**99.57±0.14**	86.16±1.95
	FNN	99.60±0.07	98.31±0.36	71.72±4.31	98.50±0.24	90.85±1.79	98.76±0.21	**92.96±1.10**
	CNN	99.15±0.21	97.83±0.48	70.40±4.22	98.49±0.19	**91.78±1.38**	99.05±0.13	92.78±1.10
400 ms	NB	85.92±1.31	89.53±0.96	81.83±0.97	88.12±1.06	84.47±1.28	89.30±1.02	86.53±0.50
	SVM	**99.64±0.14**	98.58±0.42	46.98±3.93	98.83±0.26	83.22±2.30	99.17±0.18	87.74±1.68
	FNN	99.57±0.07	98.49±0.49	83.03±3.81	99.24±0.10	94.63±1.05	**99.30±0.11**	95.71±0.80
	CNN	99.49±0.07	**98.77±0.25**	**90.81±1.30**	**99.36±0.10**	**95.92±0.58**	99.26±0.14	**97.27±0.34**
800 ms	NB	86.35±1.11	90.40±0.98	82.50±1.14	90.62±0.87	84.99±1.23	89.39±1.06	87.38±0.49
	SVM	99.66±0.10	98.17±0.46	57.27±3.66	98.37±0.26	85.36±1.90	98.79±0.20	89.61±1.38
	FNN	**99.70±0.05**	98.66±0.24	78.43±3.83	99.13±0.12	94.40±1.28	99.28±0.12	94.93±0.89
	CNN	99.58±0.07	**99.20±0.15**	**92.78±1.09**	**99.47±0.08**	**97.30±0.32**	**99.60±0.04**	**97.99±0.27**

Precision measures the proportion of which positive predictions are correct. Table 16 shows the precision results when various methods with different parameters were used to classify cognitive activities in design creativity. These results indicated that a clear trend of increasing precision with increasing frame lengths no matter what kinds of algorithms are using. These findings are in line with the trend of sensitivity.

For each task condition, the highest and lowest precision were demonstrated as follows. For REST, the highest precision was 84.66% using the frame length of 800 ms with the CNN-based classifier while the lowest precision was 7.50% using the frame length of 100 ms with the SVM-based classifier. For PU, the highest precision was 91.27% using the frame length of 800 ms with the CNN-based classifier while the lowest precision was

12.99% using the frame length of 100 ms with the SVM-based classifier. For IG, the highest precision was 93.02% using the frame length of 800 ms with the CNN-based classifier while the lowest precision was 52.91% using the frame length of 100 ms with the SVM-based classifier. For RIG, the highest precision was 92.90% using the frame length of 800 ms with the CNN-based classifier while the lowest precision was 11.75% using the frame length of 100 ms with the NB-based classifier. For IE, the highest precision was 92.90% using the frame length of 800 ms with the CNN-based classifier while the lowest precision was 36.89% using the frame length of 100 ms with the NB-based classifier. For RIE, the highest precision was 92.88% using the frame length of 800 ms with the CNN-based classifier while the lowest precision was 9.96% using the frame length of 100 ms with the NB-based classifier.

Table 16: Precision results for classification of EEG microstate sequences considering frame length and method. The results are presented as Mean ± S.E. across subjects, while the best results are marked by bold font.

Frame Length	**Method**	**Task Condition**						
		REST	PU	IG	RIG	IE	RIE	AVG
100 ms	NB	9.17±0.70	12.99±1.13	56.77±1.99	11.75±0.73	36.89±1.93	9.96±0.61	22.92±1.51
	SVM	7.50±3.33	22.36±3.76	52.91±1.66	23.39±3.51	41.23±3.04	25.15±4.20	28.76±1.77
	FNN	40.10±5.78	45.55±2.39	**65.08±1.72**	50.82±2.06	61.74±2.54	48.93±2.48	52.04±1.44
	CNN	**42.67±3.83**	**53.95±2.02**	60.94±1.52	**57.34±2.41**	**64.99±1.99**	**56.19±2.86**	**56.01±1.16**
200 ms	NB	11.08±0.82	14.60±1.28	59.50±2.03	13.15±0.81	39.29±2.08	11.59±0.75	24.87±1.55
	SVM	34.44±7.00	35.15±4.27	55.25±1.65	31.37±3.62	46.68±2.17	32.49±3.38	39.23±1.77
	FNN	**60.00±4.30**	63.94±3.39	**77.01±2.37**	67.87±3.40	76.98±2.62	63.66±3.93	68.24±1.46
	CNN	59.94±3.20	**67.20±2.60**	75.86±2.24	**70.37±2.17**	**77.80±1.96**	**73.67±2.63**	**70.81±1.11**
400 ms	NB	13.56±1.06	17.69±1.52	62.95±2.20	16.13±1.05	45.33±2.56	14.88±1.04	28.42±1.64
	SVM	57.51±5.49	41.54±3.97	59.90±1.76	38.65±3.46	53.90±2.44	40.11±2.79	48.60±1.58
	FNN	78.26±2.94	78.48±2.84	85.86±2.38	82.38±2.83	86.35±1.92	81.98±2.67	82.22±1.08
	CNN	**78.27±3.16**	**86.42±1.50**	**90.63±1.16**	**90.71±1.16**	**90.18±0.99**	**88.40±1.42**	**87.44±0.77**
800 ms	NB	14.81±2.00	20.01±2.08	66.75±2.31	20.78±1.60	49.36±2.89	17.85±1.53	31.59±1.75
	SVM	67.50±4.84	55.35±3.17	65.71±1.82	54.31±2.38	61.00±2.61	56.17±2.75	60.01±1.30
	FNN	74.98±3.29	75.65±3.02	83.07±2.08	80.35±2.67	85.75±2.19	81.58±2.90	80.23±1.14
	CNN	**84.66±1.71**	**91.27±0.87**	**93.02±0.82**	**92.90±0.79**	**92.90±0.81**	**92.88±0.69**	**91.27±0.47**

Table 17 shows the F-measure results when various methods with different parameters were used to classify cognitive activities in design creativity. Generally, these results indicated relatively higher F-measure for the longer frame lengths of 400 ms and 800 ms.

For REST, the highest F-measure was 61.31% using the frame length of 800 ms with the CNN-based classifier while the lowest F-measure was 2.64% using the frame length of 100 ms with the SVM-based classifier. For PU, the highest F-measure was 61.31% using the frame length of 800 ms with the CNN-based classifier while the lowest F-measure was 2.64% using the frame length of 100 ms with the SVM-based classifier. For IG, the highest F-measure was 86.01% using the frame length of 800 ms with the CNN-based classifier while the lowest F-measure was 3.97% using the frame length of 100 ms with the SVM-based classifier. For RIG, the highest F-measure was 94.83% using the frame length of 800 ms with the CNN-based classifier while the lowest F-measure was 33.20% using the frame length of 100 ms with the NB-based classifier. For IE, the highest F-measure was 92.29% using the frame length of 800 ms with the CNN-based classifier while the lowest F-measure was 4.79% using the frame length of 100 ms with the SVM-based classifier. For RIE, the highest F-measure was 93.22% using the frame length of 800 ms with the CNN-based classifier while the lowest F-measure was 3.82% using the frame length of 100 ms with the SVM-based classifier.

In sum, the classification performance heavily depended on the frame lengths no matter what kinds of algorithms were used. The longer frame lengths of 400 ms and 800 ms resulted in higher classification accuracy compared to the shorter frame lengths of 100 ms and 200 ms. This observation suggested long-range temporal correlations underlying EEG microstate sequences in design creativity.

6.4 Conclusion

To conclude, we show that temporal dynamics of network oscillations in design creativity can be captured by LSTM and GRU; the frame length of 200 ms can predict the next 48 ms and 100 ms with around 75% predication accuracy; the captured temporal dynamics of

Table 17: F-measure results for classification of EEG microstate sequences considering frame length and method. The results are presented as Mean ± S.E. across subjects, while the best results are marked by bold font.

Frame Length	**Method**	**Task Condition**						
		REST	PU	IG	RIG	IE	RIE	AVG
100 ms	NB	**13.74±1.07**	14.40±1.18	33.20±1.99	14.44±1.05	30.15±2.58	12.80±1.09	19.79±0.93
	SVM	2.64±1.37	3.97±1.28	64.23±2.07	4.79±1.54	35.69±3.61	3.82±1.36	19.19±2.01
	FNN	6.69±2.37	17.72±2.76	**73.35±1.93**	**28.25±4.04**	**57.88±3.13**	**24.22±3.74**	**34.68±2.21**
	CNN	8.12±1.70	**19.37±2.61**	71.77±1.75	26.78±3.61	49.44±3.64	23.52±3.42	33.17±2.04
200 ms	NB	16.28±1.13	16.30±1.38	36.99±2.38	16.61±1.10	33.20±2.63	14.98±1.19	22.39±1.00
	SVM	5.74±2.37	6.93±1.86	66.19±1.92	9.30±2.08	40.12±3.79	7.08±1.95	22.56±2.05
	FNN	25.30±4.07	45.31±5.34	**83.62±1.72**	56.07±5.80	**71.99±4.09**	52.44±6.00	55.79±2.40
	CNN	**29.87±3.37**	**50.75±4.33**	82.44±1.71	**58.79±4.94**	70.73±3.46	**57.76±5.13**	**58.39±2.06**
400 ms	NB	20.06±1.41	20.06±1.57	44.64±2.22	20.52±1.30	38.24±2.84	19.21±1.43	27.12±1.11
	SVM	19.51±3.95	14.12±2.47	69.86±1.88	19.93±3.08	48.32±4.02	15.31±2.59	31.17±2.06
	FNN	48.49±5.03	67.49±5.42	89.64±1.70	74.15±4.87	83.99±3.20	72.66±5.04	72.74±2.05
	CNN	**57.99±3.38**	**79.89±2.45**	**92.66±0.85**	**88.68±1.39**	**90.39±1.11**	**87.90±1.61**	**82.92±1.23**
800 ms	NB	19.86±1.68	22.01±2.19	49.44±2.57	25.09±1.84	43.15±3.24	22.82±1.65	30.40±1.28
	SVM	26.73±4.93	26.36±3.35	74.25±1.81	33.67±3.73	57.08±3.92	28.15±3.42	41.04±2.05
	FNN	38.15±5.28	62.42±5.12	88.47±1.48	68.86±5.23	81.12±3.77	69.20±4.36	68.04±2.17
	CNN	**61.31±3.54**	**86.01±1.62**	**94.83±0.45**	**93.18±0.56**	**92.79±1.06**	**93.22±0.47**	**86.89±1.15**

network oscillations can be used to classify different cognitive activities in design creativity. EEG microstate sequences can be reconstructed for frame lengths of 100 ms and 200 ms but the reconstruction accuracy decreases significantly for longer frame lengths. This observation supports that EEG microstate sequences are nonstationary. In addition, the results of classification accuracy show a trend of increasing accuracy with increasing frame lengths for the same classifiers during the design process. However, the results across classifiers will be discussed in the future work. These results stress the long-range correlations in charactering network oscillations in design creativity.

Chapter 7

Conclusion and future work

7.1 Conclusion

This research investigated neurocognition in design creativity by EEG microstate analysis under loosely controlled experiments. The loosely controlled experiments can trigger some critical characteristics of design creativity, such as incubation and mind wandering. The loosely controlled experiments provide sufficient time for participants to generate and evaluate solutions freely. Some solutions may be creative, while others may be inconclusive. In addition, the thinking and sketching are integrated into one phase to avoid any interruption or interference. At the same time, the loosely controlled experiments maintain certain degrees of control.

However, such loosely controlled experiments would increase data analysis difficulties since the EEG signals are unstructured, and the causal relationships between a stimulus and its response are complex and hidden. Meanwhile, the simulated design creativity would activate the large-scale brain networks to support complex and complicate cognitions.

This research addressed these difficulties of data analysis approaches. Firstly, this research tested the effectiveness of loosely controlled experiments by comparing its findings on phenomena that have been effectively studied by validated experimental research. It

was found that idea generation and idea evolution were associated with decreases in alpha power, while the decreases were significantly larger during idea generation compared to idea evolution. It was also found that problem understanding, rating idea generation, and rating idea evaluation were associated with increases in theta and beta power while the increases were largest during problem understanding. These findings are in line with those from visual creativity and higher-order cognition research based on ERD/ERS and TRP. In addition, these findings suggest that idea generation is associated with the lowest cognitive control and highest cognitive workload.

Secondly, EEG microstate analysis was applied to structure and segment the unstructured EEG signals collected from the loosely controlled experiments in design creativity. Each microstate class was associated with EEG-defined large-scale brain networks, such as the default mode network and cognitive control network. It was found that microstate class C was more prominent during idea generation, while microstate class F was more prevalent during idea evolution. Further temporal dynamics analysis found that idea generation was consistently associated with the shortest correlation times, as measured by the finite entropy rate, AIF, and Hurst exponent. These findings suggest that the interplay of functional brain networks is less restricted during idea generation, supporting the idea that the brain has more degrees of freedom during tasks involving creativity.

Thirdly, RNN techniques with the autoencoder framework were used to capture temporal dynamics of network oscillations in design creativity. Around 94% reconstruction accuracy of frame lengths of 100 ms and 200 ms corroborated that RNN techniques are capable of capturing temporal dynamics of network oscillations in design creativity. The reconstruction accuracy decreased significantly when frame lengths of EEG microstate sequences were 400 ms and 800 ms. Besides, the CNN-based classifier with encoded EEG microstate sequences has a good performance on multitask classification, including rest, problem understanding, idea generation, rating idea generation, idea evaluation, and rating

idea evaluation. The F-measure of CNN-based classifier was around 83% and 87% for frame lengths of 400 ms and 800 ms, respectively. These findings support that EEG signals are nonstationary. Also, these findings suggest that RNN techniques with the autoencoder framework are capable of capturing temporal dynamics of network oscillations, which can be further used to classify cognitive activities in design creativity.

In sum, the loosely controlled experiment supported by EEG microstate analysis appears to offer an effective approach to facilitating an ecologically valid neurocognitive study. In addition, this research is able to help design researchers to establish neurocognitive mechanisms during the design process. This neurocognitive mechanisms may help designers to improve their creativity and productivity through brainwave entrainment and identifying implementation barriers [232].

7.2 Limitations and future directions

A few limitations of the current study need to be addressed in the future. First, the objective of this research is to understand the brain activities in design creativity. We did not take into account participants' behaviour data except for NASA-LTX, since some aspects of behaviour analysis heavily rely on subjective criteria. For instance, evaluating design solutions depends on experts' knowledge and experience, as well as sample size. Future studies should consider how to analyse participants' behaviour data in an objective manner and relate them to neurocognitive data.

Second, the aim of EEG microstate analysis is to infer the activity of functional brain networks from characteristic EEG topographic patterns. As the EEG signal is affected by volume conduction, tissue-dependent signal filtering, and discrete sampling via an electrode array, the relationship between microstates and functional networks is not one-to-one. Thus, functionally different networks may be represented by only one microstate map. To

further clarify the networks involved in design creativity execution, future studies may benefit from methods such as high-density EEG combined with source localization, or functional MR imaging approaches, although the latter imposes restrictions on the experimental setting.

Bibliography

[1] D. Norman, *The design of everyday things: Revised and expanded edition*. Cambridge: MIT Press, 2013.

[2] Y. Zeng and G. Cheng, "On the logic of design," *Des. Stud.*, vol. 12, no. 3, pp. 137–141, 1991.

[3] Y. Zeng, "Environment-based formulation of design problem," *J. Integr. Des. Process. Sci.*, vol. 8, no. 4, pp. 45–63, 2004.

[4] Y. Zeng, "Environment-based design (EBD)," in *International Design Engineering Technical Conferences and Computers and Information in Engineering Conference*, vol. 54860, (Washington), pp. 237–250, 2011.

[5] H. A. Simon, *The Sciences of the Artificial*. Cambridge: MIT press, 3rd ed., 1969.

[6] D. A. Schön, *The Reflective Practitioner: How Professionals Think in Action*. New York: Basic Books, 1983.

[7] K. Dorst and J. Dijkhuis, "Comparing paradigms for describing design activity," *Des. Stud.*, vol. 16, no. 2, pp. 261–274, 1995.

[8] M. C. Corballis, *The Recursive Mind: The Origins of Human Language, Thought, and Civilization*. Princeton: Princeton University Press, 2011.

[9] Y. Hui, *Recursivity and Contingency*. London: Rowman & Littlefield International, 2019.

[10] H. Bergson and P. A. Gunter, *Creative evolution*. New York: Henry Holt and Company, 1911.

[11] M. L. Maher and J. Poon, "Modeling Design Exploration as Co-evolution," *Comput-Aided. Civ. Inf.*, vol. 11, pp. 195–209, 1996.

[12] K. Dorst and N. Cross, "Creativity in the design process: co-evolution of problem–solution," *Des. Stud.*, vol. 22, no. 5, pp. 425–437, 2001.

[13] L. Hay, A. H. Duffy, C. McTeague, L. M. Pidgeon, T. Vuletic, and M. Grealy, "A systematic review of protocol studies on conceptual design cognition: Design as search and exploration," *Des. Sci.*, vol. 3, p. e10, 2017.

[14] J. S. Gero and J. Milovanovic, "A framework for studying design thinking through measuring designers' minds, bodies and brains," *Des. Sci.*, vol. 6, p. e19, 2020.

[15] M. Zhao, W. Jia, D. Yang, P. Nguyen, T. A. Nguyen, and Y. Zeng, "A tEEG framework for studying designer's cognitive and affective states," *Des. Sci.*, vol. 6, p. e29, 2020.

[16] L. W. Anderson and D. R. Krathwohl, *A taxonomy for learning, teaching, and assessing : a revision of Bloom's taxonomy of educational objectives*. New York: Longman, 2011.

[17] K. A. Ericsson and H. A. Simon, *Protocol Analysis Verbal Reports as Data Revised edition*. Cambridge: MIT Press, 1993.

[18] J. S. Gero and T. Mc Neill, "An approach to the analysis of design protocols," *Des. Stud.*, vol. 19, no. 1, pp. 21–61, 1998.

[19] Z. Bilda and H. Demirkan, "An insight on designers' sketching activities in traditional versus digital media," *Des. Stud.*, vol. 24, no. 1, pp. 27–50, 2003.

[20] C. J. Atman, R. S. Adams, M. E. Cardella, J. Turns, S. Mosborg, and J. Saleem, "Engineering design processes: A comparison of students and expert practitioners," *J. Eng. Educ.*, vol. 96, no. 4, pp. 359–379, 2007.

[21] H. Cheong, G. M. Hallihan, and L. Shu, "Design problem solving with biological analogies: A verbal protocol study," *Artif. Intell. Eng. Des. Anal. Manuf.*, vol. 28, no. 1, pp. 27–47, 2014.

[22] J. Austin and P. F. Delaney, "Protocol Analysis as a Tool for Behavior Analysis," *Anal. Verbal Behav.*, vol. 15, no. 1, pp. 41–56, 1998.

[23] D. A. Schon and G. Wiggins, "Kinds of seeing and their functions in designing," *Des. Stud.*, vol. 13, no. 2, pp. 135–156, 1992.

[24] M. Suwa and B. Tversky, "What architects see in their sketches: Implications for design tools," in *Conference Companion on Human Factors in Computing Systems*, pp. 191–192, 1996.

[25] U. A. Athavankar, "Mental imagery as a design tool," *Cybern. Syst*, vol. 28, no. 1, pp. 25–42, 1997.

[26] Y. Zeng, A. Pardasani, J. Dickinson, Z. Li, H. Antunes, and, V. Gupta, and D. Baulier, "Mathematical Foundation for Modeling Conceptual Design Sketches," *J. Comput. Inf. Sci. Eng.*, vol. 4, no. 2, pp. 150–159, 2004.

[27] Z. Bilda, J. S. Gero, and T. Purcell, "To sketch or not to sketch? that is the question," *Des. Stud.*, vol. 27, no. 5, pp. 587–613, 2006.

[28] Z. Bilda and J. S. Gero, "The impact of working memory limitations on the design process during conceptualization," *Des. Stud.*, vol. 28, no. 4, pp. 343–367, 2007.

[29] V. Goel, *Sketches of thought*. Cambridge: MIT Press, 1995.

[30] C.-S. Chan, "Cognitive processes in architectural design problem solving," *Des. Stud.*, vol. 11, no. 2, pp. 60–80, 1990.

[31] L. A. Stauffer and D. G. Ullman, "Fundamental processes of mechanical designers based on empirical data," *J. Eng. Des.*, vol. 2, no. 2, pp. 113–125, 1991.

[32] Y. Zeng and P. Gu, "A science-based approach to product design theory part I: formulation and formalization of design process," *Robot. Comput. Integr. Manuf.*, vol. 15, no. 4, pp. 331–339, 1999.

[33] Y. Zeng and P. Gu, "A science-based approach to product design theory part II: formulation of design requirements and products," *Robot. Comput. Integr. Manuf.*, vol. 15, no. 4, pp. 341–352, 1999.

[34] J. W. Asher, "Experimental controls," in *The concise Corsini Encyclopedia of Psychology and Behavioral Science* (W. E. Craighead and C. B. Nemeroff, eds.), pp. 347–349, New York: Wiley, 2001.

[35] B. Baird, J. Smallwood, M. D. Mrazek, J. W. Kam, M. S. Franklin, and J. W. Schooler, "Inspired by Distraction: Mind Wandering Facilitates Creative Incubation," *Psychol. Sci.*, vol. 23, no. 10, pp. 1117–1122, 2012.

[36] H. Yang, A. Chattopadhyay, K. Zhang, and D. W. Dahl, "Unconscious creativity: When can unconscious thought outperform conscious thought?," *J. Consum. Psychol.*, vol. 22, no. 4, pp. 573–581, 2012.

[37] S. M. Ritter and A. Dijksterhuis, "Creativity-the unconscious foundations of the incubation period," *Front. Hum. Neurosci.*, vol. 8, p. 215, 2014.

[38] S. Kühn, S. M. Ritter, B. C. Müller, R. B. Van Baaren, M. Brass, and A. Dijksterhuis, "The Importance of the Default Mode Network in Creativity-A Structural MRI Study," *J. Creat. Behav.*, vol. 48, no. 2, pp. 152–163, 2014.

[39] W. Jia and Y. Zeng, "EEG signals respond differently to idea generation, idea evolution and evaluation in a loosely controlled creativity experiment," *Sci. Rep.*, vol. 11, p. 2119, 2021.

[40] Y. Zeng, "Environment: The First Thing to Look at in Conceptual Design," *J. Integr. Des. Process. Sci.*, no. Preprint, pp. 1–22, 2020.

[41] G. S. Altshuller, *Creativity as an exact science: the theory of the solution of inventive problems*. New York: Gordon and Breach, 1984.

[42] R. A. Shirwaiker and G. E. Okudan, "Triz and axiomatic design: a review of case-studies and a proposed synergistic use," *J. Intell. Manuf.*, vol. 19, no. 1, pp. 33–47, 2008.

[43] I. M. Ilevbare, D. Probert, and R. Phaal, "A review of TRIZ, and its benefits and challenges in practice," *Technovation*, vol. 33, no. 2-3, pp. 30–37, 2013.

[44] J. S. Gero, "Design prototypes: a knowledge representation schema for design," *AI magazine*, vol. 11, no. 4, pp. 26–26, 1990.

[45] J. S. Gero and U. Kannengiesser, "The situated function–behaviour–structure framework," *Des. Stud.*, vol. 25, no. 4, pp. 373–391, 2004.

[46] D. Corne, T. Smithers, and P. Ross, *Solving design problems by computational exploration*. University of Edinburgh, Department of Artificial Intelligence, 1994.

[47] B. Logan and T. Smithers, "Creativity and design as exploration," in *Modelling Creativity and Knowledge-Based Creative Design* (S. G. John and L. M. Mary, eds.), pp. 139–175, New Jersey: Lawrence Erlbaum Associates, 1993.

[48] M. Maher and H.-H. Tang, "Co-evolution as a computational and cognitive model of design," *Res. Eng. Des.*, vol. 14, no. 1, pp. 47–64, 2003.

[49] J. S. Gero, "Future Directions for Design Creativity Research," in *Design Creativity 2010* (T. Taura and Y. Nagai, eds.), pp. 15–22, London: Springer, 2011.

[50] R. J. Sternberg and T. I. Lubart, "Investing in creativity.," *American Psychologist*, vol. 51, no. 7, p. 677, 1996.

[51] R. Weisberg, *Creativity: Beyond the myth of genius*. New York: WH Freeman, 1993.

[52] D. K. Simonton, "Taking the US Patent Office Criteria Seriously: A Quantitative Three-Criterion Creativity Definition and Its Implications," *Creat. Res. J.*, vol. 24, no. 2-3, pp. 97–106, 2012.

[53] J. P. Guilford, "The structure of intellect.," *Psychol. Bull.*, vol. 53, no. 4, pp. 267–293, 1956.

[54] R. A. Finke, T. B. Ward, and S. M. Smith, *Creative cognition: theory, research, and applications*. Cambridge: MIT Press, 1992.

[55] P. T. Sowden, A. Pringle, and L. Gabora, "The shifting sands of creative thinking: Connections to dual-process theory," *Think. Reason.*, vol. 21, no. 1, pp. 40–60, 2015.

[56] V. Goel, "Creative brains: designing in the real world," *Front. Hum. Neurosci.*, vol. 8, p. 241, 2014.

[57] J. S. Gero, "Creativity, emergence and evolution in design," *Knowl. Based. Syst.*, vol. 9, no. 7, pp. 435–448, 1996.

[58] T. A. Nguyen and Y. Zeng, "A Theoretical Model of Design Creativity: Nonlinear Design Dynamics and Mental Stress-Creativity Relation," *Int. J. Des. Creativity Innov.*, vol. 16, no. 3, pp. 65–88, 2012.

[59] G. E. Corazza, "Potential Originality and Effectiveness: The Dynamic Definition of Creativity," *Creat. Res. J.*, vol. 28, no. 3, pp. 258–267, 2016.

[60] P. L. Broadhurst, "Emotionality and the yerkes-dodson law.," *J. Exp. Psychol.*, vol. 54, no. 5, p. 345, 1957.

[61] T. J. Howard, S. J. Culley, and E. Dekoninck, "Describing the creative design process by the integration of engineering design and cognitive psychology literature," *Des. Stud.*, vol. 29, no. 2, pp. 160–180, 2008.

[62] M. Suwa, T. Purcell, and J. Gero, "Macroscopic analysis of design processes based on a scheme for coding designers' cognitive actions," *Des. Stud.*, vol. 19, no. 4, pp. 455–483, 1998.

[63] N. Cross, "Design cognition: Results from protocol and other empirical studies of design activity," in *Design knowing and learning: Cognition in design education* (C. M. Eastman, W. M. McCracken, and W. C. Newstetter, eds.), pp. 79–103, Amsterdam: Elsevier, 2001.

[64] H. Christiaans and K. H. Dorst, "Cognitive models in industrial design engineering: a protocol study," *Design theory and methodology*, vol. 42, no. 1, pp. 131–140, 1992.

[65] C. J. Atman, J. R. Chimka, K. M. Bursic, and H. L. Nachtmann, "A comparison of freshman and senior engineering design processes," *Des. Stud.*, vol. 20, no. 2, pp. 131–152, 1999.

[66] B. R. Lawson, "Cognitive Strategies in Architectural Design," *Ergonomics*, vol. 22, no. 1, pp. 59–68, 1979.

[67] P. Lloyd and P. Scott, "Discovering the design problem," *Des. Stud.*, vol. 15, no. 2, pp. 125–140, 1994.

[68] D. G. Jansson and S. M. Smith, "Design fixation," *Des. Stud.*, vol. 12, no. 1, pp. 3–11, 1991.

[69] A. T. Purcell and J. S. Gero, "The effects of examples on the results of a design activity," in *Artificial Intelligence in Design'91* (J. S. Gero, ed.), pp. 525–542, Oxford: Elsevier, 1991.

[70] A. Purcell, P. Williams, J. Gero, and B. Colbron, "Fixation effects: Do they exist in design problem solving?," *Environ. Plann. B Plann. Des.*, vol. 20, no. 3, pp. 333–345, 1993.

[71] A. T. Purcell and J. S. Gero, "Design and other types of fixation," *Des. Stud.*, vol. 17, no. 4, pp. 363–383, 1996.

[72] T. A. Nguyen and Y. Zeng, "A theoretical model of design fixation," *Int. J. Des. Creativity Innov.*, vol. 5, no. 3-4, pp. 185–204, 2017.

[73] P. G. Rowe, *Design thinking*. Cambridge: MIT press, 1987.

[74] D. G. Ullman, *The mechanical design process*. New York: McGraw-Hill, 5th ed., 2015.

[75] L. J. Ball, J. S. B. Evans, and I. Dennis, "Cognitive processes in engineering design: A longitudinal study," *Ergonomics*, vol. 37, no. 11, pp. 1753–1786, 1994.

[76] R. P. Smith and P. Tjandra, "Experimental observation of iteration in engineering design," *Res. Eng. Des.*, vol. 10, no. 2, pp. 107–117, 1998.

[77] K. Christoff, Z. C. Irving, K. C. Fox, R. N. Spreng, and J. R. Andrews-Hanna, "Mind-wandering as spontaneous thought: a dynamic framework," *Nat. Rev. Neurosci.*, vol. 17, no. 11, pp. 718–731, 2016.

[78] S. M. Smith, "Getting into and out of mental ruts: a theory of fixation, incubation, and insight.," in *The nature of insight* (R. J. Sternberg and J. E. Davidson, eds.), Cambridge: MIT Press, 1995.

[79] D. L. Stufflebeam, "Foundational models for 21 st century program evaluation," in *Evaluation Models: Viewpoints on Educational and Human Services Evaluation* (D. S. Daniel, F. M. George, and K. Thomas, eds.), pp. 33–83, Boston: Kluwer Academic Publishers, 2000.

[80] T. Nakao, H. Ohira, and G. Northoff, "Distinction between externally vs. internally guided decision-making: operational differences, meta-analytical comparisons and their theoretical implications," *Front. Neurosci.*, vol. 6, p. 31, 2012.

[81] J. W. Schooler, S. Ohlsson, and K. Brooks, "Thoughts beyond words: When language overshadows insight.," *J. Exp. Psychol. Gen.*, vol. 122, no. 2, pp. 166–183, 1993.

[82] P. Lloyd, B. Lawson, and P. Scott, "Can concurrent verbalization reveal design cognition?," *Des. Stud.*, vol. 16, no. 2, pp. 237–259, 1995.

[83] J. Nielsen, T. Clemmensen, and C. Yssing, "Getting access to what goes on in people's heads? reflections on the think-aloud technique," in *Proceedings of the second Nordic conference on Human-computer interaction*, pp. 101–110, 2002.

[84] C. M. Michel and T. Koenig, "EEG microstates as a tool for studying the temporal dynamics of whole-brain neuronal networks: A review," *Neuroimage*, vol. 180, pp. 577–593, 2018.

[85] P. Olejniczak, "Neurophysiologic basis of EEG," *J. Clin. Neurophysiol.*, vol. 23, no. 3, pp. 186–189, 2006.

[86] K. H. Jawabri and S. Sharma, "Physiology, cerebral cortex functions," *StatPearls [Internet]*, 2019.

[87] C. L. Dickter and P. D. Kieffaber, *EEG methods for the psychological sciences*. Los Angeles: SAGE Publications Ltd., 2014.

[88] U. Ghani, N. Signal, I. Niazi, and D. Taylor, "ERP based measures of cognitive workload: A review," *Neurosci. Biobehav. Rev.*, vol. 118, pp. 18–26, 2020.

[89] M. Kutas and K. D. Federmeier, "Thirty years and counting: finding meaning in the N400 component of the event-related brain potential (ERP)," *Annu. Rev. Psychol.*, vol. 62, pp. 621–647, 2011.

[90] E. Başar, C. Başar-Eroglu, S. Karakaş, and M. Schürmann, "Gamma, alpha, delta, and theta oscillations govern cognitive processes," *Int. J. Psychophysiol.*, vol. 39, no. 2-3, pp. 241–248, 2001.

[91] G. Pfurtscheller, "Quantification of ERD and ERS in the time domain," in *Handbook of Electroencephalography and Clinical Neurophysiology* (G. Pfurtscheller and F. H. Lopes da Silva, eds.), pp. 89–105, Amsterdam: Elsevier, 1999.

[92] A. Fink and M. Benedek, "EEG alpha power and creative ideation," *Neurosci. Biobehav. Rev.*, vol. 44, pp. 111–123, 2014.

[93] P. Sauseng, B. Griesmayr, R. Freunberger, and W. Klimesch, "Control mechanisms in working memory: A possible function of EEG theta oscillations," *Neurosci. Biobehav. Rev.*, vol. 34, no. 7, pp. 1015–1022, 2010.

[94] J. F. Cavanagh and M. J. Frank, "Frontal theta as a mechanism for cognitive control," *Trends Cogn. Sci.*, vol. 18, no. 8, pp. 414–421, 2014.

[95] D. P. Allen and C. D. MacKinnon, "Time–frequency analysis of movement-related spectral power in EEG during repetitive movements: A comparison of methods," *Journal of neuroscience methods*, vol. 186, no. 1, pp. 107–115, 2010.

[96] T. A. Nguyen and Y. Zeng, "Analysis of design activities using EEG signals," in *International Design Engineering Technical Conferences and Computers and Information in Engineering Conference*, pp. 277–286, 2010.

[97] T. A. Nguyen and Y. Zeng, "A physiological study of relationship between designer's mental effort and mental stress during conceptual design," *Comput. Aided. Des.*, vol. 54, pp. 3–18, 2014.

[98] T. A. Nguyen and Y. Zeng, "Effects of stress and effort on self-rated reports in experimental study of design activities," *J. Intell. Manuf.*, vol. 28, no. 7, pp. 1609–1622, 2017.

[99] P. Nguyen, T. A. Nguyen, and Y. Zeng, "Empirical approaches to quantifying effort, fatigue and concentration in the conceptual design process," *Res. Eng. Design*, vol. 29, no. 3, pp. 393–409, 2018.

[100] P. Nguyen, T. A. Nguyen, and Y. Zeng, "Segmentation of design protocol using EEG," *Artif. Intell. Eng. Des. Anal. Manuf.*, vol. 33, no. 1, pp. 11–23, 2019.

[101] K. Alexiou, T. Zamenopoulos, J. Johnson, and S. Gilbert, "Exploring the neurological basis of design cognition using brain imaging: some preliminary results," *Des. Stud.*, vol. 30, no. 6, pp. 623–647, 2009.

[102] S. J. Gilbert, T. Zamenopoulos, K. Alexiou, and J. H. Johnson, "Involvement of right dorsolateral prefrontal cortex in ill-structured design cognition: An fMRI study," *Brain Res.*, vol. 1312, pp. 79–88, 2010.

[103] M. Ellamil, C. Dobson, M. Beeman, and K. Christoff, "Evaluative and generative modes of thought during the creative process," *Neuroimage*, vol. 59, no. 2, pp. 1783–1794, 2012.

[104] L. Hay, A. H. Duffy, S. J. Gilbert, L. Lyall, G. Campbell, D. Coyle, and M. Grealy, "The neural correlates of ideation in product design engineering practitioners," *Des. Sci.*, vol. 5, p. e29, 2019.

[105] M. Saggar, E.-M. Quintin, E. Kienitz, N. T. Bott, Z. Sun, W.-C. Hong, Y.-h. Chien, N. Liu, R. F. Dougherty, A. Royalty, *et al.*, "Pictionary-based fMRI paradigm to study the neural correlates of spontaneous improvisation and figural creativity," *Sci. Rep.*, vol. 5, p. 10894, 2015.

[106] R. E. Beaty, Y. N. Kenett, A. P. Christensen, M. D. Rosenberg, M. Benedek, Q. Chen, A. Fink, J. Qiu, T. R. Kwapil, M. J. Kane, *et al.*, "Robust prediction of individual creative ability from brain functional connectivity," *Proc. Natl. Acad. Sci. U.S.A.*, vol. 115, no. 5, pp. 1087–1092, 2018.

[107] O. M. Kleinmintz, T. Ivancovsky, and S. G. Shamay-Tsoory, "The two-fold model of creativity: the neural underpinnings of the generation and evaluation of creative ideas," *Curr. Opin. Behav. Sci.*, vol. 27, pp. 131–138, 2019.

[108] K. Goucher-Lambert and J. Cagan, "Crowdsourcing inspiration: Using crowd generated inspirational stimuli to support designer ideation," *Des. Stud.*, vol. 61, pp. 1–29, 2019.

[109] M. Saggar, E.-M. Quintin, N. T. Bott, E. Kienitz, Y.-h. Chien, D. W. Hong, N. Liu, A. Royalty, G. Hawthorne, and A. L. Reiss, "Changes in Brain Activation Associated with Spontaneous Improvization and Figural Creativity After Design-Thinking-Based Training: A Longitudinal fMRI Study," *Cereb. Cortex*, vol. 27, no. 7, pp. 3542–3552, 2017.

[110] S. Vieira, J. S. Gero, J. Delmoral, V. Gattol, C. Fernandes, M. Parente, and A. A. Fernandes, "The neurophysiological activations of mechanical engineers and industrial designers while designing and problem-solving," *Des. Sci.*, vol. 6, p. e26, 2020.

[111] T. Shealy, J. Gero, M. Hu, and J. Milovanovic, "Concept generation techniques change patterns of brain activation during engineering design," *Des. Sci.*, vol. 6, p. e31, 2020.

[112] H. Kuusela and P. Pallab, "A comparison of concurrent and retrospective verbal protocol analysis," *Am. J. Psychol.*, vol. 113, no. 3, pp. 387–404, 2000.

[113] S. Agnoli, M. Zanon, S. Mastria, A. Avenanti, and G. E. Corazza, "Predicting response originality through brain activity: An analysis of changes in EEG alpha power during the generation of alternative ideas," *Neuroimage*, vol. 207, p. 116385, 2020.

[114] D. Lehmann, H. Ozaki, and I. Pal, "EEG alpha map series: brain micro-states by space-oriented adaptive segmentation," *Electroencephalogr. Clin. Neurophysiology*, vol. 67, no. 3, pp. 271–288, 1987.

[115] J. Britz, D. Van De Ville, and C. M. Michel, "BOLD correlates of EEG topography reveal rapid resting-state network dynamics," *Neuroimage*, vol. 52, no. 4, pp. 1162–1170, 2010.

[116] R. D. Pascual-Marqui, C. M. Michel, and D. Lehmann, "Segmentation of brain electrical activity into microstates: model estimation and validation," *IEEE. Trans. Biomed. Eng.*, vol. 42, no. 7, pp. 658–665, 1995.

[117] A. T. Poulsen, A. Pedroni, N. Langer, and L. K. Hansen, "Microstate EEGlab toolbox: An introductory guide," *BioRxiv*, no. 289850, 2018.

[118] M. M. Murray, D. Brunet, and C. M. Michel, "Topographic ERP analyses: a step-by-step tutorial review," *Brain Topogr.*, vol. 20, no. 4, pp. 249–264, 2008.

[119] G. Pourtois, S. Delplanque, C. Michel, and P. Vuilleumier, "Beyond conventional event-related brain potential (ERP): exploring the time-course of visual emotion processing using topographic and principal component analyses," *Brain Topogr.*, vol. 20, no. 4, pp. 265–277, 2008.

[120] S. Makeig, S. Debener, J. Onton, and A. Delorme, "Mining event-related brain dynamics," *Trends Cogn. Sci.*, vol. 8, no. 5, pp. 204–210, 2004.

[121] F. Von Wegner, P. Knaut, and H. Laufs, "EEG microstate sequences from different clustering algorithms are information-theoretically invariant," *Front. Comput. Neurosci.*, vol. 12, p. 70, 2018.

[122] R. Efron, "The minimum duration of a perception," *Neuropsychologia*, vol. 8, no. 1, pp. 57–63, 1970.

[123] B. J. Baars, "The conscious access hypothesis: origins and recent evidence," *Trends Cogn. Sci.*, vol. 6, no. 1, pp. 47–52, 2002.

[124] A. Delorme and S. Makeig, "EEGLAB: an open source toolbox for analysis of single-trial EEG dynamics including independent component analysis," *J. Neurosci. Methods*, vol. 134, no. 1, pp. 9–21, 2004.

[125] L. J. Gabard-Durnam, A. S. Mendez Leal, C. L. Wilkinson, and A. R. Levin, "The Harvard Automated Processing Pipeline for Electroencephalography (HAPPE): Standardized Processing Software for Developmental and High-Artifact Data," *Front. Neurosci.*, vol. 12, p. 97, 2018.

[126] H. Nolan, R. Whelan, and R. B. Reilly, "FASTER: Fully Automated Statistical Thresholding for EEG artifact Rejection," *J. Neurosci. Methods*, vol. 192, no. 1, pp. 152–162, 2010.

[127] S. Karakaş, "A review of theta oscillation and its functional correlates," *Int. J. Psychophysiol.*, vol. 157, pp. 82–99, 2020.

[128] T. Koenig, D. Lehmann, M. C. Merlo, K. Kochi, D. Hell, and M. Koukkou, "A deviant EEG brain microstate in acute, neuroleptic-naive schizophrenics at rest," *Eur. Arch. Psychiatry. Clin. Neurosci.*, vol. 249, no. 4, pp. 205–211, 1999.

[129] F. Von Wegner, "Partial Autoinformation to Characterize Symbolic Sequences," *Front. Physiol.*, vol. 9, p. 1382, 2018.

[130] F. von Wegner, E. Tagliazucchi, and H. Laufs, "Information-theoretical analysis of resting state EEG microstate sequences - non-Markovianity, non-stationarity and periodicities," *Neuroimage*, vol. 158, pp. 99–111, 2017.

[131] C.-K. Peng, S. Havlin, H. E. Stanley, and A. L. Goldberger, "Quantification of scaling exponents and crossover phenomena in nonstationary heartbeat time series," *Chaos*, vol. 5, no. 1, pp. 82–87, 1995.

[132] D. Van de Ville, J. Britz, and C. M. Michel, "EEG microstate sequences in healthy humans at rest reveal scale-free dynamics," *Proc. Natl. Acad. Sci. U.S.A.*, vol. 107, no. 42, pp. 18179–18184, 2010.

[133] M. Saggar, E. Volle, L. Q. Uddin, E. G. Chrysikou, and A. E. Green, "Creativity and the brain: An editorial introduction to the special issue on the neuroscience of creativity.," *Neuroimage*, p. 117836, 2021.

[134] D. Schwab, M. Benedek, I. Papousek, E. M. Weiss, and A. Fink, "The time-course of EEG alpha power changes in creative ideation," *Front. Hum. Neurosci.*, vol. 8, p. 310, 2014.

[135] S. Jaarsveld, A. Fink, M. Rinner, D. Schwab, M. Benedek, and T. Lachmann, "Intelligence in creative processes: An EEG study," *Intelligence*, vol. 49, pp. 171–178, 2015.

[136] C. Rominger, I. Papousek, C. M. Perchtold, M. Benedek, E. M. Weiss, A. Schwerdtfeger, and A. Fink, "Creativity is associated with a characteristic U-shaped function of alpha power changes accompanied by an early increase in functional coupling," *Cogn. Affect. Behav. Neurosci.*, vol. 19, pp. 1012–1021, 2019.

[137] N. Hao, Y. Ku, M. Liu, Y. Hu, M. Bodner, R. H. Grabner, and A. Fink, "Reflection enhances creativity: Beneficial effects of idea evaluation on idea generation," *Brain Cogn.*, vol. 103, pp. 30–37, 2016.

[138] C. Rominger, I. Papousek, C. M. Perchtold, B. Weber, E. M. Weiss, and A. Fink, "The creative brain in the figural domain: Distinct patterns of EEG alpha power during idea generation and idea elaboration," *Neuropsychologia*, vol. 118, pp. 13–19, 2018.

[139] C. Rominger, I. Papousek, C. M. Perchtold, M. Benedek, E. M. Weiss, B. Weber, A. R. Schwerdtfeger, M. T. Eglmaier, and A. Fink, "Functional coupling of brain networks during creative idea generation and elaboration in the figural domain," *Neuroimage*, vol. 22, p. 116395, 2019.

[140] T. A. Nguyen and Y. Zeng, "A preliminary study of EEG spectrogram of a single subject performing a creativity test," in *Proceedings of the 2014 International Conference on Innovative Design and Manufacturing (ICIDM)*, pp. 16–21, IEEE, 2014.

[141] A. Custo, D. Van De Ville, W. M. Wells, M. I. Tomescu, D. Brunet, and C. M. Michel, "Electroencephalographic Resting-State Networks: Source Localization of Microstates," *Brain Connect.*, vol. 7, no. 10, pp. 671–682, 2017.

[142] L. M. Pidgeon, M. Grealy, A. H. Duffy, L. Hay, C. McTeague, T. Vuletic, D. Coyle, and S. J. Gilbert, "Functional neuroimaging of visual creativity: a systematic review and meta-analysis," *Brain Behav.*, vol. 6, no. 10, p. e00540, 2016.

[143] B. Barbot, "The Dynamics of Creative Ideation: Introducing a New Assessment Paradigm," *Front. Psychol.*, vol. 9, p. 2529, 2018.

[144] K. Dorst, "Co-evolution and emergence in design," *Des. Stud.*, vol. 65, pp. 60–77, 2019.

[145] T. I. Lubart, "Models of The Creative Process: Past, Present and Future," *Creat. Res. J.*, vol. 13, no. 3-4, pp. 295–308, 2001.

[146] L. Zeng, R. W. Proctor, and G. Salvendy, "Can Traditional Divergent Thinking Tests Be Trusted in Measuring and Predicting Real-World Creativity?," *Creat. Res. J.*, vol. 23, no. 1, pp. 24–37, 2011.

[147] G. E. Corazza, "The Dynamic Universal Creativity Process," in *Dynamic Perspectives on Creativity : New Directions for Theory, Research, and Practice in Education* (R. A. Beghetto and G. E. Corazza, eds.), pp. 297–319, Cham: Springer International Publishing, 2019.

[148] A. Dietrich, "Where in the brain is creativity: a brief account of a wild-goose chase," *Curr. Opin. Behav. Sci.*, vol. 27, pp. 36–39, 2019.

[149] H. Yuan, V. Zotev, R. Phillips, W. C. Drevets, and J. Bodurka, "Spatiotemporal dynamics of the brain at rest-exploring EEG microstates as electrophysiological signatures of BOLD resting state networks," *Neuroimage*, vol. 60, no. 4, pp. 2062–2072, 2012.

[150] P. Milz, P. L. Faber, D. Lehmann, T. Koenig, K. Kochi, and R. D. Pascual-Marqui, "The functional significance of EEG microstates-Associations with modalities of thinking," *Neuroimage*, vol. 125, pp. 643–656, 2016.

[151] E. Pirondini, M. Coscia, J. Minguillon, J. d. R. Millán, D. Van De Ville, and S. Micera, "EEG topographies provide subject-specific correlates of motor control," *Sci. Rep.*, vol. 7, no. 1, p. 13229, 2017.

[152] M. Murphy, R. Stickgold, M. E. Parr, C. Callahan, and E. J. Wamsley, "Recurrence of task-related electroencephalographic activity during post-training quiet rest and sleep," *Sci. Rep.*, vol. 8, no. 1, pp. 1–10, 2018.

[153] P. Ruggeri, H. B. Meziane, T. Koenig, and C. Brandner, "A fine-grained time course investigation of brain dynamics during conflict monitoring," *Sci. Rep.*, vol. 9, no. 1, p. 3667, 2019.

[154] F. Zappasodi, M. G. Perrucci, A. Saggino, P. Croce, P. Mercuri, R. Romanelli, R. Colom, and S. J. Ebisch, "EEG microstates distinguish between cognitive components of fluid reasoning," *Neuroimage*, vol. 189, pp. 560–573, 2019.

[155] W. Klimesch, "EEG alpha and theta oscillations reflect cognitive and memory performance: a review and analysis," *Brain Res. Rev.*, vol. 29, no. 2-3, pp. 169–195, 1999.

[156] N. Jaušovec and K. Jaušovec, "EEG activity during the performance of complex mental problems," *Int. J. Psychophysiol.*, vol. 36, no. 1, pp. 73–88, 2000.

[157] E. Verstraeten and R. Cluydts, "Attentional switching-related human EEG alpha oscillations," *Neuroreport*, vol. 13, no. 5, pp. 681–684, 2002.

[158] M. Doppelmayr, W. Klimesch, W. Stadler, D. Pöllhuber, and C. Heine, "EEG alpha power and intelligence," *Intelligence*, vol. 30, no. 3, pp. 289–302, 2002.

[159] W. Klimesch, M. Doppelmayr, H. Russegger, T. Pachinger, and J. Schwaiger, "Induced alpha band power changes in the human EEG and attention," *Neurosci. Lett.*, vol. 244, no. 2, pp. 73–76, 1998.

[160] N. V. Shemyakina and Z. V. Nagornova, "EEG "Signs" of Verbal Creative Task Fulfillment with and without Overcoming Self-Induced Stereotypes," *Behav. Sci.*, vol. 10, no. 1, p. 17, 2020.

[161] B. Kraus, C. Cadle, and S. Simon-Dack, "EEG alpha activity is moderated by the serial order effect during divergent thinking," *Biol. Psychol.*, vol. 145, pp. 84–95, 2019.

[162] N. F. Roozenburg, "On the pattern of reasoning in innovative design," *Des. Stud.*, vol. 14, no. 1, pp. 4–18, 1993.

[163] M. Doppelmayr, W. Klimesch, P. Sauseng, K. Hödlmoser, W. Stadler, and S. Hanslmayr, "Intelligence related differences in EEG-bandpower," *Neurosci. Lett.*, vol. 381, no. 3, pp. 309–313, 2005.

[164] M. Doppelmayr, W. Klimesch, K. Hödlmoser, P. Sauseng, and W. Gruber, "Intelligence related upper alpha desynchronization in a semantic memory task," *Brain Res. Bull.*, vol. 66, no. 2, pp. 171–177, 2005.

[165] W. Klimesch, M. Doppelmayr, and S. Hanslmayr, "Upper alpha ERD and absolute power: their meaning for memory performance," *Prog. Brain Res.*, vol. 159, pp. 151–165, 2006.

[166] R. B. Cattell, *Intelligence: its structure, growth and action*. Amsterdam: Elsevier, 1987.

[167] M. Benedek and A. Fink, "Toward a neurocognitive framework of creative cognition: the role of memory, attention, and cognitive control," *Curr. Opin. Behav. Sci.*, vol. 27, pp. 116–122, 2019.

[168] M. D. Fox, A. Z. Snyder, J. L. Vincent, M. Corbetta, D. C. Van Essen, and M. E. Raichle, "The human brain is intrinsically organized into dynamic, anticorrelated functional networks," *Proc. Natl. Acad. Sci. USA*, vol. 102, no. 27, pp. 9673–9678, 2005.

[169] M. D. Fox and M. E. Raichle, "Spontaneous fluctuations in brain activity observed with functional magnetic resonance imaging," *Nat. Rev. Neurosci.*, vol. 8, no. 9, pp. 700–711, 2007.

[170] R. Leech and D. J. Sharp, "The role of the posterior cingulate cortex in cognition and disease," *Brain*, vol. 137, no. 1, pp. 12–32, 2014.

[171] M. Corbetta, J. M. Kincade, and G. L. Shulman, "Neural Systems for Visual Orienting and Their Relationships to Spatial Working Memory," *J. Cogn. Neurosci.*, vol. 14, no. 3, pp. 508–523, 2002.

[172] K. Gilhooly, E. Fioratou, S. Anthony, and V. Wynn, "Divergent thinking: Strategies and executive involvement in generating novel uses for familiar objects," *Br. J. Psychol.*, vol. 98, no. 4, pp. 611–625, 2007.

[173] M. Benedek, E. Jauk, A. Fink, K. Koschutnig, G. Reishofer, F. Ebner, and A. C. Neubauer, "To create or to recall? Neural mechanisms underlying the generation of creative new ideas," *Neuroimage*, vol. 88, pp. 125–133, 2014.

[174] A. Shenhav, J. D. Cohen, and M. M. Botvinick, "Dorsal anterior cingulate cortex and the value of control," *Nat. Neurosci.*, vol. 19, no. 10, p. 1286, 2016.

[175] E. G. Chrysikou, "Creativity in and out of (cognitive) control," *Curr. Opin. Behav. Sci.*, vol. 27, pp. 94–99, 2019.

[176] E. Jauk, "A bio-psycho-behavioral model of creativity," *Curr. Opin. Behav. Sci.*, vol. 27, pp. 1–6, 2019.

[177] A. P. Zanesco, E. Denkova, and A. P. Jha, "Associations between self-reported spontaneous thought and temporal sequences of EEG microstates," *Brain Cogn*, vol. 150, p. 105696, 2021.

[178] B. A. Seitzman, M. Abell, S. C. Bartley, M. A. Erickson, A. R. Bolbecker, and W. P. Hetrick, "Cognitive manipulation of brain electric microstates," *Neuroimage*, vol. 146, pp. 533–543, 2017.

[179] L. Bréchet, D. Brunet, G. Birot, R. Gruetter, C. M. Michel, and J. Jorge, "Capturing the spatiotemporal dynamics of self-generated, task-initiated thoughts with EEG and fMRI," *Neuroimage*, vol. 194, pp. 82–92, 2019.

[180] F. von Wegner, E. Tagliazucchi, V. Brodbeck, and H. Laufs, "Analytical and empirical fluctuation functions of the EEG microstate random walk-short-range vs. long-range correlations," *Neuroimage*, vol. 141, pp. 442–451, 2016.

[181] J. D. Cohen, W. M. Perlstein, T. S. Braver, L. E. Nystrom, D. C. Noll, J. Jonides, and E. E. Smith, "Temporal dynamics of brain activation during a working memory task," *Nature*, vol. 386, no. 6625, pp. 604–608, 1997.

[182] A. Stipacek, R. Grabner, C. Neuper, A. Fink, and A. Neubauer, "Sensitivity of human EEG alpha band desynchronization to different working memory components and increasing levels of memory load," *Neurosci. Lett.*, vol. 353, no. 3, pp. 193–196, 2003.

[183] C. M. Krause, L. Sillanmäki, M. Koivisto, C. Saarela, A. Häggqvist, M. Laine, and H. Hämäläinen, "The effects of memory load on event-related EEG desynchronization and synchronization," *Clin. Neurophysiol.*, vol. 111, no. 11, pp. 2071–2078, 2000.

[184] E. Koechlin, C. Ody, and F. Kouneiher, "The Architecture of Cognitive Control in the Human Prefrontal Cortex," *Science*, vol. 302, no. 5648, pp. 1181–1185, 2003.

[185] G. A. Buzzell, T. V. Barker, S. V. Troller-Renfree, E. M. Bernat, M. E. Bowers, S. Morales, L. C. Bowman, H. A. Henderson, D. S. Pine, and N. A. Fox, "Adolescent cognitive control, theta oscillations, and social observation," *Neuroimage*, vol. 198, pp. 13–30, 2019.

[186] C. E. Davis, J. D. Hauf, D. Q. Wu, and D. E. Everhart, "Brain function with complex decision making using electroencephalography," *Int. J. Psychophysiol.*, vol. 79, no. 2, pp. 175–183, 2011.

[187] C. C. Williams, M. Kappen, C. D. Hassall, B. Wright, and O. E. Krigolson, "Thinking theta and alpha: Mechanisms of intuitive and analytical reasoning," *Neuroimage*, vol. 189, pp. 574–580, 2019.

[188] J. Riddle, D. A. Vogelsang, K. Hwang, D. Cellier, and M. D'Esposito, "Distinct Oscillatory Dynamics Underlie Different Components of Hierarchical Cognitive Control," *J. Neurosci.*, vol. 40, no. 25, pp. 4945–4953, 2020.

[189] V. v. Veen and C. S. Carter, "Conflict and Cognitive Control in the Brain," *Curr. Dir. Psychol. Sci.*, vol. 15, no. 5, pp. 237–240, 2006.

[190] J. F. Cavanagh, M. X. Cohen, and J. J. Allen, "Prelude to and Resolution of an Error: EEG Phase Synchrony Reveals Cognitive Control Dynamics during Action Monitoring," *J. Neurosci.*, vol. 29, no. 1, pp. 98–105, 2009.

[191] P. S. Cooper, F. Karayanidis, M. McKewen, S. McLellan-Hall, A. S. Wong, P. Skippen, and J. F. Cavanagh, "Frontal theta predicts specific cognitive control-induced behavioural changes beyond general reaction time slowing," *Neuroimage*, vol. 189, pp. 130–140, 2019.

[192] T. Amer, K. L. Campbell, and L. Hasher, "Cognitive Control As a Double-Edged Sword," *Trends Cogn. Sci.*, vol. 20, no. 12, pp. 905–915, 2016.

[193] A. Fink, R. Grabner, C. Neuper, and A. Neubauer, "EEG alpha band dissociation with increasing task demands," *Brain Res. Cogn. Brain Res.*, vol. 24, no. 2, pp. 252–259, 2005.

[194] A. Keil, T. Mussweiler, and K. Epstude, "Alpha-band activity reflects reduction of mental effort in a comparison task: A source space analysis," *Brain Res.*, vol. 1121, no. 1, pp. 117–127, 2006.

[195] P. S. Tsang and M. A. Vidulich, "Mental Workload and Situation Awareness.," in *Handbook of Human Factors and Ergonomics* (G. Salvendy, ed.), pp. 243–268, John Wiley & Sons, Inc., 3 ed., 2006.

[196] A.-M. Brouwer, M. A. Hogervorst, M. Holewijn, and J. B. van Erp, "Evidence for effects of task difficulty but not learning on neurophysiological variables associated with effort," *Int. J. Psychophysiol.*, vol. 93, no. 2, pp. 242–252, 2014.

[197] K. J. Jaquess, L.-C. Lo, H. Oh, C. Lu, A. Ginsberg, Y. Y. Tan, K. R. Lohse, M. W. Miller, B. D. Hatfield, and R. J. Gentili, "Changes in Mental Workload and Motor Performance Throughout Multiple Practice Sessions Under Various Levels of Task Difficulty," *Neuroscience*, vol. 393, pp. 305–318, 2018.

[198] M. Doppelmayr, W. Klimesch, K. Hödlmoser, P. Sauseng, and W. Gruber, "Intelligence related upper alpha desynchronization in a semantic memory task," *Brain Res. Bull.*, vol. 66, no. 2, pp. 171–177, 2005.

[199] W. Klimesch, "Alpha-band oscillations, attention, and controlled access to stored information," *Trends Cogn. Sci.*, vol. 16, no. 12, pp. 606–617, 2012.

[200] S. Mun, M. Whang, S. Park, and M.-C. Park, "Effects of mental workload on involuntary attention: A somatosensory ERP study," *Neuropsychologia*, vol. 106, pp. 7–20, 2017.

[201] A.-M. Brouwer, M. A. Hogervorst, J. B. Van Erp, T. Heffelaar, P. H. Zimmerman, and R. Oostenveld, "Estimating workload using EEG spectral power and ERPs in the n-back task," *J. Neural Eng.*, vol. 9, no. 4, p. 045008, 2012.

[202] K. Fukuda, I. Mance, and E. K. Vogel, "α Power Modulation and Event-Related Slow Wave Provide Dissociable Correlates of Visual Working Memory," *J. Neurosci.*, vol. 35, no. 41, pp. 14009–14016, 2015.

[203] W. Klimesch, P. Sauseng, and S. Hanslmayr, "EEG alpha oscillations: The inhibition–timing hypothesis," *Brain Res. Rev.*, vol. 53, no. 1, pp. 63–88, 2007.

[204] T. A. Rihs, C. M. Michel, and G. Thut, "Mechanisms of selective inhibition in visual spatial attention are indexed by α-band EEG synchronization," *Eur. J. Neurosci.*, vol. 25, no. 2, pp. 603–610, 2007.

[205] M. Benedek, S. Bergner, T. Könen, A. Fink, and A. C. Neubauer, "EEG alpha synchronization is related to top-down processing in convergent and divergent thinking," *Neuropsychologia*, vol. 49, no. 12, pp. 3505–3511, 2011.

[206] D. W. Grupe and J. B. Nitschke, "Uncertainty and anticipation in anxiety: an integrated neurobiological and psychological perspective," *Nat. Rev. Neurosci.*, vol. 14, no. 7, pp. 488–501, 2013.

[207] J. Morriss, M. Gell, and C. M. van Reekum, "The uncertain brain: A co-ordinate based meta-analysis of the neural signatures supporting uncertainty during different contexts," *Neurosci. Biobehav. Rev.*, vol. 96, pp. 241–249, 2019.

[208] J. F. Cavanagh, L. Zambrano-Vazquez, and J. J. Allen, "Theta lingua franca: A common mid-frontal substrate for action monitoring processes," *Psychophysiology*, vol. 49, no. 2, pp. 220–238, 2012.

[209] A. K. Engel and P. Fries, "Beta-band oscillations-signalling the status quo?," *Curr. Opin. Neurobiol.*, vol. 20, no. 2, pp. 156–165, 2010.

[210] E. S. Darowski, E. Helder, R. T. Zacks, L. Hasher, and D. Z. Hambrick, "Age-related differences in cognition: the role of distraction control.," *Neuropsychology*, vol. 22, no. 5, p. 638, 2008.

[211] I. Mund, R. Bell, and A. Buchner, "Aging and interference in story recall," *Exp. Aging Res.*, vol. 38, no. 1, pp. 20–41, 2012.

[212] R. Radel, K. Davranche, M. Fournier, and A. Dietrich, "The role of (dis) inhibition in creativity: Decreased inhibition improves idea generation," *Cognition*, vol. 134, pp. 110–120, 2015.

[213] E. G. Chrysikou, "The Costs and Benefits of Cognitive Control for Creativity," in *The Cambridge Handbook of the Neuroscience of Creativity* (R. E. Jung and O. Vartanian, eds.), p. 299âĂŞ317, New York: Cambridge University Press, 2018.

[214] D. S. Rosen, Y. Oh, B. Erickson, F. Z. Zhang, Y. E. Kim, and J. Kounios, "Dual-process contributions to creativity in jazz improvisations: An SPM-EEG study," *Neuroimage*, vol. 213, p. 116632, 2020.

[215] C. J. Limb and A. R. Braun, "Neural Substrates of Spontaneous Musical Performance: An fMRI Study of Jazz Improvisation," *PLoS One*, vol. 3, no. 2, p. e1679, 2008.

[216] R. E. Beaty, M. Benedek, P. J. Silvia, and D. L. Schacter, "Creative Cognition and Brain Network Dynamics," *Trends Cogn. Sci.*, vol. 20, no. 2, pp. 87–95, 2016.

[217] W. Zhang, Z. Sjoerds, and B. Hommel, "Metacontrol of human creativity: The neurocognitive mechanisms of convergent and divergent thinking," *Neuroimage*, vol. 210, p. 116572, 2020.

[218] M. Gärtner, V. Brodbeck, H. Laufs, and G. Schneider, "A stochastic model for EEG microstate sequence analysis," *Neuroimage*, vol. 104, pp. 199–208, 2015.

[219] V. Brodbeck, A. Kuhn, F. von Wegner, A. Morzelewski, E. Tagliazucchi, S. Borisov, C. M. Michel, and H. Laufs, "EEG microstates of wakefulness and NREM sleep," *Neuroimage*, vol. 62, no. 3, pp. 2129–2139, 2012.

[220] A. P. Zanesco, B. G. King, A. C. Skwara, and C. D. Saron, "Within and between-person correlates of the temporal dynamics of resting EEG microstates," *Neuroimage*, vol. 211, p. 116631, 2020.

[221] M. Gschwind, C. M. Michel, and D. Van De Ville, "Long-range dependencies make the difference-Comment on" A stochastic model for EEG microstate sequence analysis".," *Neuroimage*, vol. 117, pp. 449–455, 2015.

[222] J. Mao, W. Xu, Y. Yang, J. Wang, Z. Huang, and A. Yuille, "Deep captioning with multimodal recurrent neural networks (m-rnn)," *arXiv preprint arXiv:1412.6632*, 2014.

[223] Y. Bengio, P. Simard, and P. Frasconi, "Learning long-term dependencies with gradient descent is difficult," *IEEE Trans. Neural. Netw.*, vol. 5, no. 2, pp. 157–166, 1994.

[224] S. Hochreiter and J. Schmidhuber, "Long short-term memory," *Neural Comput.*, vol. 9, no. 8, pp. 1735–1780, 1997.

[225] K. Cho, B. Van Merriënboer, C. Gulcehre, D. Bahdanau, F. Bougares, H. Schwenk, and Y. Bengio, "Learning phrase representations using RNN encoder-decoder for statistical machine translation," *arXiv preprint arXiv:1406.1078*, 2014.

[226] F. A. Gers, N. N. Schraudolph, and J. Schmidhuber, "Learning precise timing with LSTM recurrent networks," *J. Mach. Learn. Res.*, vol. 3, pp. 115–143, 2002.

[227] S. Alhagry, A. A. Fahmy, and R. A. El-Khoribi, "Emotion recognition based on EEG using LSTM recurrent neural network," *Emotion*, vol. 8, no. 10, pp. 355–358, 2017.

[228] P. Wang, A. Jiang, X. Liu, J. Shang, and L. Zhang, "LSTM-based EEG classification in motor imagery tasks," *IEEE Trans. Neural Syst. Rehabilitation Eng.*, vol. 26, no. 11, pp. 2086–2095, 2018.

[229] A. Sikka, H. Jamalabadi, M. Krylova, S. Alizadeh, J. N. van der Meer, L. Danyeli, M. Deliano, P. Vicheva, T. Hahn, T. Koenig, *et al.*, "Investigating the temporal dynamics of electroencephalogram (EEG) microstates using recurrent neural networks," *Hum. Brain Mapp.*, vol. 41, no. 9, pp. 2334–2346, 2020.

[230] U. Güçlü and M. A. van Gerven, "Modeling the dynamics of human brain activity with recurrent neural networks," *Front. Comput. Neurosci.*, vol. 11, p. 7, 2017.

[231] M. Sokolova and G. Lapalme, "A systematic analysis of performance measures for classification tasks," *Inf. Process. Manag.*, vol. 45, no. 4, pp. 427–437, 2009.

[232] J. Yang, L. Yang, H. Quan, and Y. Zeng, "Implementation Barriers: A TASKS Framework," *Journal of Integrated Design and Process Science*, vol. 25, 2021.